

UC San Diego

UC San Diego Electronic Theses and Dissertations

Title

Assessing the impact of climate-change related lower pH and lower salinity conditions on the physiology and behavior of a luminous marine invertebrate

Permalink

<https://escholarship.org/uc/item/9zr0x9qw>

Author

LaFace, Kira

Publication Date

2019

Peer reviewed|Thesis/dissertation

UNIVERSITY OF CALIFORNIA SAN DIEGO

Assessing the impact of climate-change related lower pH and lower salinity conditions on
the physiology and behavior of a luminous marine invertebrate

A Thesis submitted in partial satisfaction of the
requirements for the degree Master of Science

in

Marine Biology

by

Kira Marie Price LaFace

Committee in charge:

Dimitri Deheyn, Chair
Deirdre Lyons
Jennifer Taylor

2019

Copyright

Kira Marie Price LaFace, 2019

All rights reserved.

The Thesis of Kira Marie Price LaFace is approved, and it is acceptable in quality and form for publication on microfilm and electronically:

Chair

University of California San Diego

2019

DEDICATION

I would like to dedicate this thesis to all of my family and friends who supported me in my endeavor to achieve my childhood dream of becoming a marine biologist. I would not have been able to reach this point without all of your love and guidance. I would also like to dedicate this thesis to my advisor Dr. Deheyn and the Deheyn Lab for all of the helpful advice, and support that made this work possible and transform this project into a publication in the future. I am eternally grateful and I will carry the memories of our time together with me as I move forward onto the next stages of my career and life. Thank you.

TABLE OF CONTENTS

Signature Page.....	iii
Dedication.....	iv
Table of Contents.....	v
List of Abbreviations.....	vi
List of Figures.....	vii
List of Tables.....	xi
Acknowledgements.....	xii
Abstract of the Thesis.....	xiv
Introduction.....	1
Materials and Methods.....	10
Results.....	25
Discussion.....	52
References.....	81

LIST OF ABBREVIATIONS

ACC	Amorphous Calcium Carbonate
Ach	Acetylcholine chloride
ASW	Artificial Seawater
CaCO ₃	Calcium carbonate
CO ₂	Carbon dioxide
CO ₃ ²⁻	Carbonate
EDS	Energy Dispersive Spectroscopy
H ₂ CO ₃	Carbonic acid
HCO ₃ ⁻	Bicarbonate
H ₂ O	Water
KCl	Potassium chloride
MgCl ₂	Magnesium chloride
MgCO ₃	Magnesium carbonate
pH ⁻	Low pH (7.6)
pH ⁻ S ⁻	Low pH low salinity (7.6; 25 PSU)
PSU	Practical Salinity Units
RLU	Relative Light Units
S ⁻	Low salinity (25 PSU)
SEM	Scanning Electron Microscopy

LIST OF FIGURES

Figure 1. Graphic representation of the experimental setup and four individual treatments: pH ⁻ (green), S ⁻ (red), pH-S ⁻ (blue) and the control (orange).....	12
Figure 2. Progression of the brittlestars natural flipping response. Photo credit goes to Roan Wooley (Deheyn Lab intern, High Tech High).....	18
Figure 3. Flow chart of methods for the ossicle porosity analysis of both the non-regenerated and regenerated ossicles imaged with SEM during the arm regeneration experimental tests. These measurements were made using the program Fiji for Mac OS X.....	21
Figure 4. Fluorescence of <i>A. squamata</i> after the occurrence of bioluminescence (525 nm). The luminescence occurs at the brightest parts of fluorescence on the sides of the arm of the brittlestar. Despite the center disk displaying fluorescence, it does not produce bioluminescence.....	24
Figure 5. Box plot analysis of average flipping times for the brittlestars exposed to both the altered water chemistry and control conditions.....	26
Figure 6. Box plot analysis of average flipping times for the brittlestars showing slower flipping times in the S ⁻ after the treatments have been removed (crossed-circle sign). The left side box plot depicts the average flipping times when the treatments were present.....	27
Figure 7. Distribution of brittlestars used in the chi-squared statistical tests with the treatments present. These brittlestars were unable to flip for over 120 s and expressed stressed behaviors during the flipping process of either curling into a ball or lying flat upside down.....	28
Figure 8. Distribution of brittlestars used in the chi-squared statistical tests once the treatments were removed. These brittlestars were unable to flip for over 120 s and expressed stressed behaviors during the flipping process of either curling into a ball or lying flat upside down.....	29
Figure 9. Frequency (in percentages) of occurrence of the four flipping behaviors the brittlestars displayed during the flipping process for each of the four experimental treatments.....	30
Figure 10. Effect of treatment removed: frequency (in percentages) of occurrence of the four flipping behaviors brittlestars displayed during the flipping process when each treatment was removed for each of the four previous experimental treatments.....	31
Figure 11. Median flipping times of each flip trial for the brittlestars exposed to the experimental treatments demonstrates flipping fatigue for each treatment, with an increase linear trend from trial 1 to trial 10. Error bars are displayed as percentage error.....	33
Figure 12. Median flipping times of each flip trial for the brittlestars previously exposed to the experimental treatments demonstrates continuous flipping fatigue with an increase linear trend from trial 1 to trial 10 after the treatments were removed. Error bars are displayed as percentage error. Note: The Y-axis is different compared to Figure 11.....	34

Figure 13. The progression of brittlestar arm regeneration in each of the four experimental treatments over time. The blue circles highlight the area of regeneration. N.A.: Data Not Available (due to brittlestars death). Scale bars: 7.5 μ m.....37

Figure 14. Images of the non-regenerated ossicles of the brittlestar arm (skeleton) after being exposed to each of the four experimental treatments over time. The pictures show the 3rd dorsal ossicle (skeleton) from the original amputation site. The green x's and labels mark where the EDS measurements occurred (n=4).....40

Figure 15. Progression of brittlestar arm regeneration compared to the original arm ossicles in each of the four experimental treatments over time. The pictures show both the 3rd dorsal ossicle from the original amputation site (left) and the dorsal ossicle from the regenerated site (right). The green x's and labels mark where the EDS measurements occurred (n=4).....41

Figure 16. Average values of mean intensity and mean percent porosity \pm SD for day 28 present in the non-regenerated and regenerated dorsal ossicles for the brittlestars exposed to the four different treatments over time. Data was collected from SEM images from Figure 15 using Fiji for Mac OS X after images were binarized and thresholded.....43

Figure 17. Average values of mean intensity and mean percent porosity \pm SD for day 49 present in the non-regenerated and regenerated dorsal ossicles for the brittlestars exposed to the four different treatments over time. Data was collected from SEM images from Figure 15 using Fiji for Mac OS X after images were binarized and thresholded.....43

Figure 18. Average concentrations of magnesium in mass percent \pm SD present in the non-regenerated original dorsal ossicle for the brittlestars exposed to the four different treatments over time. The dotted lines indicate the upper and lower limits of the control range.....46

Figure 19. Average concentrations of calcium in mass percent \pm SD present in the non-regenerated original dorsal ossicle for the brittlestars exposed to the four different treatments over time. The dotted lines indicate the upper and lower limits of the control range.....47

Figure 20. Ratios of calcium to magnesium in mass percent \pm SD of the non-regenerated original dorsal ossicle for the brittlestars exposed to the four different treatments over time. The dotted lines indicate the upper and lower limits of the control range.....47

Figure 21. Average concentrations of magnesium in mass percent \pm SD present in the regenerated dorsal ossicle for each brittlestar exposed to the four treatments over time. There was no regeneration for pH⁻S⁻ during day 49 (N.A.).....48

Figure 22. Average concentrations of calcium in mass percent \pm SD present in the regenerated dorsal ossicle for each brittlestar exposed to the four treatments over time. There was no regeneration for pH⁻S⁻ during day 49 (N.A.).....49

Figure 23. Ratios of calcium to magnesium in mass percent \pm SD of the regenerated dorsal ossicle for each brittlestar exposed to the four treatments over time. There was no regeneration for pH⁻S⁻ during day 49 (N.A.).....50

Figure 24. Comparison between average concentrations of magnesium in mass percent \pm SD present in the both the regenerated and non-regenerated dorsal ossicles for each brittlestar exposed to the four treatments over time (n=4 per bar). The dotted lines indicate the upper and lower limits of the control range.....51

Figure 25. Comparison between average concentrations of calcium in mass percent \pm SD present in the both the regenerated and non-regenerated dorsal ossicles for each brittlestar exposed to the four treatments over time (n=4 per bar). The dotted lines indicate the upper and lower limits of the control range.....52

Figure 26. Raw bioluminescence data of spontaneous light showing the sum light (A), peak light intensity (B) and peak time of the light response (C) for the brittlestars exposed to each treatment. The colored lines represent the best fit lines of the raw data to show a general trend. The peak intensity plot corresponds most closely with the light profiles.....60

Figure 27. Raw bioluminescence data of spontaneous light showing the sum light (A), peak light intensity (B) and peak time of the light response (C) for the brittlestars after the treatments were removed. The colored lines represent the best fit lines of the raw data to show a general trend. The peak intensity plot corresponds most closely with the light profiles.....62

Figure 28. Typical profiles of spontaneous light production (RLU/s) for the brittlestars exposed to each treatment on Day 0 (A), Day 30 (B), Day 46 (C) and Day 67 (D). Day 67 (D) occurred while the brittlestars were placed back into the control conditions to determine if recovery was possible.....64

Figure 29. Raw bioluminescence data of Ach light showing the sum light (A), peak light intensity (B) and peak time of the light response (C) for the brittlestars exposed to each treatment. The colored lines represent the best fit lines of the raw data to show a general trend. The peak intensity plot corresponds most closely with the light profiles.....66

Figure 30. Raw bioluminescence data of KCl light showing the sum light (A), peak light intensity (B) and peak time of the light response (C) for the brittlestars exposed to each treatment. The colored lines represent the best fit lines of the raw data to show a general trend. The peak intensity plot corresponds most closely with the light profiles.....67

Figure 31. Raw bioluminescence data of Ach light showing the sum light (A), peak light intensity (B) and peak time of the light response (C) for the brittlestars after the treatments were removed. The colored lines represent the best fit lines of the raw data to show a general trend. The peak intensity plot corresponds most closely with the light profiles.....68

Figure 32. Raw bioluminescence data of KCl light showing the sum light (A), peak light intensity (B) and peak time of the light response (C) for the brittlestars after the treatments were removed. The colored lines represent the best fit lines of the raw data to show a general trend. The peak intensity plot corresponds most closely with the light profiles.....69

Figure 33. Typical profiles of Ach light production (RLU/s) for the brittlestars exposed to each treatment on Day 0 (A), Day 30 (B), Day 46 (C) and Day 67 (D). Day 67 (D) occurred while the

brittlestars were placed back into the control conditions to determine if recovery was possible.....71

Figure 34. Typical profiles of KCl light production (RLU/s) for the brittlestars exposed to each treatment on Day 0 (A), Day 30 (B), Day 46 (C) and Day 67 (D) and measured without the use of the filter. Day 67 (D) occurred while the brittlestars were placed back into the control conditions to determine if recovery was possible.....72

LIST OF TABLES

Table 1. Temperature and water carbonate chemistry parameters used throughout the experiments. The values with an asterisk refer to the measured parameters from the Dickson lab. The measured value of temperature and calculated value of pH using CO₂sys and the Dickson lab measurements have a sample size of n=147.....14

Table 2. Chemicals used throughout the brittlestar flipping, bioluminescence, and arm regeneration experiments as well as their chemical composition and reason for use in the experiments.....16

Table 3. R² value for the trendlines on the flipping fatigue (Figure 10) with mean flipping times for both trials 1 and 10 and the percent increase in flipping time from trial 1 to trial 10 for each of the experimental conditions.....33

Table 4. R² value for the trendlines on the flipping fatigue (Figure 11) are shown along with the mean flipping times for both trials 1 and 10 and the percent increase in flipping time from trial 1 to trial 10 when each of the experimental conditions the brittlestars were exposed to had been removed.....35

Table 5. Length and area in μm of the regeneration highlighted by the blue circles in Figure 13 (from left to right) N.A.: Data Not Available (due to brittlestars death). The measurements were measured using the program Fiji for Mac OS X.....37

Table 6. Length and width measurements of the non-regenerated and regenerated portions of the brittlestar arms imaged with SEM and measured with the program Image J. The red colored font indicates the length of the regenerated portion of the brittlestar arm.....39

Table 7. Measurements of mean intensity (the gray areas in a black and white binarized image; see Figure 15) and mean percent porosity (how much bone is present) for the images shown in Figure 15 above (from left top to bottom to right top to bottom). N.A.: Data Not Available (due to no regeneration occurring).....44

ACKNOWLEDGEMENTS

I would like to express my gratitude to my advisor Dr. Deheyn for his consistent support and guidance during this project and I would also like to extend my thanks to all of the members of the Deheyn Lab for providing me with words of encouragement and advice throughout my time with the lab and this project. I would like to especially recognize, Daniel Wangpraseurt for writing a code in MATLAB to help expedite the process of the bioluminescence data analysis, and Michael Allen for taking all of the SEM photos and performing the EDS analysis on the regenerated arms.

I would like to also say thank you to the other people on my committee, Assistant Professor Jennifer Taylor and Assistant Professor Deirdre Lyons. Your guidance was invaluable and I would not have been able to complete my thesis without your words of support. Thank you for believing in me.

I would like to extend my thanks to the Dickson, Taylor, and Tresguerres Labs for providing seawater chemistry analysis, and experimental data collection tools and resources, respectively. A special thanks goes out to Garfield Kwan in the Tresguerres Lab for training me on the experimental aquarium system. I would also like to say thank you to Sebastian Kruppert in the Taylor Lab for his help downloading and receiving the pH data.

I would also like to say thank you to Phil Zerofski for collecting the experimental specimens that made this work possible. Lastly, I would like to say thank you to all of the undergraduate and high school volunteers who donated their time to help with the experimental set up and data collection. A very special thanks to: Alexa Zonderman, Roan Wooley, and Trevor Pickett.

None of this work would have been possible without the funding from the SIO Department Graduate Student Excellence Travel/Research Award, so thank you to those who made receiving the award possible.

I would also like to specially thank my parents Marjorie Price-LaFace and Drake LaFace for financially and emotionally supporting me through this exciting but difficult time of completing my thesis. You have always been there for me and encouraged me to follow my passions in life and for that I am eternally grateful.

ABSTRACT OF THE THESIS

Assessing the impact of climate-change related lower pH and lower salinity conditions on the physiology and behavior of a luminous marine invertebrate

by

Kira Marie Price LaFace

Master of Science in Marine Biology

University of California San Diego, 2019

Dimitri Deheyn, Chair

Increases in water precipitation and ocean acidification—consequences of climate change and CO₂ emissions—affects the physiology and behavior of marine invertebrates. We postulated changes would occur in nervous system-controlled predator defense mechanisms, including bioluminescence, arm regeneration, and neuro-coordination abilities, such as the ability to return to upright after being flipped upside down. This hypothesis was tested by exposing the luminous brittlestar *Amphipholis squamata* (Echinodermata) to conditions of lower pH (pH 7.7, from pH 7.9), lower salinity (25 PSU, from 33 PSU), and lower pH and salinity combined. Exposure to

the changes in experimental seawater chemistry for up to 7 weeks resulted in slower flipping times in the low salinity and in the low pH treatments and in high levels of leaking light in their bioluminescence response. These results indicated a negative effect on the neuro-muscular coordination and possibly the neuro-control of the light production. Brittlestar arms exposed to lower pH and salinity conditions experienced stunted regenerative growth, evidenced by shorter and narrower regenerative arm tips that were also less calcified. Brittlestars demonstrated difficulty expressing normal (control) predator defense functions following a 7-week exposure to low salinity conditions suggesting long term exposure resulted in prolonged effects on maintenance and repair mechanisms sustaining the brittlestar defense strategies. These data suggest compensatory energy reallocation toward maintaining normal function of other vital processes under stress. Quantifying the brittlestars behavioral and physiological responses can provide a clue for how their survivability will be impacted under projected low pH and low salinity conditions in the future.

Introduction

Climate change has been occurring at a rapid rate since the 1950s after the industrial revolution, where a boom in population and fossil fuel use caused, amongst other things, a shift in the pH and salinity of the oceans. This shift in biogeochemical factors can have an impact on osmoconformer marine invertebrates because their internal chemical environment matches the external chemical environment (Rivera-Ingraham and Lignot, 2017). Therefore, the change in pH and salinity expected during these times of anthropogenic induced climate change could have an impact on physiological processes that are integral to the survival of organisms, such as feeding, growth, locomotion and predator defenses (Turner and Meyer, 1980).

Climate change

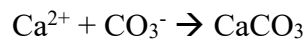
Ocean pH has declined because it acts like a carbon sink and absorbs 30% of emitted carbon dioxide from the atmosphere (Orr, 2011). However, in the last few decades, there have been negative consequences of this absorption because they can no longer buffer carbon dioxide at the rate that humans are emitting it into the atmosphere (Andersson et al., 2013). Although the scientific term to explain this process is called ‘ocean acidification’, it does not imply that the pH of the oceans will become acidic, only that the pH is decreasing. The phenomenon causing this decrease in ocean pH results from the absorbed atmospheric carbon dioxide (CO₂) reacting with water (H₂O) in the ocean to form carbonic acid (H₂CO₃). This acid complex and excess hydrogen ions produced in the chemical reaction act to decrease the pH of the ocean. The chemical reaction is shown below (Gattuso and Hansson, 2011):



The Intergovernmental Panel on Climate Change (IPCC) synthesis report from 2014 predicts a drop of 0.2-0.3 in pH units by the year 2100 if we continue with our current energy source habits and our current disproportionate mitigation efforts. This may not seem like a large decrease, but

the pH scale is logarithmic, so a decrease of 0.3 pH units is approximately a 100% decrease in ocean pH, which is significant for the species living in this environment.

The above chemical reaction also changes the most prevalent species of carbon from carbonate (CO_3^{2-}), a key component in calcium carbonate (CaCO_3), to bicarbonate (HCO_3^-). The hydrogen ions (H^+) from the chemical reaction above are more attracted to the carbonate species than the calcium ions (Ca^{2+}) are, so they bind to the available carbonate ions creating bicarbonate. Carbon in this bicarbonate form is less usable to many marine calcifying organisms, affecting the calcification abilities of some organisms (Andersson et al., 2013). The excess hydrogen ions that are not bound to carbonate also act to dissolve already established CaCO_3 precipitates, such as the skeletons and shells of marine invertebrates. Ocean acidification has the potential to influence the calcification and dissolution rates of marine calcifying organisms. There are three types of CaCO_3 mineral precipitates that could be damaged under ocean acidification conditions: aragonite, magnesium calcite (Mg-calcite) and calcite. The CaCO_3 calcification reaction is the following (Gattuso and Hansson, 2011):



The dissolution (reverse reaction) of CaCO_3 is often favored by ocean acidification and most notably affects marine invertebrate calcifiers. Carbonate dissolution occurs for the more metastable carbonate phases first, such as high-Mg Mg-calcites (Andersson et al., 2013), which echinoderms use to build their carbonate skeleton. The Mg-calcite mineral structure is similar to calcite, but calcium ions have been randomly replaced by magnesium ions. The available concentrations and ratio of calcium to magnesium (Ca:Mg) necessary for skeleton formation could also be impacted as a function of the changing seawater chemistry due to ocean acidification and changes in salinity (Andersson et al., 2011).

The changing climate also has an impact on the rate of water precipitation. In the near future, the wet geographical areas are projected to get wetter while the dry areas are predicted to get even drier. There has already been an observed increase in the frequency and intensity of storms and floods in the past few decades leading to a higher number of freshwater sources entering the ocean in the form of runoff. This can have an impact on the salinity levels of coastal areas (IPPC AR5, 2014). Freshwater runoff can also carry higher concentrations of CO₂ leading to a potential synergistic effect of lower salinity and further lowering ocean pH (National Research Council, 2010). Decreasing the salinity of the oceans dilutes all of the available ions in seawater, such as calcium and magnesium. This decrease in salinity may make ion transport more difficult and result in an organismal reduction of solutes and consequently the osmotic uptake of water in osmoconforming species (Le François et al., 2015).

Organismal susceptibility

Coastal areas are usually subjected to more extreme levels of temperature, pH and salinity due to their proximity to the shore. However, even though coastal organisms are accustomed to highly variable environments, they have been shown to respond to forecasted changes in lower pH with impaired performance, such as in growth, calcification, and survival (Barry et al., 2011). The effects of ocean acidification are expected to impact the organisms living in the surface ocean first. Nevertheless, CO₂ has already managed to penetrate down to 1,000 m globally, causing a shoaling of the carbonate saturation horizons for all three CaCO₃ mineral phases (Andersson et al., 2011). This means that the saturation state (Ω) is becoming undersaturated ($\Omega < 1$) at shallower depths (Zeebe and Ridgwell, 2011) and organisms could experience increased difficulty calcifying at larger ranges of the water column. Benthic organisms in coastal systems are also likely to be more vulnerable to ocean acidification sooner

because coastal waters tend to contain more elements that can be corrosive to types of CaCO_3 (Barry et al., 2011).

Echinoderms

Echinoderms are prevalent in coastal environments and are known to be susceptible to environmental stressors. One of these echinoderms, that could express negative consequences to changes in their environment, is the brittlestar. These negative impacts from climate change manifest in the brittlestar nervous system and can be deduced by studying the brittlestars natural defensive abilities. The brittlestar nervous system is comprised of radial nerve cords that run inside the length of each arm and connect to form a nerve ring (Kano et al., 2017). The decentralized brittlestar nervous system assigns distinct roles using neurotransmitter signals to each of the muscle networks in their arms. This process coordinates the arm movement of each arm during locomotion (Kano et al., 2017). The overarching role of the nervous system could be disturbed by changes in water chemistry such as low pH and low salinity, but it is not clear which specific mechanisms will be affected.

Brittlestars have a few methods of survival and predator avoidance that this study examines, such as the neuro-coordination of arms to flip over, and bioluminescence. The brittlestar relies on its decentralized nervous system to coordinate the muscles in the arms to flip right side up after it has been flipped over. This flipping behavior is mostly used to escape from predation in the water column by curling into a ball first so that the brittlestar can sink out of reach from the predator. The behavior can also be used to recover from a near-predation experience on the benthos (Emson and Wilkie, 1982). The nervously controlled process of bioluminescence occurs through a biochemical reaction within light cells located on the lateral sides of the brittlestar arm, and the intense flashes of light propagating up and down the arm are

also usually associated with predator defense function (Herring, 1995; Deheyn et al., 1999, 2000c).

Another important metric of animal health is growth, which in brittlestars involves both calcification and regeneration and reflects the capacity to survive sublethal predation experiences, where a predator consumes part of the organism, such as an arm, and the interaction does not result in prey mortality (Lawrence and Vasquez, 1996). This regeneration ability is crucial to locomotion and feeding abilities, which help the brittlestar survive. Brittlestars arms are made up of a series of ossicles composed of Mg-calcite. Ossicles are mineral composites that, when linked by tendons, muscles and tissue, form the endoskeleton and give it the necessary rigidity for body support and locomotion. There are four separate outer rows of ossicles in each arm, two lateral rows, one aboral (dorsal) row, and one aboral (ventral) row (Märkel and Röser, 1985; Wilt et al., 2003). These outer ossicles are held together via a central “vertebrae ossicle” and also have protruding lateral spines (Deheyn et al., 2015). Re-forming these ossicles are the essential component to the arm regeneration process.

The brittlestar in this study also experiences extreme environments because its habitat ranges from intertidal zones to approximately 1,330 meters deep. Furthermore, it is a cosmopolitan species, so it can be found all over the world. (Deheyn et al., 2000b; Dupont et al., 2001). And, similar to many coastal invertebrates, changes in pH and salinity could cause negative effects on the survival mechanisms of the brittlestar by causing stress to the organism.

Experimental parameters

This project studies the effects of both future-projected decreased pH and decreased salinity levels both independently and combined on a species of luminous intertidal brittlestar, the dwarf brittlestar *Amphipholis squamata*. These particular invertebrates were chosen as the model organism for this study because they are easy to obtain, and are self-fertilizing brooders.

This means that many individuals can be produced at a single time and the clones are genetically similar to one another (Deheyn et al., 2000b). Thus, any results observed are more likely to be physiologically driven instead of genetically predetermined. It is expected that the brittlestar system will suffer from these changes in water chemistry and consequently the functionality of their innate predator defense abilities will diminish. To address this research topic, and test the predicted hypotheses, experimental manipulations in aquaria were performed, where brittlestars were exposed to conditions of low salinity, low pH and their combination.

The performances of certain bioreporters (flipping times, regeneration, bioluminescence ability) were measured over time during pulse exposure treatments, but also after exposure (for flipping times and bioluminescence ability only) when the treatments were reversed back to ambient seawater control conditions (to assess possible “recovery”). Testing these specific parameters helped to gain an understanding of how the brittlestars survival rate may be affected by changing environmental conditions as a consequence of climate change. Nervously controlled parameters of behavior and physiology (flipping response and arm regeneration) were studied to determine the overall health of *A. squamata* and deduce how it behaves under stress due to altered carbonate chemistry conditions (Lawrence and Cowell, 1996) of reduced pH and reduced salinity. The natural bioluminescence ability of *A. squamata* was used to determine if the nervously controlled process of light production would behave similarly or differently from the other parameters of flipping response and arm regeneration in response to the experimental treatments.

Brittlestar *flipping response behavior* is innate to predator escape and defense. This behavior has the ability to indicate the health or stress levels of the individual in the sea star *Stichaster striatus* (Lawrence and Cowell, 1996) and could apply to *A. squamata* as well.

Brittlestar flipping coordination could become slower in conditions of low salinity and low pH

exposure (independently and combined) because the treatments could alter the message for arm movement from nervous system. One of the ways that brittlestars transmit messages from the nervous system to the arms to activate movement is through ATP or Ca^{2+} channels to induce active movements (Fieber, 2017). If the concentration of Ca^{2+} is decreased by lower salinity conditions, the brittlestar may have a harder time sending messages from the nervous system to the muscles. The lower pH conditions could also impede the nervous control of the brittlestar by causing stress to the organism and making it more difficult to relay signals to the arms in a timely manner (Hu et al., 2014).

The *Arm regeneration ability*, of the brittlestar is vital for organismal survival after experiencing an act of predation. It can take a few weeks for the arm to grow back to functional conditions. During this time, feeding may be impaired because brittlestars use their arms for suspension feeding (Sides, 1987). Also, while the arm is regenerating, growth and reproduction functions are slowed or halted to allocate more energy to the regrowth of a new arm. The nervous system is also imperative for controlling this regrowth process in echinoderms, because it is one of the first things to grow back during the regeneration process (Huet, 1975; Kumar and Brockes, 2012).

The regeneration process may be slowed in lower pH and lower salinity conditions (independently and combined). Hypoosmotic conditions (lower salinity) tend to decrease the rate of metabolic performance in the decapod crab, *Carcinus aestuarii* (Rivera-Ingraham and Lignot, 2017). Metabolic depression in lower salinity conditions could limit the energetic resources available for growth and survival, including regeneration processes in other invertebrates, such as brittlestars as well. Studies have also shown that exposure to low pH conditions reduces the metabolic rate of organisms (Dupont, 2010), further increasing the difficulty to regenerate under conditions of environmental stress. Additionally, when exposed to low salinity conditions,

reduced presence of the necessary calcification elements, magnesium and calcium, may also add to the difficulty in properly forming the ossicle structures (Deheyn et al., 2015). This is exacerbated by low pH conditions, reducing the carbonate ions necessary for calcification (Feely et al., 2004).

Because the flipping response and regeneration process are so tightly associated with the integrative function of the nervous system, it was important to assess more directly the state of the nervous system in specimens of *A. squamata* under the treatment conditions. To achieve that, the brittlestars ability to create light, a process known as *bioluminescence*, was studied as another proxy to test if the nervous system was leaking light in response to the experimental conditions. In the brittlestar, the chemical reaction of light production requires the activation of a light-emitting photoprotein system that involves the binding of calcium as a cofactor (Shimomura, 1986; Haddock et al., 2010). Although the neuronal control of the light production has been well characterized (De Bremaeker et al., 1999) the photoprotein system still remains to be identified and characterized (Shimomura and Shimomura, 1985; Brehm and Morin, 1997). Nevertheless, we know that the light production is tightly associated with the nervous system, with the light producing cells (photocytes) possibly being neutrally derived (Brehm, 1977), and that the light production will therefore depend on the functional integrity of the nervous system, and/or the amount of photoprotein available. The light production is not spontaneously produced by the brittlestar, but only when mechanically stimulated, or when exposed to exogenous (experimental) sources of neuromodulators or calcium (Deheyn et al., 1996; De Bremaeker et al., 1999), which were used here as functional assays.

If brittlestars are exposed to low pH and low salinity treatment conditions, they might have less control over their light production ability. When chemically stimulated, brittlestars may produce less light, leading to a weakened defense mechanism. This could be due either to a

decrease in concentration of the necessary cofactor Ca^{2+} as a consequence of the dilution of seawater ions in lower salinity conditions (Haddock et al., 2010) or due to the stress of low pH interfering with the mechanisms required to produce a light reaction response.

The factors of stress interfering with the brittlestars ability to perform their normal mechanisms of flipping and regeneration, but also bioluminescence, could mainly be attributed to the production of reactive oxygen species (ROS). Under normal circumstances, ROS are useful as second messengers for the expression of multiple transcription factors and signal transduction molecules (Lesser, 2006). However, excess ROS can occur with a change in seawater chemistry (increase in CO_2) and salinity. The production of ROS has shown to be detrimental to key cellular components such as proteins that could play an essential role in maintaining organismal homeostasis. A common organismal response to oxidative stress caused by the production of excess ROS is metabolic depression (Rivera-Ingraham and Lignot, 2017), which severely decreases the energy reserves the brittlestars have to maintain the normal function of their survival mechanisms.

To address this research topic, and test the predicted hypotheses, experimental manipulations in aquaria were performed, where the brittlestars were exposed to various conditions of salinity, pH and their combination. The performances of certain bioreporters were measured (flipping times and regeneration abilities, with some bioluminescence testing when pertinent) over time during pulse exposure treatments, but also after exposure (for flipping times and bioluminescence ability only), when the treatments were reversed back to ambient seawater control conditions (to assess possible “recovery”). Testing these specific parameters helped to gain an understanding of how the brittlestars survival rate may be affected by changing environmental conditions as a consequence of climate change.

Materials and methods

The behavioral and physiological/morphological responses of *A. squamata* were studied through testing flipping response, arm regeneration and bioluminescence to determine how they are impacted by low pH, low salinity, and their combination. To quantify the behavioral flipping response, the time of the flipping, behavior of flipping and flipping fatigue rate were tested to measure the rate of increase from the first flip time to the last flip time of each brittlestar. The arm regeneration responses were tested using observational microscopic imaging and quantitative elemental analysis of the skeleton. The light response of the brittlestars was tested by analyzing the difference in their bioluminescent abilities with and without neurochemical stimulation of the light production. Experimental treatment values used in these tests were the following: low pH, low salinity and the combination of low pH and low salinity in accordance with the predicted values in the year 2100 by the IPCC synthesis report of 2014.

There were two separate independent experiments conducted consecutively in time. The first experiment was to test the arm regeneration capabilities of the brittlestars, which lasted for seven weeks, from November 1st to December 20th 2017. The second experiment was intended to measure the flipping response and bioluminescence response to the various treatments and lasted another seven weeks from February 5th to March 25th 2018. The second experiment also had an additional experimental portion where all the brittlestars were placed into the control treatment conditions of ambient seawater for the duration of three weeks, from March 26th to April 15th 2018 to determine if brittlestar recovery in their flipping response and bioluminescence ability from the treatments was possible.

Animals and experimental design

A total of 120 brittlestars were obtained, from the Marine Biology Research Division experimental aquarium at Scripps Institution of Oceanography. All brittlestars were clones of 5

individuals, that were originally collected by Dimitri Deheyn in the late 1990s. Brittlestars were placed in individual cages made from plastic tubes and mesh for the duration of the experiments. 30 brittlestars were assigned to each of four treatments: [1] *low pH* and ambient salinity (pH = 7.77 ± 0.05 , salinity = 33.46 PSU), [2] *low pH and low salinity* combined (pH = 7.80 ± 0.02 , salinity = 25.40 PSU), [3] *low salinity* and ambient pH (pH = 8.13 ± 0.04 , salinity = 25.37 PSU), and [4] the control (pH = 8.06 ± 0.03 , salinity = 33.45 PSU), which was ambient pH and salinity seawater pumped from the Scripps pier. These experimental treatments will herein be referred to as pH⁻, pH⁻S⁻, S⁻, and control respectively. Ocean pH of La Jolla Shores, San Diego, CA, where *A. squamata* is abundant, is around 8.1 (Andersson et al., 2013) and is projected to decrease by 0.06 or 0.07 units (IPPC AR5, 2014). Salinity typically ranges between 33-35 PSU, but is projected to drop 0.1 to 0.2 PSU as well (IPPC AR5, 2014). However, these values are based on open ocean measurements and assumed to be applied to coastal waters as it is more complex and difficult to accurately model and forecast coastal regions.

The experimental aquaria system consisted of three 20 L header tanks feeding flow through water to twelve 2.5 L tanks (three tanks per treatment). The treatment tanks each had ten cages (one brittlestar per cage) fastened to the bottom with suction cup clips (Figure 1). Reduced pH was achieved by bubbling in 100% CO₂ gas and regulated with a solenoid (Fluid Concept GmbH, G1/8 DN2.3, 21JN1ROV23NL LBA, 110V-50Hz/2.5 Watt, Sutensee-Spöck, Germany) that had a ± 0.03 range above and below pH 7.7. The low salinity (S⁻, and pH⁻S⁻) treatments were administered to the brittlestars for 7 hours through exposure/pulse conditions for each day, because that is how long it took before the pH in the treatment tanks started rising due to acclimation to the ambient aquarium pCO₂. During this 7-hour period, water flow to all of the 12 treatment tanks was stopped. The brittlestars were exposed to the pH⁻ treatments for 24 hours

each day, with the exception of the pH⁻S⁻ treatment, whereby the brittlestars were exposed to ambient pH for 24 hours each day.

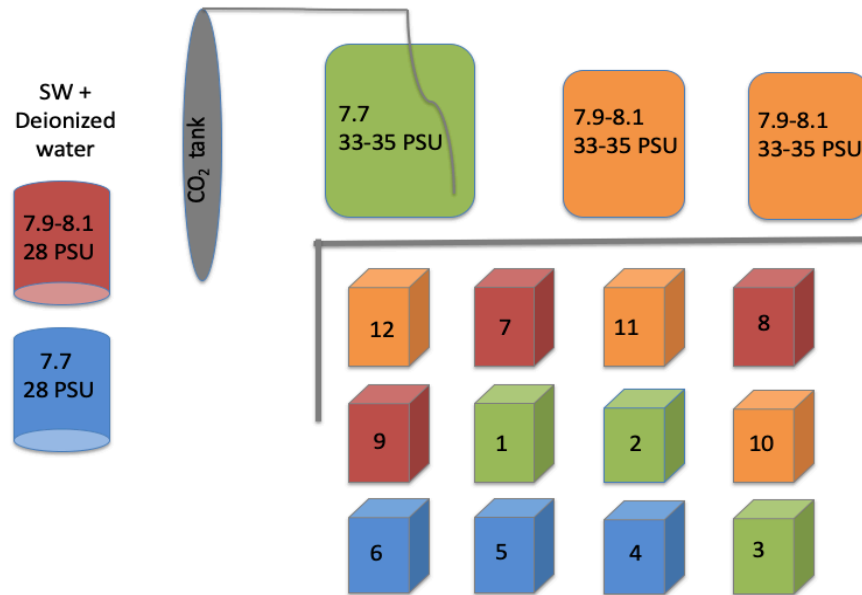


Figure 1. Graphic representation of the experimental setup and four individual treatments: pH⁻ (green), S⁻ (red), pH⁻S⁻ (blue) and the control (orange).

To reduce the salinity, seawater was manually mixed every day in two separate carboys (2.5 gal, Thermo Scientific Nalgene, OH, USA). One carboy held deionized water mixed with seawater from the low pH header tank and the other carboy held deionized water mixed with seawater from the two ambient condition header tanks (refer to Figure 1). The mixtures in the carboys were administered to the individual treatment tanks manually each day for a total of 7-hour exposure time. To keep the administration of the experimental treatments consistent, the treatment water was poured out from each tank until all tanks had the same volume of 6,570 mL before the 7-hour exposure period began. At the end of each 7-hour exposure window, water flow (approximately 25 mL per second) to all of the treatment tanks were turned back on to flush out the low salinity treatments until the next 7-hour exposure period the following day.

Throughout the duration of these experiments daily pH, temperature and salinity data was collected for each of the twelve experimental tanks and the three header tanks. The pH and salinity levels were controlled with the exception of the 7 hours where the brittlestars did not experience water flow. The temperature levels were monitored for water chemistry analysis purposes but allowed to fluctuate naturally throughout the experiments.

Water chemistry analysis

pH from the header tanks were measured with glass electrode probes (IKS ComputerSysteme GmbH, accuracy 0.01 pH, Friedrich-Speidel-Str.36 76307 Karlsbad, Germany) and monitored every two minutes using an IKS Aquastar machine (Karlsbad, Germany) connected to a laptop computer in the experimental aquarium that could be accessed remotely with the software aquastar version 2.19 to download the data every three days. The pH probes in the header tanks were calibrated every other day using standard calibration buffers (IKS Aquaristic Products, Karlsbad, Germany). In addition, the pH and temperature data were logged for each header tank and for all 12 treatment tanks twice per day using a handheld pH probe (HQ40d, probe PHC201, accuracy 0.01 pH, 0.1 temperature, Hach, Loveland, CO, USA). The handheld portable pH probe was calibrated with the NBS buffer solutions (Fisher Scientific, Fair Lawn, NJ, USA) every two weeks.

Water samples were taken from the low pH, and ambient pH (control) header tanks and two randomly selected treatment tanks with low salinity and ambient salinity combined with low pH at the start of the experiment. The water collections were made following standard operating procedures (Carter et al., 2013) and submitted to the Dickson laboratory at Scripps for analysis of pH and total alkalinity at 25°C (Table 1).

Water chemistry values, such as the carbonate saturation state, and the concentrations of carbonate, bicarbonate and $p\text{CO}_2$ (with the exception of temperature) were calculated using

CO2Sys 2.3. For the calculations, parameters from the Dickson laboratory were used based on salinity, total alkalinity (TA) and pH measured with the total seawater scale. The dissociation constants of K_1 , and K_2 from Mehrbach et al. (1973) refit by Dickson and Millero (1987), the HSO_4 constant from Dickson (1990), the HF constant from Dickson and Riley (1979), and The $[\text{B}]_T$ value was used from Uppstrom (1974) were used in the calculations. The total seawater pH scale was also used for all of the carbonate chemistry calculations (Table 1). The analyzed water samples were used to calculate the average difference between the Dickson lab measurements and the Hach pH probe readings. This was then applied to the daily pH measurements taken with the Hach probe as corrected values and averaged for each treatment between the three experimental replicate tanks.

Table 1. Temperature and water carbonate chemistry parameters used throughout the experiments. The values with an asterisk refer to the measured parameters from the Dickson lab. The measured value of temperature and calculated value of pH using CO2sys and the Dickson lab measurements have a sample size of $n=147$. The other carbonate chemistry parameters are from the Dickson laboratory and have a sample size of $n=1$.

Variable	Treatments			
	pH [*]	pH·S ⁻	S ⁻	Control
pCO₂ (μatm)	990.13	739.56	324.85	464.84
pH_{sws} [*]	7.77±0.05	7.80±0.02	8.13±0.04	8.06±0.03
Temperature (°C)	14.56±0.78	14.25±0.82	14.28±0.97	33.45±0.00
Salinity	33.46	25.40	25.37	33.45
TA [*] ($\mu\text{mol/kgSW}$)	2222.60	1685.90	1683.80	2222.10
HCO₃ ($\mu\text{mol/kgSW}$)	2035.60	1559.02	1438.27	1881.81
CO₃ ($\mu\text{mol/kgSW}$)	75.52	50.29	97.37	137.44
Ω Ca	1.82	1.28	2.47	3.31

Chemical solutions

The composition of the solutions made and used for the flipping response, arm regeneration and bioluminescence tests are detailed in Table 2.

Table 2. Chemicals used throughout the brittlestar flipping, bioluminescence, and arm regeneration experiments as well as their chemical composition and reason for use in the experiments.

Name of Solution	Chemical Composition	Purpose
3.5% Magnesium Chloride (MgCl₂)	3.5 g of MgCl ₂ in 100 mL of ASW	To anesthetize the brittlestars
500 mL Artificial Seawater (ASW)	11.69 g of NaCl, 0.3575 g of KCl, 5.315 g of magnesium chloride hexahydrate, 0.7275 g of calcium chloride dehydrate, 1.967 g of sodium sulfate and 1.211 g of Tris buffer base in 450 mL of MilliQ water with HCl added to lower the pH; pH=8.1	Replacement for seawater when making chemical solutions
2 mM Acetylcholine chloride (Ach)	0.00363 g of Ach (M.W.=) in 10 mL of ASW	To neurostimulate the isolated brittlestar arms during the bioluminescence experiment
400 mM Potassium chloride (KCl)	2.98205 g of KCl (M.W.=) in 100 mL of ASW	To depolarize the light cells in the isolated brittlestar arms during the bioluminescence experiment
Skin arm fixative	2.5% Glutaraldehyde, 2.0% Paraformaldehyde and 0.1 M Cacodylic buffer in 100 mL of MilliQ water; pH=7.4	A storage solution for the isolated regenerated arms used in the skin analysis
0.1 M Cacodylic buffer	50 mL of 0.2 M cacodylic buffer in 50 mL of MilliQ water, 2.876 g of NaCl; osmolarity= 1214 mmol/kg; pH=7.4	Used in the process of replacing the fixative that the arms were stored in with 100% ethanol
37% ethanol	19.47 mL of 95% ethanol with 30.53 mL of 0.1 M cacodylic buffer	Used in the process of replacing the fixative that the arms were stored in with 100% ethanol
67% ethanol	35.26 mL of 95% ethanol with 14.74 mL of 0.1 M cacodylic buffer	Used in the process of replacing the fixative that the arms were stored in with 100% ethanol
95% ethanol	Pre-made from 200% ethanol mixture	Used in the process of replacing the fixative that the arms were stored in with 100% ethanol
0.75% Protease from <i>Streptomyces griseus</i> (pronase)	0.0075 g of pronase in 1 mL of ASW	Used to dissolve the skin on the brittlestar arms to make the skeleton visible

Flipping response analysis

For the flipping response tests, 6 brittlestars were placed in each of 3 tanks per treatment for a total of 72 brittlestars. Each day 6 brittlestars from a single tank from each treatment were flipped until all 72 were flipped. A total of 18 brittlestar specimens (n =18) were flipped for each

experimental treatment both when the treatments were present (7 weeks) and absent (3 weeks) for a total of 72 brittlestars flipped each week. Brittlestars were flipped once every week for the 10-week duration of the experiment. The brittlestars were exposed to the treatments for the first seven weeks and then placed into ambient seawater conditions (control conditions) for the last three weeks of the experiment.

For the flipping process, the brittlestars were put into 20 mL of seawater and flipped consecutively inside a 60 mm wide and 10 mm tall petri dish. The brittlestars that experienced (pH^- , S^- , or $\text{pH}\cdot\text{S}^-$) were flipped in the water of their respective treatment, while the brittlestars in the control treatments were flipped in ambient seawater. The protocol for flipping the brittlestars upside down was to use small angled tweezers to scoop underneath their arms; it was usually best to catch the underneath of their arms closest to the disk and carefully turn them over so that their oral side was facing upwards. Once they were upside down and their disk was resting on the bottom of the petri dish, the timer was started. The timer was not stopped until the brittlestar had flipped itself over and the disk was lying flat against the petri dish with its oral side down once again (Lawrence and Cowell, 1996). The one other case in which the timer was stopped was if the timer had reached and or exceeded two minutes (120 s) and the brittlestar had either not flipped because it was lying flat upside down or still curled into a ball. Once the brittlestar had either completed a successful flip or once 120 s had passed, the brittlestar was then immediately flipped over again and the timer was restarted. This procedure continued for each of the ten flipping trials. The righting responses of 6 brittlestars were measured at one time and captured on video with an iPhone 6S camera attached to a 2-foot-long ring stand. Only the first ten flips were used in the analysis although, some individuals were flipped more than ten times.

The rate at which the brittlestars flipped from trial 1 to trial 10 is known as the flipping fatigue and was analyzed along with the flipping time and behavior of each flip. The absence

and/or presence of behaviors such as flipping, curling into a ball and then flipping, staying in a ball for over 120 s, and not flipping for over 120 s were observed and recorded for each brittlestar. The normal flipping response progression of the brittlestar is demonstrated in Figure 2.

Upside down

Upright



Figure 2. Progression of the brittlestars natural flipping response. Photo credit goes to Roan Wooley (Deheyn Lab intern, High Tech High).

Arm regeneration analysis

This subsequent experiment, followed the same protocols as described in the flipping response experiment. The water quality measurements for this subsequent experiment are also represented in Table 1. The arms of the brittlestar were induced to regenerate on Day 0 by severing 1/3 of their total arm length from the tip of the arm. It was assumed that the regeneration process was equal among all individuals. To measure regeneration, the regenerated arms were collected at six different times (from 10 individual brittlestars per collection day) within the first two weeks of the experiment: on days 0, 2, 4, 7, 10, and 14 and then once a week until day 49, the last day of the experiment. Analyses were only performed on the days where the brittlestar arms demonstrated the most change (i.e. days 0, 2, 7, 28 and 49). On the 21st day of the experiment, no collection was made because the arms were beginning to slow in growth and not much changed in their appearance from day 14 to day 21.

Brittlestars were anesthetized (in $MgCl_2$) for five minutes before their disk diameter and arm length were measured using millimetric paper (each square represented 2 mm) under a Wild

Heerburgg dissecting microscope. During this measuring process, the brittlestars were placed in a few milliliters of their treatment water. Two out of the five arms were cut for each brittlestar using this method. Images were taken (Nikon SMZ 1500 stereoscope at 50x magnification) to document the progression of regeneration and collected over time to better visualize the regeneration process at a closer scale.

For each collection day, the regenerated arm was re-measured and the two longest arms from the brittlestar body closest to the base of the arm (right next to the oral disk) were isolated before storing the arms. One arm went into the fixative and was stored in a 4°C refrigerator and the other arm was stored with no solution in a -80°C freezer to later be digested and used for skeleton (ossicles) analysis (Deheyn et al., 2000a). The arms that were collected and stored in fixative were analyzed with a scanning electron microscopy (SEM) equipped with an energy dispersive spectroscopy (EDS) function.

Preparation of the samples for SEM

To properly dehydrate the brittlestar arms, the osmolarity of the ethanol solutions had to match the osmolarity of the fixative that the brittlestar arms were stored in. This was an important step so that the arm would not experience a change in osmolarity during the ethanol replacement (otherwise possibly affecting the integrity of the soft tissue), which was carefully followed using a Wescor 5500 Vapor Pressure Osmometer. Arms were dehydrated with increased rinses of a series of ethanol concentrations in 0.1 M cacodylic buffer (37%, 67%, 95%, and 100%) using techniques adapted from previously established protocols for SEM sample preparation (Murtey and Ramasamy, 2016). SEM carbon conductive 12 mm double-sided sticky spectro tabs were used to mount the arms to specialized SEM metal stubs for analysis. 20 µL of 70% ethanol was put on the carbon tape to facilitate positioning. The arms were oriented with their dorsal side up and podia down.

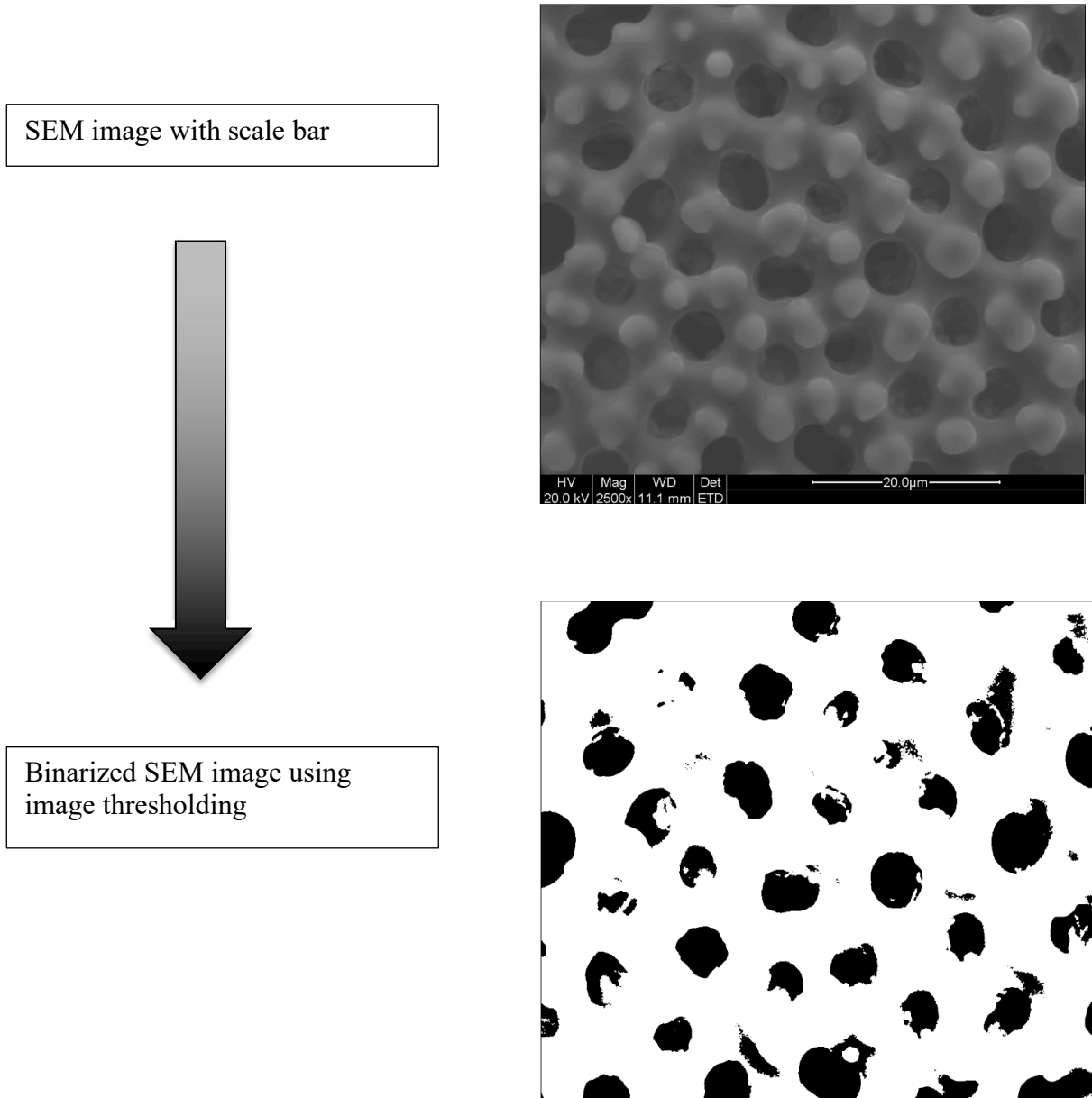
The arms intended for ossicle analysis underwent additional preparation; the tissue of the arm was digested with 0.75% of Protease from *Streptomyces griseus* (pronase Type XIV P5147-1G; lot #: SLBS6732; Sigma Aldrich) to digest the soft tissue and expose the ossicle skeleton structure. The pronase was made new each day to prevent degradation. Then, 20 μ L of pronase was pipetted onto the arm where it remained for 35 minutes. Afterwards, the remaining pronase was absorbed using a KimWipe and 20 μ L of new pronase was added to the arm for another 35 minutes. This process continued until each mounted brittlestar arm went through 8-10 rotations of pronase additions depending on the state of digestion for each arm. The process was repeated until all the tissue was dissolved and the ossicles could be clearly seen (under a stereoscope), but ended before the center vertebrae ossicle was visible. After the 5th pronase addition, a new batch of 0.75% pronase was made and used for the remaining digestion periods. Prepared arms were positioned on SEM stubs in a similar method as those used for tissue analysis.

The SEM and EDS analysis process as well as sample carbon coating was performed by Michael Allen (Deheyn Lab, Staff Researcher) following a known protocol (Deheyn et al., 2015). Digested arms were examined at 2,500x magnification to perform EDS analysis on four separate points on the trabeculae (bumps) of the dorsal ossicle shield of the third ossicle from the site of initial amputation. A whole view of both the non-digested arm under the SEM at 30x and 40x magnification were also imaged.

From these images, measurements were made of the length and width of the regenerated and non-regenerated portions of the brittlestar arm and the percent porosity of the non-regenerated and regenerated ossicle structures. The sample size was $n = 4$ for each treatment per day and there were five different days analyzed over time. The EDS analysis was measured for each of the treatments on day 0, 2, 7, 28 and the last day of the experiment, day 49. The SEM images of the brittlestar arm ossicles were first binarized to black (0 pixels) and white (255

pixels) using the program Fiji for Mac OS X. After which, the mean gray intensity of the image and the mean percent porosity of each arm ossicle imaged could be measured (see Figure 3).

Figure 3. Flow chart of methods for the ossicle porosity analysis of both the non-regenerated and regenerated ossicles imaged with SEM during the arm regeneration experimental tests. These measurements were made using the program Fiji for Mac OS X. Each image was measured three separate times to obtain mean gray intensity and a mean percent porosity (n=3).



Bioluminescence analysis

Light production in the brittlestar *A. squamata* is not naturally spontaneous, but rather triggered by mechanical stimulus and experimentally by neuro-induction. Only the arms produce light (Figure 4), and the light producing cells, photocytes, are intimately controlled by the nervous system. Hence, using neuro-mediators experimentally can help assess the neuro-control of the light producing cells (Deheyn et al., 2015).

A total of 102 arms were analyzed for bioluminescence while brittlestars were exposed to treatment conditions and a total of 45 arms were analyzed following removal from treatment conditions during the same time as the flipping response experiment. The arms that were analyzed came from 48 brittlestars that were designated for use for the bioluminescence measurements (the other 72 brittlestars exposed to treatment conditions were used to measure the flipping response).

Luminometer protocol

The luminometer was used, primed, and cleaned before each use following standard lab protocols. A solution of 2 mM Acetylcholine chloride (ACh) solution was made new each time due to its degenerative properties. The ACh solution was injected volume to volume (v:v) into the tube inside the luminometer with the arm in ASW, bringing the final ACh concentration to 1 mM. A 400 mM solution of Potassium chloride (KCl) was also prepared and v:v injected into the tube inside the luminometer with the arm, bringing its final concentration to 200 mM. ASW was used to make the chemical solutions in lieu of normal seawater to avoid contamination of the solutions with unwanted microbes or algae that are often found in seawater. All chemical solutions were kept in the refrigerator at 4°C to preserve the integrity of the solutions when not in use.

After making the necessary solutions above, brittlestars were anesthetized with 3.5% MgCl_2 and examined in seawater from their treatment. Measurements were made of the length of two of their longest arms using a millimetric scale under a dissecting microscope. The arms of the brittlestar were manually straightened using forceps until the arm length could be accurately measured.

Luminescence was measured with a luminometer where it ran for three minutes total at a 0.2 s acquisition rate. The first minute was to measure background light [machine noise and/or any spontaneous (stress-related) light leaking from the brittlestar arm]. The second minute was to measure the light production of the brittlestar arm when it was stimulated by 1 mM of ACh. The last minute was to measure the light production of the brittlestar arm when it was stimulated by 200 mM KCl, which depolarized the arm and triggered the maximal possible chemical reaction (positive control). The measured light production units are known as Relative Light Units (RLU) per second. Two arms were isolated from each brittlestar, one arm was analyzed in the luminometer and the other arm was analyzed in the same luminometer but with the addition of a Kodak Wratten gelatin N. D. 2.00 filter to block 99% of the luminescence reading (only 1% of the light was measured to avoid saturation of the detector). The reason for this was that the addition of KCl released all of the available light in the photocytes, most often resulting in a saturated reading of RLU/s. The filter was necessary to observe the total possible light intensity that the brittlestar arms could produce after being exposed to the treatments, and was used to normalize the light response for each treatment. The purpose of the unfiltered luminometer experiment was to capture the full effect of the Ach, which incited a light response from the arm that mimicked the brittlestars natural defense response (Deheyn et al., 2000c). A matlab code written by Dr. Daniel Wangpraseurt (Deheyn Lab postdoctoral researcher) was used to analyze the bioluminescence data obtained from the Sirius Luminometer. The code provided the sum,

peak value, and peak time of each brittlestar arm for the spontaneous light, Ach induced light response and the KCl induced light response parameters.

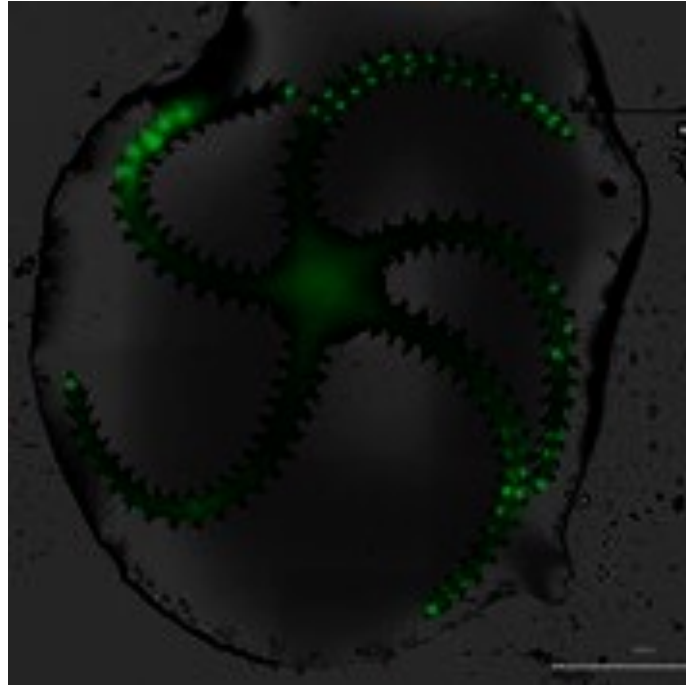


Figure 4. Fluorescence of *A. squamata* after the occurrence of bioluminescence (525 nm). The luminescence occurs at the brightest parts of fluorescence on the sides of the arm of the brittlestar. Despite the center disk displaying fluorescence (light production triggered by blue excitation), it does not produce bioluminescence. Photo credit goes to James Davis (Deheyn Lab demonstration, BioTek Instruments, Inc.).

The bioluminescence raw data were $\log(x+1)$ transformed for homoscedasticity and normality because of small sample sizes ($n = 1$) for each of the light testing parameters (Spontaneous, Ach, and KCl). The raw data were also normalized by dividing the spontaneous and the Ach light response data by the KCl light data, which acted as the positive control for the bioluminescence response. The data were analyzed by comparing the various light response effects against the individual treatments. The raw data bioluminescence values were used as a proxy to best demonstrate the integrity of the nervous system and its ability to control the light

production response of the brittlestars when they were exposed to the different treatment conditions.

The bioluminescence profiles for each of the three light emission responses (non-chemically stimulated and chemically stimulated with ACh and KCl) recorded on day 0, 23, 46, and 67 were taken from one arm analysis. The light profiles were analyzed to provide a clearer depiction of how the light production of the brittlestars exposed to the four different experimental treatments behaved when the treatments were present, and when the treatments were absent (Day 67).

Statistical analysis

Most statistical analyses were performed in JMP Pro 2013. One-way ANOVAs were used to compare brittlestar flipping response (flipping times, flipping behavior, and flipping fatigue), and arm regeneration (length and width, ossicle magnesium and calcium levels, and ossicle porosities) responses between treatments. A chi-squared test was used separately to compare brittlestars that took longer than 120 s to flip between treatments. Post hoc (Tukey HSD) tests were used when ANOVA tests demonstrated significant differences between treatments. Ordinary least squares regression in Excel 2011 was used to examine flipping fatigue and outline a trend increase in flip time from trial 1 to 10. An alpha value of 0.05 was used unless otherwise specified. All data (except bioluminescence data (n=1) were reported as mean \pm s.d. unless otherwise noted.

Results

Flipping time was increased in pH, but decreased in S⁻ and pH⁻S⁻

There was some significance between treatments when the flipping time of the brittlestars was analyzed (ANOVA: $F_{3,3323} = 166.78$, $n = 776$, $p < 0.0001$). Brittlestars displayed greater

mean flipping times (16.69 ± 11.34 s) and flipped slower in the pH^- treatment (ANOVA: $F_{3,3323} = 166.78$, $n = 776$, $p < 0.0001$; Tukey, $n = 830$, $df = 3$, $p < 0.0001$). The mean flipping time for the brittlestars in both the S^- (11.21 ± 7.55 s) and pH^-S^- (8.06 ± 5.18 s) treatments were significantly faster than the flipping times for the control treatment (14.55 ± 9.09 s), (ANOVA: $F_{3,3323} = 166.78$, $n = 776$, $p < 0.0001$; Tukey, $n = 847$, $df = 3$, $p < 0.0001$; Tukey, $n = 874$, $df = 3$, $p < 0.0001$ respectively) (Figure 5).

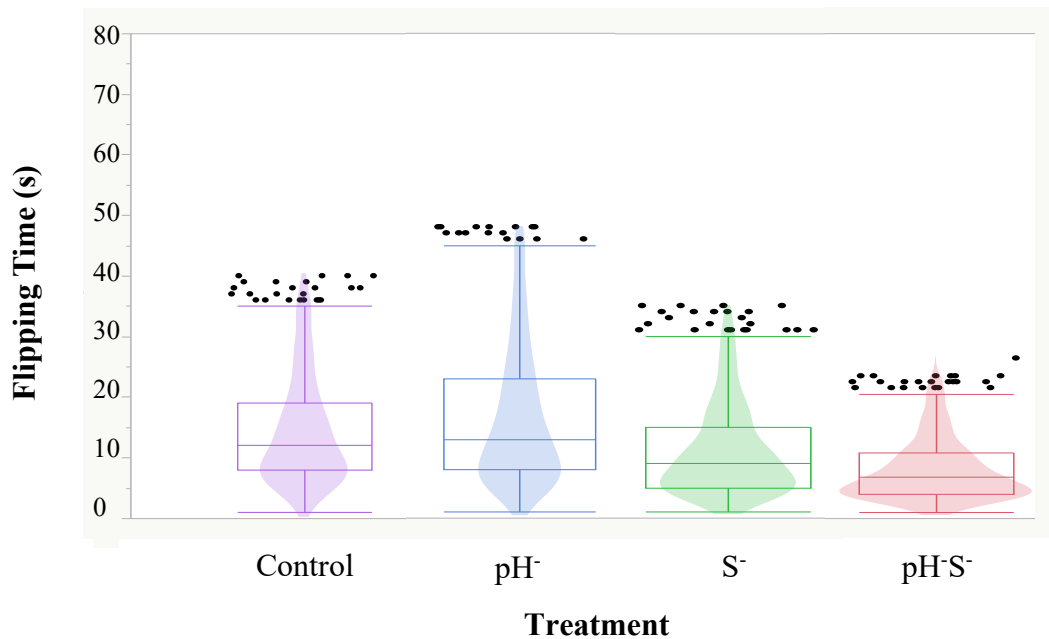


Figure 5. Box plot analysis of average flipping times for the brittlestars exposed to both the altered water chemistry and control conditions showing that the brittlestars in pH^- flipped slower and the brittlestars in the S^- , and pH^-S^- flipped faster than the brittlestars in the control condition.

Despite the pH^- treatment causing significantly slower flipping time responses in the brittlestars exposed to such conditions, when the pH^- treatment was removed and the brittlestars were placed back into ambient seawater conditions, the flipping times (22.07 ± 10.00 s) decreased back down toward levels similar to the control flipping times (26.83 ± 9.03 s), (ANOVA: $F_{3,32} = 9.31$ $n = 9$, $p < 0.0001$; Tukey, $n = 9$, $df = 3$, $p = 0.93$). This further indicates

that the brittlestars in the pH^- treatment were able to recover quickly in ambient seawater conditions despite displaying retarded flipping times when the pH^- treatment was in effect (Figure 6). The brittlestars exposed to the pH^-S^- treatment also expressed a similar mean flipping time (26.59 ± 17.69 s) to the control. The brittlestars in the S^- treatment, following treatment removal, did not demonstrate the same effect. Rather, it was the opposite and mean flipping time (59.06 ± 25.21 s) increased by roughly 50 s following treatment removal.

When the treatments were removed, the brittlestars exposed to S^- mean flipping time was significantly different from brittlestars exposed to the other treatments following treatment removal (ANOVA: $F_{3,32} = 9.31$ $n = 9$, $p < 0.0001$; Tukey, $n = 9$, $df = 3$, $p = 0.0016$). The significance of the data also demonstrates that the brittlestars exposed to the S^- had a more difficulty recovering from the treatment conditions (Figure 6).

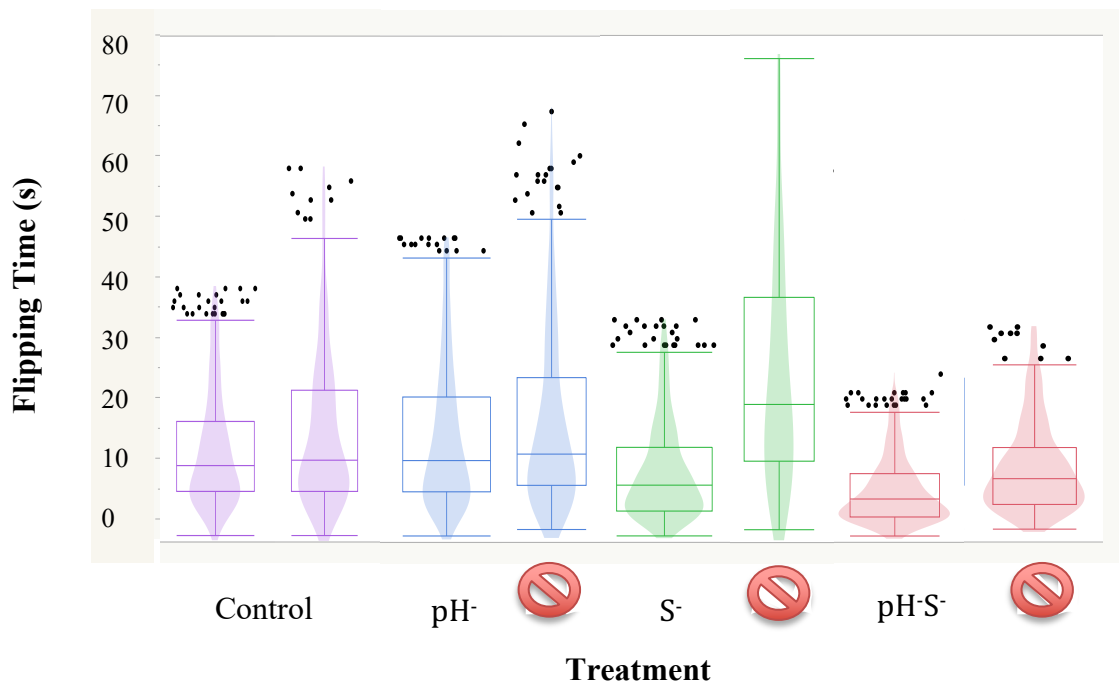


Figure 6. Box plot analysis of average flipping times for the brittlestars showing slower flipping times in the S^- after the treatments have been removed (crossed-circle sign). The left side box plot depicts the average flipping times when the treatments were present (as present in Figure 5) and the box plots to the right of the treatment with the international prohibition symbol represent the results when the treatment was removed.

None of the occurrences in which it took the brittlestar over 120 s to flip are presented in Figure 6. These data were analyzed using a chi-squared analysis to show which treatment incited this particular outcome the most frequently. In the experiment where the brittlestars were exposed to the treatment conditions, the pH⁻ and S⁻ treatments both showed significant differences from both the control treatment and the pH⁻S⁻ treatment in the amount of brittlestars that exceeded the 120 s upper flip limit ($\chi^2(0, N = 112) = 33.64, p < 0.0001$; $\chi^2(0, N = 94) = 26.76, p < 0.0001$ respectively) (Figure 7). However, when the treatments were removed, the chi-square statistical test only showed that the prior S⁻ treatment was still significantly different from the other treatments ($\chi^2(0, N = 123) = 43.04, p < 0.0001$) (Figure 8).

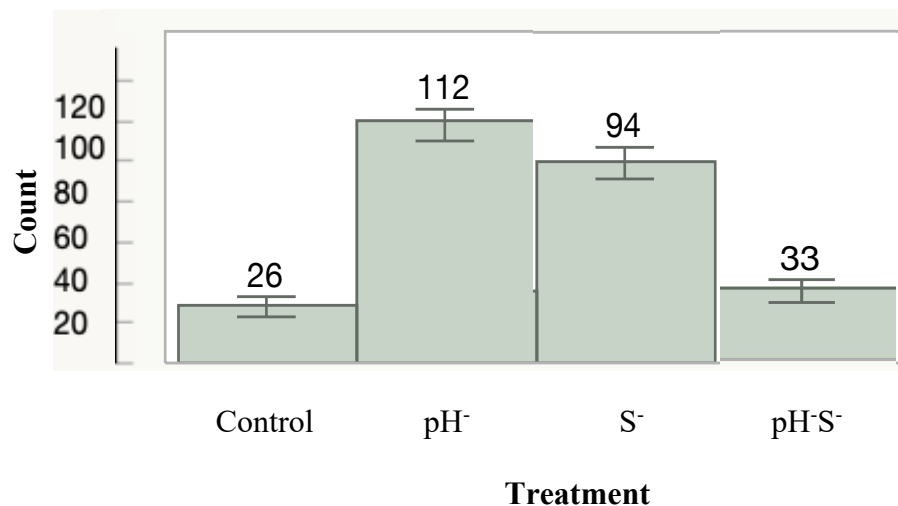


Figure 7. Distribution of brittlestars used in the chi-squared statistical tests with the treatments present. These brittlestars were unable to flip for over 120 s and expressed stressed behaviors during the flipping process of either curling into a ball or lying flat upside down.

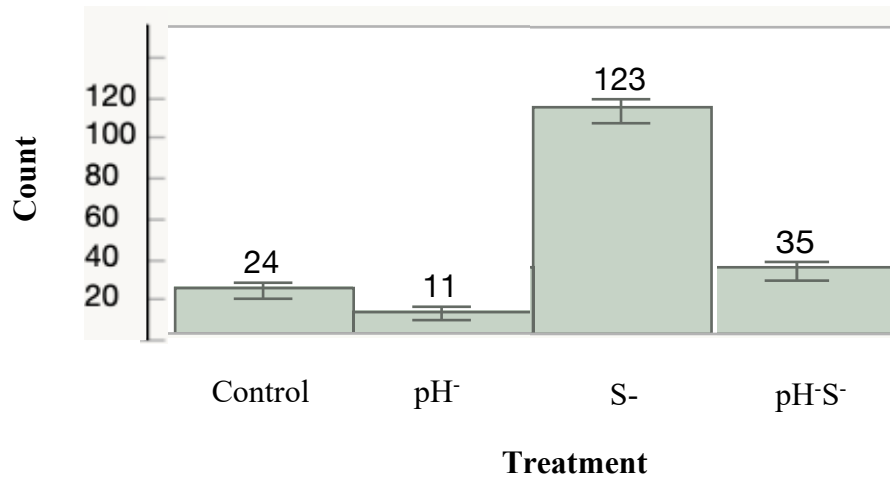


Figure 8. Distribution of brittlestars used in the chi-squared statistical tests once the treatments were removed. These brittlestars were unable to flip for over 120 s and expressed stressed behaviors during the flipping process of either curling into a ball or lying flat upside down.

Stressed flipping behaviors increased in pH⁻, S⁻, and pH⁻S⁻

The brittlestars also experienced treatment variability in their expression of flipping behaviors. The brittlestars displayed the highest proportions of these behaviors in the pH⁻, S⁻ and pH⁻S⁻ treatments, the normal flipping behavior demonstrated no significant difference (ANOVA: $F_{3,80} = 0.79$, $n = 21$, $p = 0.5013$) in frequency between the four experimental treatments (Figure 9).

The four behaviors that were expressed by the brittlestars in each treatment at varying frequencies were flipping normally within 120 s, and the more stressed behaviors such as curling into a ball and flipping within 120 s, and curling into a ball or not flipping for more than 120 s. The brittlestars in the pH⁻ condition expressed the highest frequency of no flipping (ANOVA: $F_{3,32} = 8.44$, $n = 21$, $p < 0.0001$; Tukey, $n = 21$, $df = 3$, $p = 0.001$), and had the same frequency of staying curled in a ball as the control treatment (ANOVA: $F_{3,32} = 4.02$, $n = 21$, $p = 0.01$; Tukey, $n = 21$, $df = 3$, $p = 1.0$). The S⁻ treatment had the highest percentage of brittlestars that curled up into a ball for over 120 s compared to the other treatments (ANOVA: $F_{3,32} = 4.02$, $n = 21$, $p = 0.01$; Tukey, $n = 21$, $df = 3$, $p = 0.2$). The brittlestars in the pH⁻S⁻ treatment expressed the highest

frequency of curling into a ball before flipping (ANOVA: $F_{3,32} = 4.87$ $n = 21$, $p < 0.01$) (Figure 9).

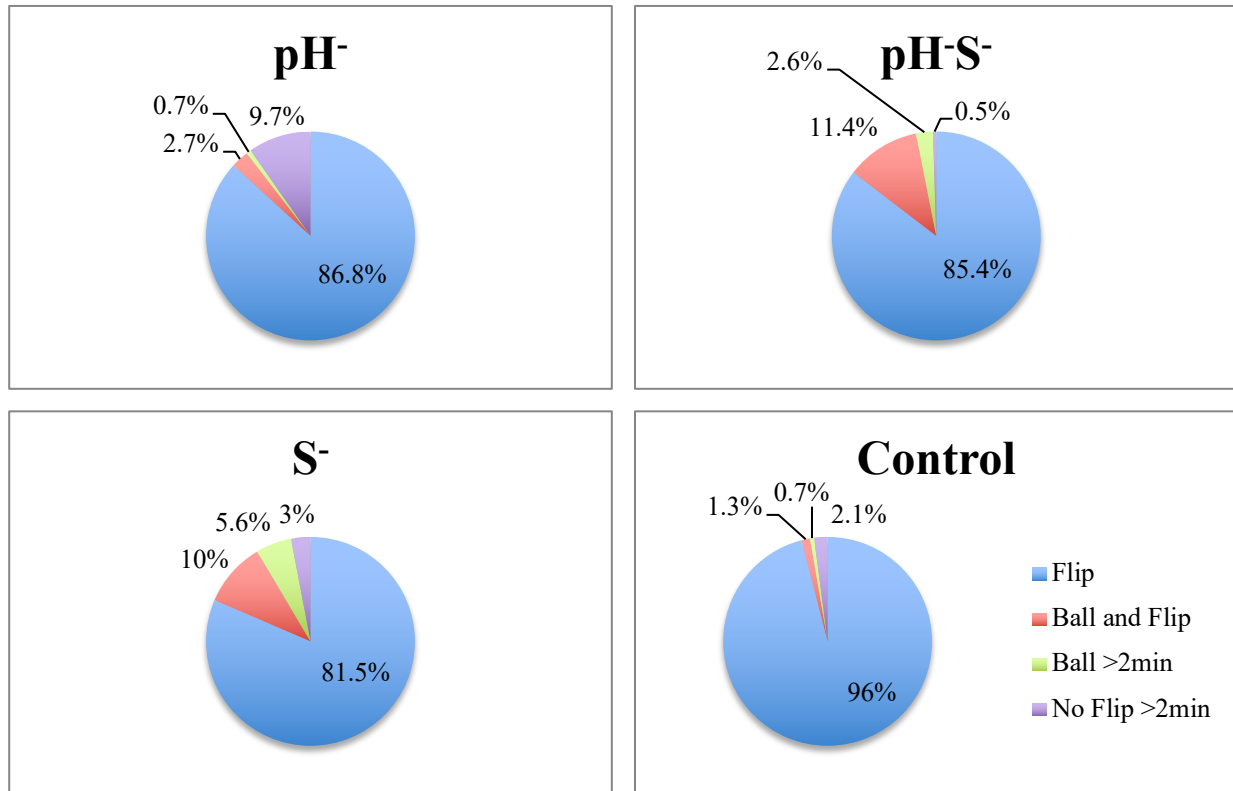


Figure 9. Frequency (in percentages) of occurrence of the four flipping behaviors the brittlestars displayed during the flipping process for each of the four experimental treatments.

When treatments were removed, the brittlestars that were exposed to the pH^- treatment ceased both behaviors of curling into a ball for longer than 120 s and curling into a ball before flipping after the treatment was removed, which significantly reduced their frequency of not flipping for over 120 s and resembled the brittlestars in the control treatment (ANOVA: $F_{3,32} = 9.61$, $n = 21$, $p < 0.0001$; Tukey, $n = 21$, $df = 3$, $p = 0.98$). On the other hand, the frequency of the brittlestars behavior of curling into a ball for longer than 120 s was significantly greater for the brittlestars from the S^- treatment than for any of the other three treatments (ANOVA: $F_{3,32} = 9.61$, $n = 21$, $p < 0.0001$; Tukey, $n = 21$, $df = 3$, $p = 0.0006$), with the exception of the ball and

flip flipping behavior (ANOVA: $F_{3,32} = 2.14$, $n = 21$, $p < 0.11$). They also displayed the largest increase in the frequency of the behavior of remaining curled in a ball for over 120 s (ANOVA: $F_{3,32} = 9.61$, $n = 21$, $p < 0.0001$; Tukey, $n = 21$, $df = 3$, $p = 0.0002$) (Figure 10). The pH-S^- brittlestars demonstrated a decrease in the ball and flip behavior and an increase in the other two stressed behaviors when the treatment was removed. The control treatment also demonstrated an increase in all of the stressed flipping behaviors, however, the increase was marginal compared to the other treatments (Figure 10).

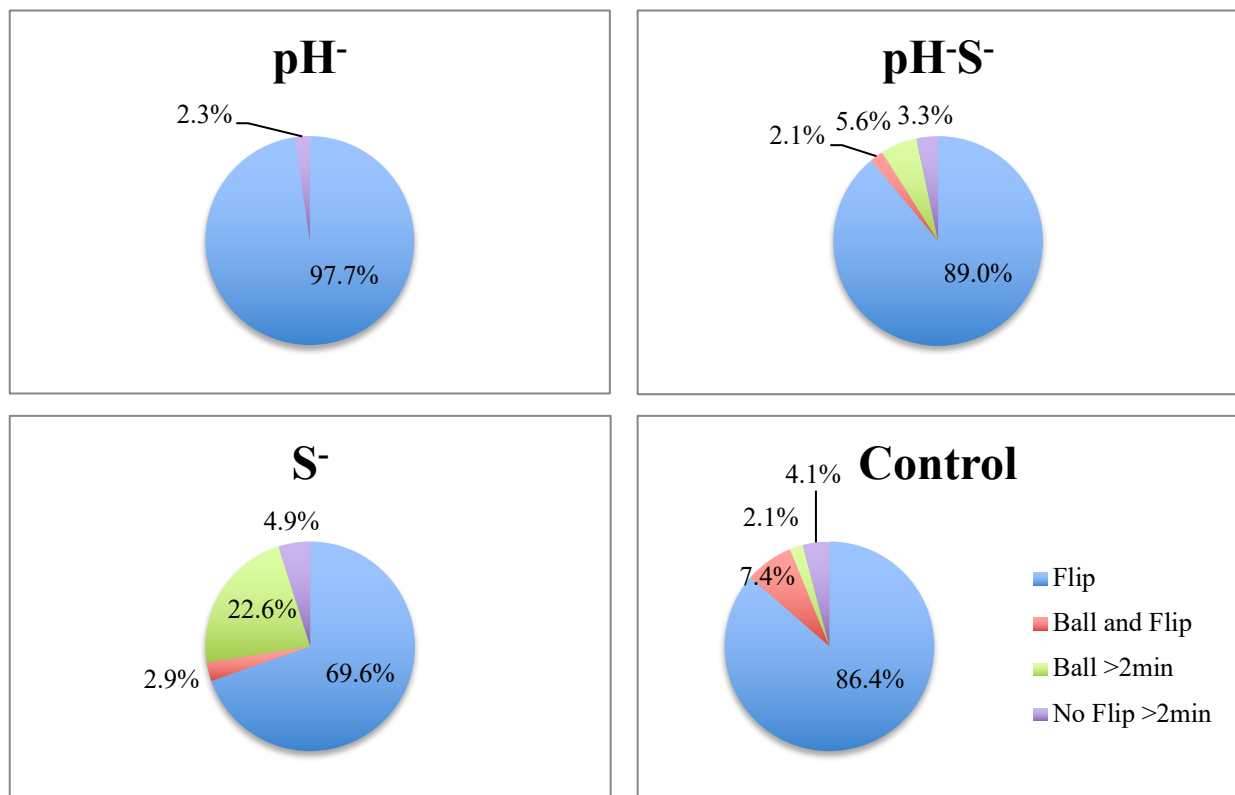


Figure 10. Effect of treatment removed: frequency (in percentages) of occurrence of the four flipping behaviors brittlestars displayed during the flipping process when each treatment was removed for each of the four previous experimental treatments.

Most of the brittlestar stressed behaviors displayed significance between the pH^- and pH-S^- treatments and the control. For instance, the ball for over 120 s behavior had significantly different frequencies between the brittlestars in the pH-S^- and S^- treatments (ANOVA: $F_{3,32} =$

9.61, $n = 21$, $p < 0.0001$; Tukey, $n = 21$, $df = 3$, $p = 0.004$) and the pH^- and S^- treatments (ANOVA: $F_{3,32} = 9.61$, $n = 21$, $p < 0.0001$; Tukey, $n = 21$, $df = 3$, $p = 0.0002$). In the situation where all the treatment conditions were removed (see Figure 10), the frequency of normal flipping behavior only showed significant difference between the prior exposure to the pH^- treatment and the S^- treatment (ANOVA: $F_{3,32} = 3.45$, $n = 21$, $p = 0.03$). There was no significance between the frequencies of any of the four treatments for the ball and flip flipping behavior and the no flipping behavior (ANOVA: $F_{3,32} = 2.14$, $n = 21$, $p = 0.11$, $F_{3,32} = 0.39$, $n = 21$, $p = 0.76$ respectively).

Flipping fatigue increased the most drastically, from trial to trial, in pH^- , and S^-

The brittlestars flipping times expressed a positive linear trend in varying flipping fatigue rates between trial 1 (the first time they were flipped) and trial 10 (the last time they were flipped) for each of the four experimental treatments where the brittlestars flipped slower on the last flip than they did on the first flip. The largest percent increase in flipping fatigue occurred in the brittlestars in the pH^- treatment (171%). The slowing of brittlestar flipping responses from trial 1 to trial 10 continued with the S^- treatment, the control, and the pH^-S^- treatment expressing the second highest (151%), third highest (110%) and least high percent increase (53%) in flip time respectively (Figure 11; Table 3).

For the brittlestars in the control condition, flip trials 1 and 10 were the most significantly distinct from the earlier flip trials 1 and 2 (ANOVA: $F_{9,200} = 5.09$, $n = 21$, $p < 0.0001$; Tukey, $n = 21$, $df = 9$, $p = 0.004$). Flip times for trial 10 were also significantly higher than flip trial 1 for the brittlestars in the pH^- treatment (ANOVA: $F_{9,200} = 5.09$, $n = 21$, $p < 0.0001$; Tukey, $n = 21$, $df = 9$, $p < 0.05$). Brittlestars in the S^- treatment also displayed an increase in flip times from trial 1 to trial 10 (ANOVA: $F_{9,200} = 5.09$, $n = 21$, $p < 0.0001$; Tukey, $n = 21$, $df = 9$, $p < 0.05$). The brittlestars in the pH^-S^- treatment expressed the least significant increase in their flipping times

from trial 1 to trial 10 (ANOVA: $F_{9,200} = 5.09$, $n = 21$, $p < 0.0001$; Tukey, $n = 21$, $df = 9$, $p > 0.05$) (Figure 11), indicating that this treatment had less of an effect on the trial-based flipping fatigue of the brittlestars. This claim is supported by the $\text{pH}\cdot\text{S}^-$ treatment having the lowest R^2 value as well showing that there was less of a linear trend for this treatment (Table 3). Although, all of the brittlestars flipping times experienced a linear increase as shown by the high R^2 values when an ordinary least squares (linear) regression trend was fit to the data of each treatment.

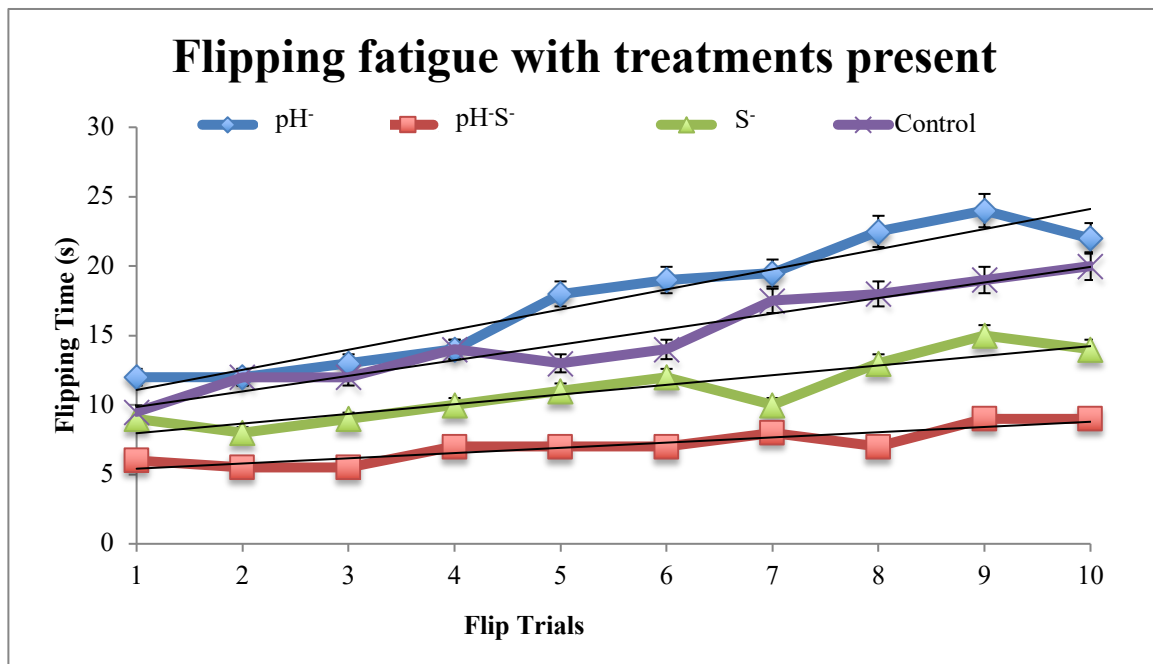


Figure 11. Median flipping times of each flip trial for the brittlestars exposed to the experimental treatments demonstrates flipping fatigue for each treatment, with an increase linear trend from trial 1 to trial 10. Error bars are displayed as percentage error.

Table 3. R^2 value for the trendlines on the flipping fatigue (Figure 11) with mean flipping times for both trials 1 and 10 and the percent increase in flipping time from trial 1 to trial 10 for each of the experimental conditions.

	pH^-	S^-	$\text{pH}\cdot\text{S}^-$	Control
R^2 values	$R^2=0.92613$	$R^2=0.81955$	$R^2=0.80892$	$R^2=0.93942$
Mean values Trial 1; Trial 10 (s)	13.6; 36.9	9.7; 24.3	6.6; 10.1	10.8; 22.7
Percent increase from Trial 1 to 10	171	151	53	110

When the treatments were removed, every treatment condition failed to show any noteworthy significance between flipping times from trial 1 through trial 10 (ANOVA: $F_{9,80} = 1.29$, $n = 21$, $p > 0.05$). However, the flip times still increased from flip trial 1 to 10 in all of the treatment conditions. In the situation where the treatments were removed (see Figure 12), the brittlestars in the S^- treatment expressed the highest percent increase (132%) in flip time from flip trial 1 to flip trial 10 (Table 4). This was followed by increased flipping times from the first flip to the last flip in the brittlestars exposed to the control (100%), pH^-S^- (99%), and pH^- (63%) treatments respectively (Table 4).

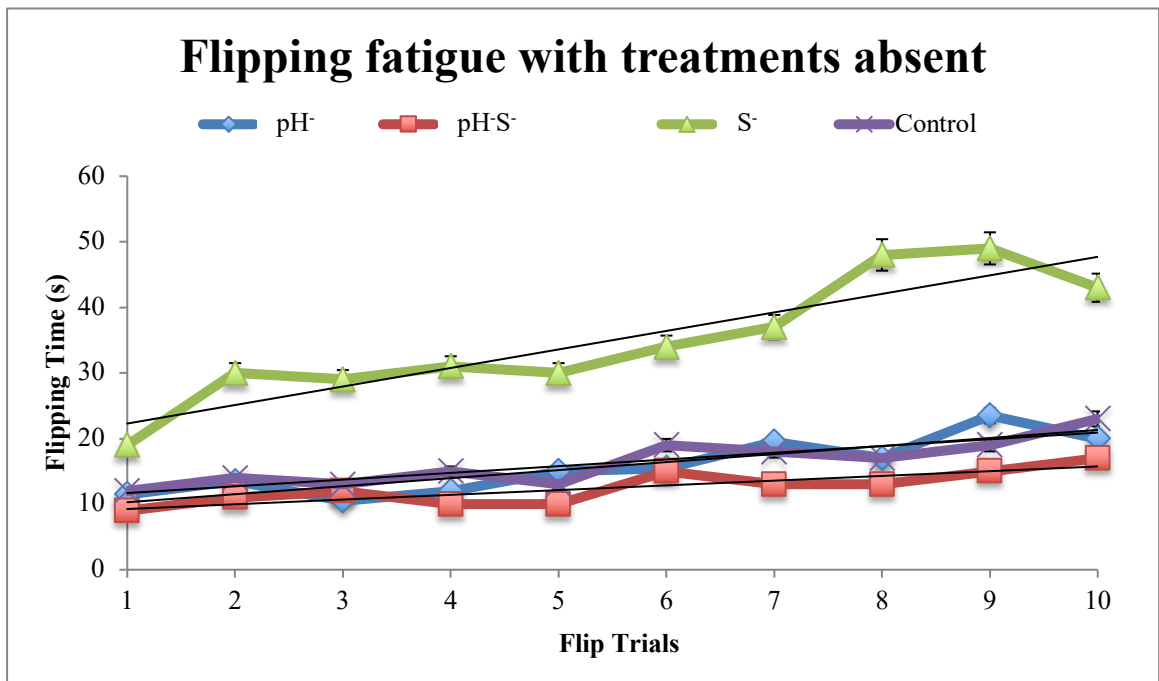


Figure 12. Median flipping times of each flip trial for the brittlestars previously exposed to the experimental treatments demonstrates continuous flipping fatigue with an increase linear trend from trial 1 to trial 10 after the treatments were removed. Error bars are displayed as percentage error. Note: The Y-axis is different compared to Figure 11

Table 4. R² value for the trendlines on the flipping fatigue (Figure 12) are shown along with the mean flipping times for both trials 1 and 10 and the percent increase in flipping time from trial 1 to trial 10 when each of the experimental conditions the brittlestars were exposed to had been removed.

	pH ⁻	S ⁻	pH ⁻ S ⁻	Control
R² values	R ² = 0.77717	R ² = 0.83087	R ² = 0.70929	R ² = 0.78609
Mean values Trial 1; Trial 10	14.8; 24.1	30.4; 70.4	12.9; 25.7	12.7; 25.4
Percent increase from Trial 1 to 10	63	132	99	100

Despite less variability of flipping time between each trial after the treatments, the brittlestar mean flipping times increased when the mean flipping times for trial 10 were compared between when the treatments were removed and when the treatments were present (Table 3 and 4). The exception was the brittlestars that were exposed to the pH⁻ treatment, whereby the mean flipping time decreased by 12.8 s (35%) from trial 10 with pH⁻ present to trial 10 with the treatment removed. The brittlestars that had been exposed to the S⁻ treatment underwent the most intense percent increase in flipping time and the mean flipping time increased by 46.1 s (190%) for trial 10. The control mean flipping time only increased by 2.7 s (12%), and the brittlestars in the pH⁻S⁻ treatment, following treatment removal, increased their mean flipping time by 15.6 s (154%) for trial 10 when comparing last flipping times with the treatments present and absent. Statistical analyses were not made comparing the trial 10 flipping times from when the treatments the brittlestars were exposed to were present and absent. Based on these results, it is clear that the treatments have lasting effects on the brittlestars even after they are placed back into current ambient seawater conditions of pH 7.9 and salinity levels of 33-35 PSU. This effect, following treatment removal, most notably occurs in the brittlestars that were exposed to the S⁻ and pH⁻S⁻ treatments.

Arm regeneration growth was stunted in pH⁻, S⁻, and pH⁻S⁻

Another natural ability of the brittlestar that was affected by exposure to changes in carbonate chemistry was their arm regenerative capabilities. When the brittlestars were put in seawater conditions of pH⁻, S⁻, and pH⁻S⁻ they experienced either stunted or slowed arm growth compared to the brittlestars regenerative arm length and width in the control treatment. The first signs of regeneration appeared for the brittlestars in the control treatment on day 7. For the other treatments measurable regeneration occurred on day 28.

As depicted in Figure 13 below, the arm regeneration capabilities of the brittlestar were severely handicapped when the brittlestars were exposed to alterations in their environment relating to lower pH and lower salinity levels. This stunted growth phenomenon was apparent when the length of regeneration was measured for the brittlestars that were exposed to the treatment conditions with lower pH and/or salinity (Table 5). The exception were the brittlestars exposed to the pH⁻ treatment (ANOVA: $F_{3,5} = 7.58$, $n = 4$, $p = 0.03$; Tukey, $n = 4$, $df = 3$, $p = 0.71$). Some of the brittlestars exposed to this treatment also started to show signs of tissue degradation making it impossible to separate one arm from the next (i.e. N.A. in weeks 6-7). However, the brittlestars exposed to the S⁻ and pH⁻S⁻ treatments did experience retardation in arm regeneration growth (ANOVA: $F_{3,5} = 7.58$, $n = 4$, $p = 0.03$; Tukey, $n = 4$, $df = 3$, $p = 0.04$, Tukey, $n = 4$, $df = 3$, $p = 0.04$ respectively). There was no significance between treatments and control when regenerated width was measured (ANOVA: $F_{3,5} = 0.88$, $n = 4$, $p = 0.51$).

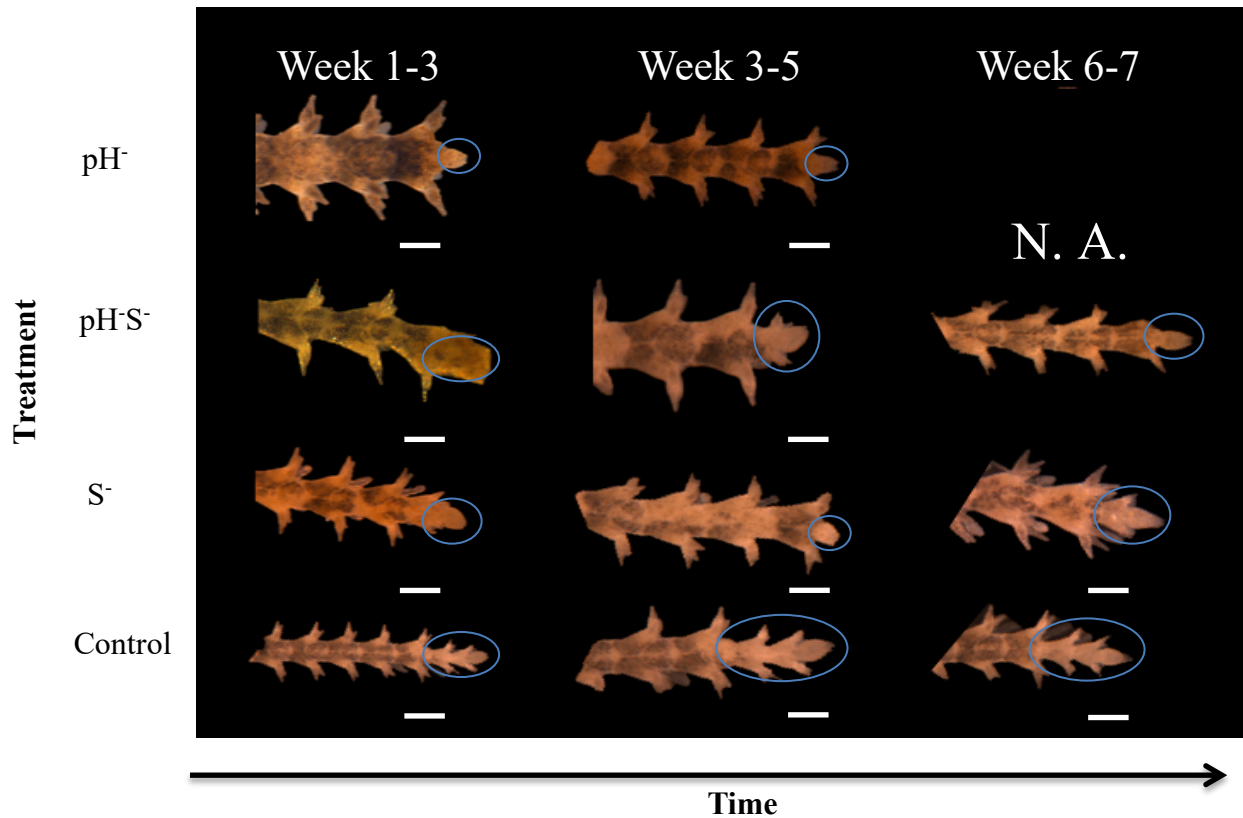


Figure 13. Progression of brittlestar arm regeneration in each of the four experimental treatments over time. The blue circles highlight the area of regeneration. N.A.: Data Not Available (due to brittlestars death). Scale bars: 7.5 μm

Table 5. Length and area in μm of the regeneration highlighted by the blue circles in Figure 13 (from left to right) N.A.: Data Not Available (due to brittlestars death). The measurements were measured using the program Fiji for Mac OS X.

Treatment	Weeks	Length (μm)	Area (μm^2)	Treatment	Weeks	Length (μm)	Area (μm^2)
pH ⁻	1-3	4.432	1.627	S ⁻	1-3	5.497	1.976
pH ⁻	3-5	4.091	1.511	S ⁻	3-5	5.497	1.976
pH ⁻	6-7	N.A.	N.A.	S ⁻	6-7	11.834	4.184
pH-S ⁻	1-3	8.189	2.905	Control	1-3	10.914	3.835
pH-S ⁻	3-5	5.465	1.976	Control	3-5	18.488	6.392
pH-S ⁻	6-7	6.861	2.441	Control	6-7	17.076	5.927

SEM showed a morphological difference between regenerated and non-regenerated ossicles in the treatments pH, S, and pH-S

After observing the treatment conditions effect on the brittlestars natural regeneration ability, additional steps were taken to observe this phenomenon on the micron scale and achieve a better understanding of how these altered conditions were affecting the reformation of the brittlestars skeleton. The stunted growth in the regenerated arms was shown to be more significant (ANOVA: $F_{3,5} = 7.58$, $n = 4$, $p = 0.03$) when the regenerated arms were imaged with SEM and their regenerated lengths were specifically measured. The measured length of the non-regenerated brittlestar arms were also significant (ANOVA: $F_{3,12} = 13.35$, $n = 4$, $p = 0.0004$). The width of the regenerated arms was also measured but there was no significant difference (ANOVA: $F_{3,5} = 0.88$, $n = 4$, $p = 0.51$) between treatments. The brittlestar arm non-regenerated widths were also measured and there was no significance between treatments (ANOVA: $F_{3,5} = 0.41$, $n = 4$, $p = 0.75$) The arm length and width measurements of both the non-regenerated and regenerated portion of the brittlestars arms exposed to each of the four experimental treatments is shown in Table 6 below.

Table 6. Length and width measurements in μm of the non-regenerated and regenerated portions of the brittlestar arms imaged with SEM and measured with the program Image J. The red font indicates the length of the regenerated portion of the brittlestar arm.

		Control	pH⁻	S⁻	pH⁻S⁻
Day 0	Length of regenerated arm	N. A.	N. A.	N. A.	N. A.
	Width of regenerated arm	N. A.	N. A.	N. A.	N. A.
	Length of non-regenerated arm	4.023	1.117	3.5	3.6
	Width of non-regenerated arm	0.224	0.272	0.248	0.27
Day 2	Length of regenerated arm	N. A.	N. A.	N. A.	N. A.
	Width of regenerated arm	N. A.	N. A.	N. A.	N. A.
	Length of non-regenerated arm	4.56	3.536	3.294	3.635
	Width of non-regenerated arm	0.253	0.242	0.227	0.245
Day 7	Length of regenerated arm	0.11	N. A.	N. A.	N. A.
	Width of regenerated arm	0.104	N. A.	N. A.	N. A.
	Length of non-regenerated arm	2.812	4.419	3.564	3.943
	Width of non-regenerated arm	0.318	0.316	0.247	0.238
Day 28	Length of regenerated arm	0.412	0.415	0.139	0.058
	Width of regenerated arm	0.173	0.085	0.112	0.13
	Length of non-regenerated arm	3.387	4.37	4.796	5.278
	Width of non-regenerated arm	0.273	0.285	0.247	0.297
Day 49	Length of regenerated arm	0.684	0.413	0.052	0.094
	Width of regenerated arm	0.104	0.083	0.084	0.051
	Length of non-regenerated arm	1.988	>4.155	>4.544	4.544
	Width of non-regenerated arm	0.214	0.207	0.261	0.171

The following qualitative and quantitative analysis regarding the appearances of the non-regenerated and regenerated arm ossicles over time are both speculations and estimations to provide further suggestion as to why the regeneration was stunted in the brittlestars exposed to the pH^- , $\text{pH}^- \text{S}^-$, and S^- treatments. The information gleaned from the SEM images cannot be accurately and fairly compared between treatments because not all of the ossicle images were captured with the same angle and orientation of the arm. There does not appear to be structural effects from the treatments on the brittlestars already present ossicles (Figure 14). The shapes and prevalence of the stroma (holes) and trabeculae (bumps) of ossicles vary greatly, even among the control, making it difficult to discern which is natural variability and which differences can be attributed to impacts of the treatments. However, the difference became more apparent when the appearance between the previously existing ossicles and the regenerated ossicles in each treatment was compared (Figure 15).

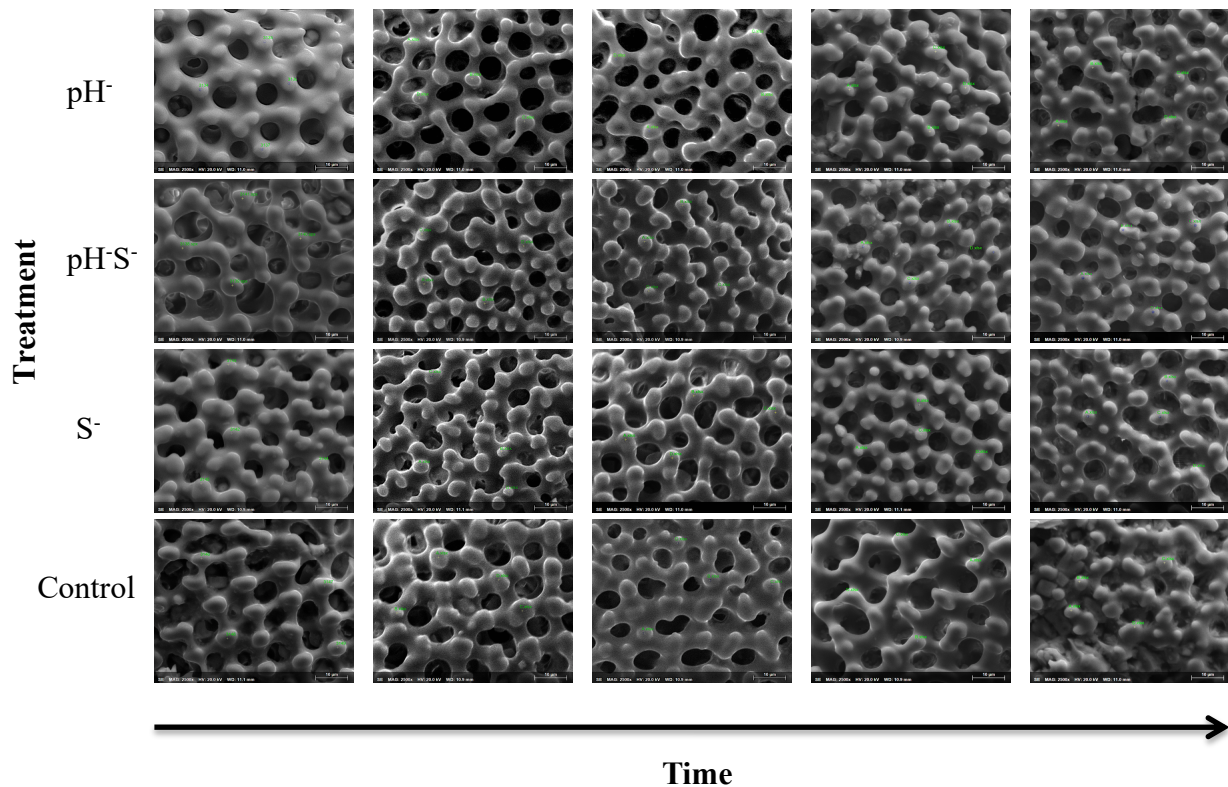


Figure 14. Images of the non-regenerated ossicles of the brittlestar arm (skeleton) after being exposed to each of the four experimental treatments over time. The pictures show the 3rd dorsal ossicle (skeleton) from the original amputation site. The green x's and labels mark where the EDS measurements occurred (n=4).

The regenerated ossicles of the brittlestars exposed to the pH^- and S^- conditions on day 28 and day 49 of the experiment demonstrated thinner ridges and less pronounced trabeculae than the regenerated ossicles of the brittlestars in the control condition. The ossicles from the $\text{pH}^- \text{S}^-$ treatment more closely resemble the appearance of the control. The stroma was also more elongated at day 28 so the shape resembled ovals rather than circles for the pH^- and S^- treatments and then at day 49 regained the circular shape. The trabeculae also became more pronounced for the pH^- treatment exposed ossicles at day 49 but not for the S^- exposed ossicles, which displayed more of a flat surface (Figure 15). It is unclear what this ultrastructural change means for the functionality and durability of the brittlestar ossicles when the brittlestars are exposed to the treatment conditions.

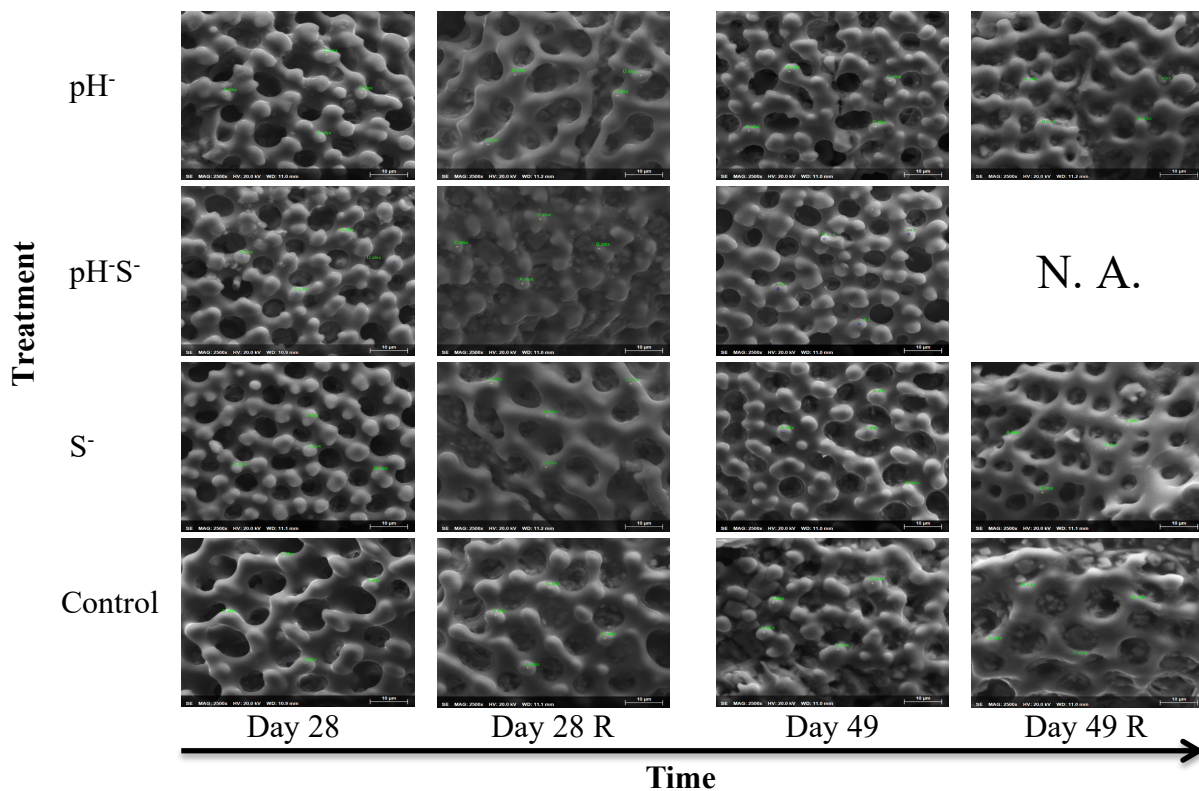


Figure 15. Progression of brittlestar arm regeneration compared to the original arm ossicles in each of the four experimental treatments over time. The pictures show both the 3rd dorsal ossicle from the original amputation site (left) and the dorsal ossicle from the regenerated site (right). The green x's and labels mark where the EDS measurements occurred (n=4).

Differences in the porosity of the non-regenerated and regenerated ossicles of the brittlestars exposed to each of the four treatments were quantified in Fiji for Mac OS X (Table 7) using image thresholding methods (refer to Figure 3). The mean gray intensity values refer to the level of white vs. gray pixels present after the SEM image of the ossicles had been binarized and image thresholded. Image thresholding separated the stroma (black) and the trabeculae and bone ridges (white). On a scale from 0-255, 0 meaning the image is completely black and 255 meaning the image is completely white. When testing the percent porosity of the ossicles, the higher the value, the more bone was present, and the lower the value, the less bone was present. When the value was higher, that meant the stroma of the ossicles was smaller or less present in the images depicted in Figure 15. The opposite was true for the lower percent porosity values.

When comparing the non-regenerated arm ossicles over time (from day 28 to day 49) the brittlestars in the pH^- and S^- treatment seemed to have a similar decrease in their overall porosity (ANOVA: $F_{3,8} = 10.23$, $n = 4$, $p = 0.0040$; Tukey, $n = 4$, $df = 3$, $p = 0.0073$) compared to the ossicles of the brittlestars exposed to the pH^-S^- and control treatments (ANOVA: $F_{3,8} = 10.23$, $n = 4$, $p = 0.0040$; Tukey, $n = 4$, $df = 3$, $p = 0.0082$) (Figure 16). Moreover, the porosity decreased in the regenerated ossicles for the brittlestars exposed to the pH^- , S^- and control treatments (ANOVA: $F_{3,8} = 4.39$, $n = 4$, $p = 0.04$). The porosity of the regenerated ossicles from the brittlestars exposed to the pH^-S^- treatment could not be observed over time due to no measurable regeneration of the ossicles occurring in the brittlestar arm imaged using SEM on day 49 (Figure 17).

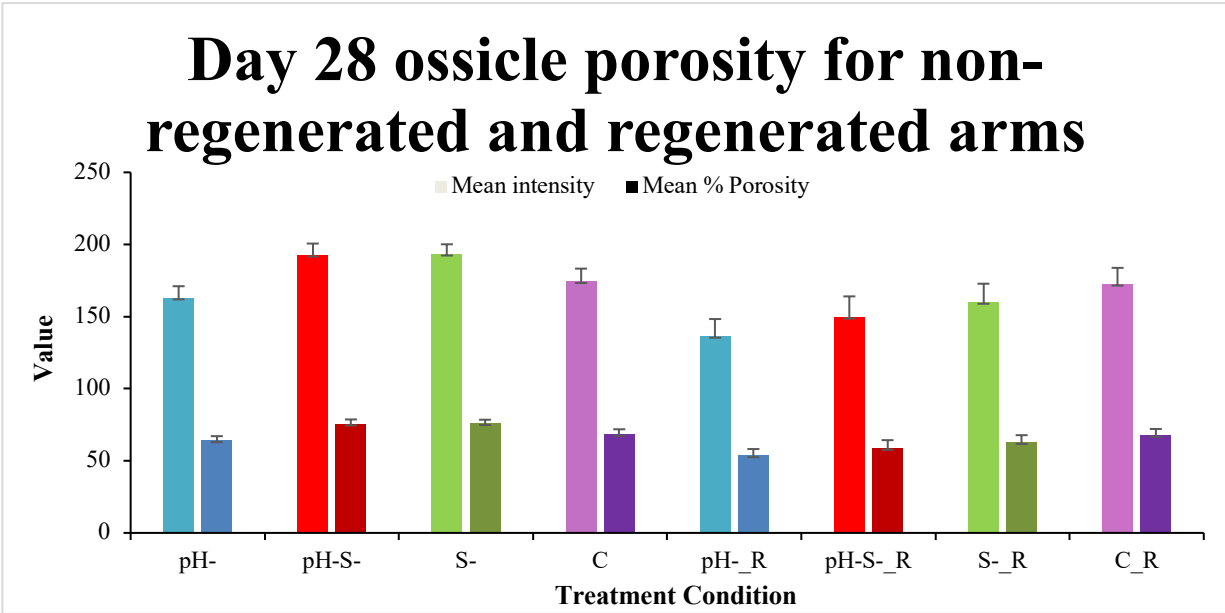


Figure 16. Average values of mean intensity and mean percent porosity \pm SD for day 28 present in the non-regenerated and regenerated dorsal ossicles for the brittlestars exposed to the four different treatments over time. Data was collected from SEM images from Figure 15 using Fiji for Mac OS X after images were binarized and thresholded.

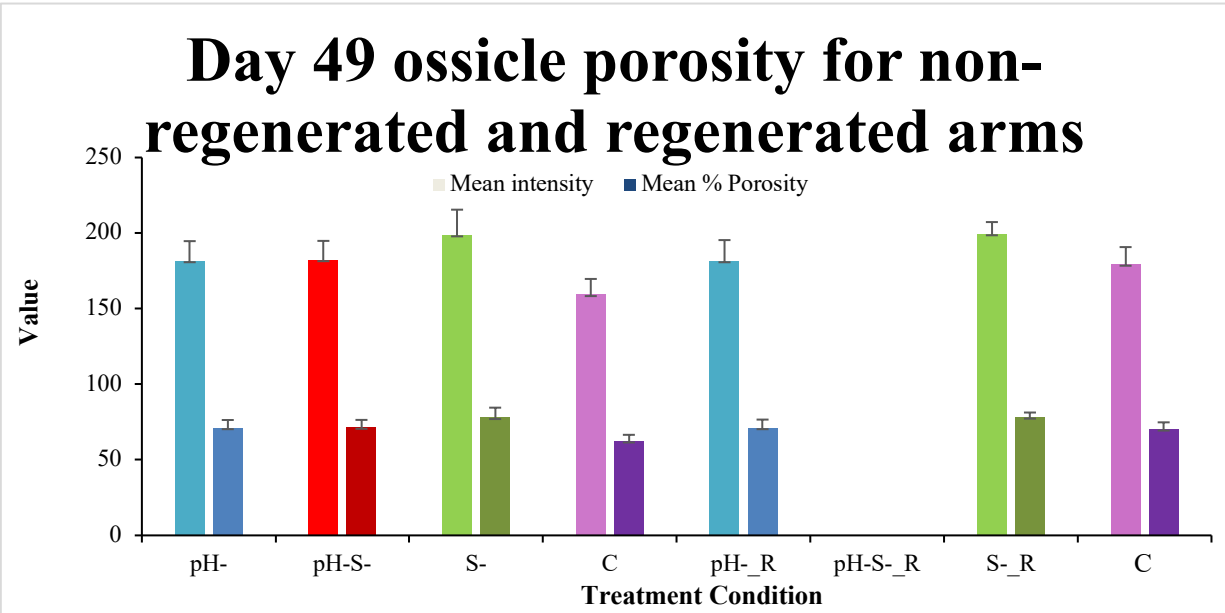


Figure 17. Average values of mean intensity and mean percent porosity \pm SD for day 49 present in the non-regenerated and regenerated dorsal ossicles for the brittlestars exposed to the four different treatments over time. Data was collected from SEM images from Figure 15 using Fiji for Mac OS X after images were binarized and thresholded.

Table 7. Measurements of mean intensity (the gray areas in a black and white binarized image; see Figure 15) and mean percent porosity (how much bone is present) for the images shown in Figure 15 above (from left top to bottom to right top to bottom). N.A.: Data Not Available (due to no regeneration occurring). The measurements were measured using the program Fiji for Mac OS X (n=3).

Treatment	Day	Arm state	Mean gray intensity	Mean % porosity
pH ⁻	28	Non-regenerated	162.93±8.12	63.89±3.19
pH ⁻ S ⁻	28	Non-regenerated	192.65±7.98	75.55±3.13
S ⁻	28	Non-regenerated	193.34±6.79	75.79±2.69
C	28	Non-regenerated	174.30±8.95	68.35±3.51
pH ⁻	28	Regenerated	136.35±11.94	53.47±4.68
pH ⁻ S ⁻	28	Regenerated	149.61±14.39	58.67±5.64
S ⁻	28	Regenerated	159.88±12.91	62.70±5.06
C	28	Regenerated	172.51±11.26	67.65±4.42
pH ⁻	49	Non-regenerated	181.74±12.95	71.27±5.08
pH ⁻ S ⁻	49	Non-regenerated	182.42±12.43	71.54±4.87
S ⁻	49	Non-regenerated	198.85±16.65	77.98±6.53
C	49	Non-regenerated	159.32±10.35	62.48±4.06
pH ⁻	49	Regenerated	181.72±13.66	71.26±5.36
pH ⁻ S ⁻	49	Regenerated	N.A.	N.A.
S ⁻	49	Regenerated	199.56±7.74	78.26±3.03
C	49	Regenerated	179.42±11.32	70.36±4.44

EDS demonstrated an increase in the Ca:Mg ratio in the non-regenerated ossicles (pH⁻) and a decrease in regenerated ossicles (pH⁻ and S⁻)

The brittlestars exposed to the pH⁻ treatment expressed a decreasing trend of absorption of magnesium over time. The mass percent of magnesium in the ossicles in the pH⁻ treatment

decreased from 20% to 11% from day 0 to day 49. The other treatments seemed to maintain relatively stable magnesium mass percent values around 15% (Figure 18). The opposite trend occurred for the mass percent levels of calcium in the brittlestars exposed to the pH^- treatment (Figure 19). This idea, that the magnesium and calcium levels in the ossicle are inversely correlated, is further supported by the abnormally high spike in magnesium on day 7 and the abnormally low peak of calcium in the brittlestar exposed to the $\text{pH}^- \text{S}^-$ treatment.

Statistical analyses demonstrated that from Day 0, before the brittlestars were exposed to the treatment conditions, the $\text{pH}^- \text{S}^-$ treatments had significantly different absorption levels of both magnesium and calcium, when the brittlestar arm ossicles were tested by EDS measurements against the levels of both the pH^- treatment and the control mass percentages (ANOVA: $F_{3,12} = 11.77$, $n = 4$, $p = 0.0007$; Tukey, $n = 4$, $df = 3$, $p = 0.0004$, Tukey, $n = 4$, $df = 3$, $p = 0.03$ respectively). The levels of magnesium and calcium in the ossicles exposed to the S^- treatment were shown to be significantly lower than the pH^- treatment mass percent magnesium levels (ANOVA: $F_{3,12} = 11.77$, $n = 4$, $p = 0.0007$; Tukey, $n = 4$, $df = 3$, $p = 0.03$) and significantly higher than the pH^- treatment mass percent calcium levels (ANOVA: $F_{3,12} = 11.77$, $n = 4$, $p = 0.0007$; Tukey, $n = 4$, $df = 3$, $p = 0.03$), respectively.

Non-regenerated ossicles contained lower levels of magnesium in pH^- and S^-

Overall the brittlestars in the $\text{pH}^- \text{S}^-$ and S^- treatments were normally taking up less magnesium into their magnesium calcite ossicle structure (Figure 18) and absorbing more calcium than the brittlestars in the control and the pH^- treatments. The opposite was true for the calcium levels (Figure 19). However, these patterns of absorption changed when the brittlestars were exposed to the pH^- and S^- water chemistry treatments over time. At day 7 of the brittlestars exposure to the experimental treatments, the brittlestars in the pH^- treatment began to absorb more calcium and less magnesium than the brittlestars in the $\text{pH}^- \text{S}^-$ treatment (ANOVA: $F_{3,12} =$

9.65, $n = 4$, $p = 0.0016$). This continued until the last day, day 49, when the brittlestars in the pH⁻ treatment contained more mass percent of calcium and less mass percent of magnesium than all of the other three experimental treatments (ANOVA: $F_{3,12} = 8.39$, $n = 4$, $p = 0.0028$). It is important to note that these changes in mass percent of calcium and magnesium depicted in Figure 16 and 17 show the changes that occurred for the already present ossicles and do not reflect the changes in elemental absorption for the regenerated ossicles under the lower pH and lower salinity experimental conditions.

When the calcium to magnesium ratios (Ca:Mg) were observed for the non-regenerated ossicles, the brittlestar ossicles exposed to the pH⁻ treatment displayed a similar pattern to the ossicle concentration of calcium over time (ANOVA: $F_{3,12} = 8.39$, $n = 4$, $p = 0.0028$) (Figure 20). The Ca:Mg ratio increased over time in pH⁻, remained relatively the same in S⁻ and decreased in pH⁻S⁻ and the control. Although, the upper and lower limits of the control range showed less variability in the Ca:Mg ratio results than the concentration of calcium results, which is probably due to the presence of magnesium also being considered as a factor.

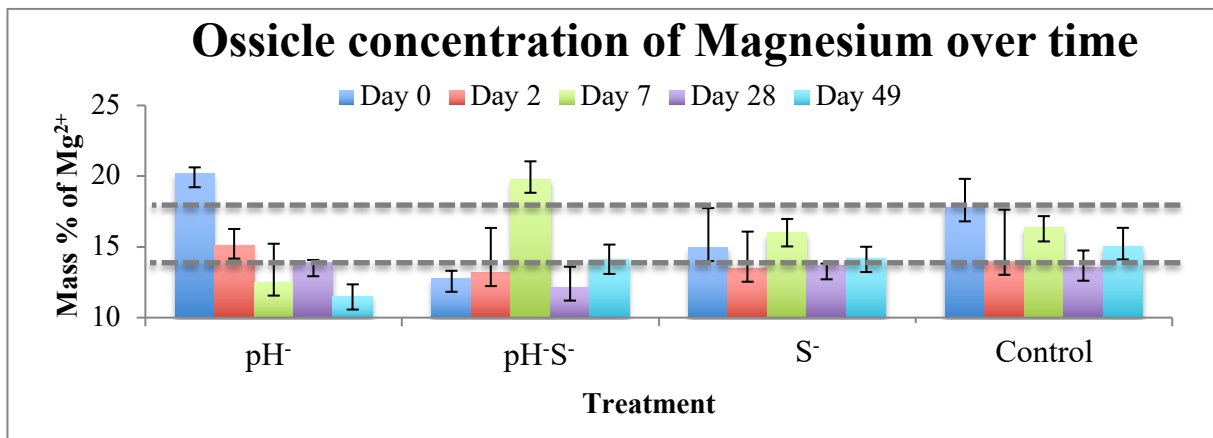


Figure 18. Average concentrations of magnesium in mass percent \pm SD present in the non-regenerated original dorsal ossicle for the brittlestars exposed to the four different treatments over time. The dotted lines indicate the upper and lower limits of the control range.

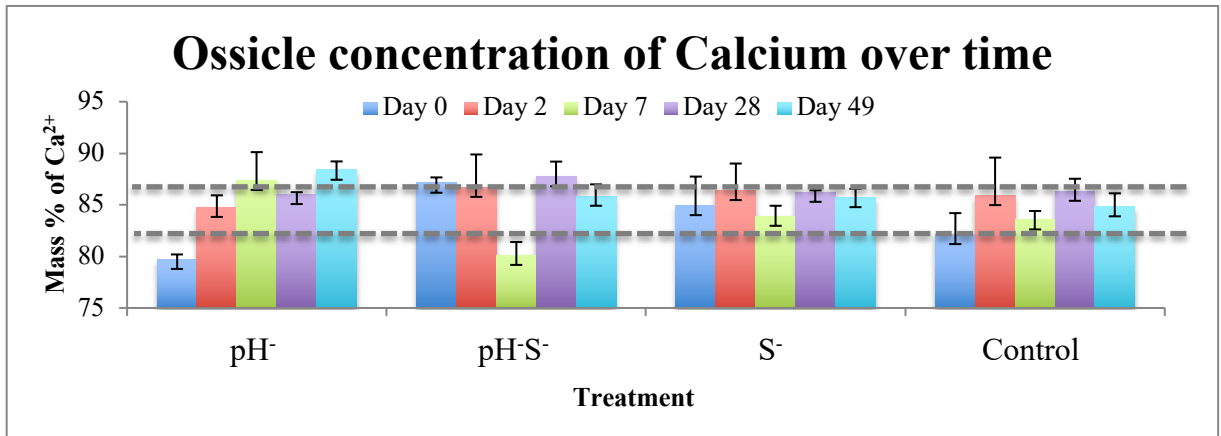


Figure 19. Average concentrations of calcium in mass percent \pm SD present in the non-regenerated original dorsal ossicle for the brittlestars exposed to the four different treatments over time. The dotted lines indicate the upper and lower limits of the control range.

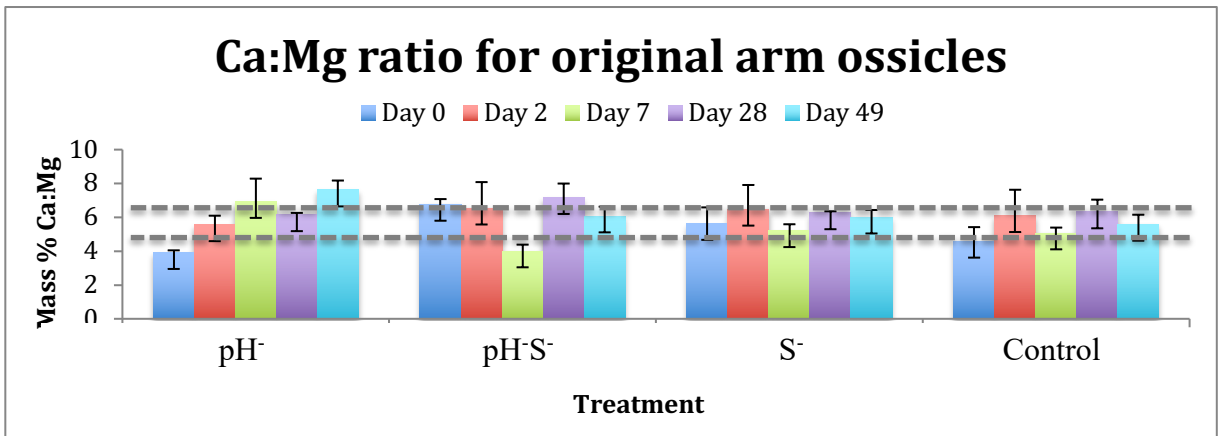


Figure 20. Ratios of calcium to magnesium in mass percent \pm SD of the non-regenerated original dorsal ossicle for the brittlestars exposed to the four different treatments over time. The dotted lines indicate the upper and lower limits of the control range.

Regenerated ossicles contained higher levels of magnesium in pH⁻ and S⁻

It appears that this trade off trend between magnesium and calcium mass percent levels continues for the regenerated arm ossicles, albeit not as drastically. Measurable regeneration occurred in brittlestars exposed to pH⁻, S⁻, and pH⁻S⁻ treatments at Day 28 and continued to Day 49. The brittlestars in the pH⁻ treatment once again displayed the largest difference in elemental absorption levels.

The statistical test performed on the EDS elemental data for Day 28 showed significant difference between the pH^- treatment magnesium and calcium mass percent levels, the pH^-S^- treatment levels (ANOVA: $F_{3,12} = 9.24$, $n = 4$, $p = 0.0019$; Tukey, $n = 4$, $df = 3$, $p = 0.0036$), and the control treatment (ANOVA: $F_{3,12} = 9.24$, $n = 4$, $p = 0.0019$; Tukey, $n = 4$, $df = 3$, $p = 0.0042$) (Figure 21 and 22). The pH^- treatment exposed brittlestars had higher calcium levels and lower magnesium levels than the pH^-S^- treatment and control exposed brittlestars. And the mass percent levels of magnesium and calcium between the pH^-S^- treatment and the control were similar (ANOVA: $F_{3,12} = 9.24$, $n = 4$, $p = 0.0019$; Tukey, $n = 4$, $df = 3$, $p = 0.9999$). Day 49 did not demonstrate the same significance, as the control elemental levels evened out with the pH^- treatment levels (ANOVA: $F_{3,12} = 0.94$, $n = 4$, $p = 0.43$) and there was no measurable regeneration for the pH^-S^- exposed brittlestars.

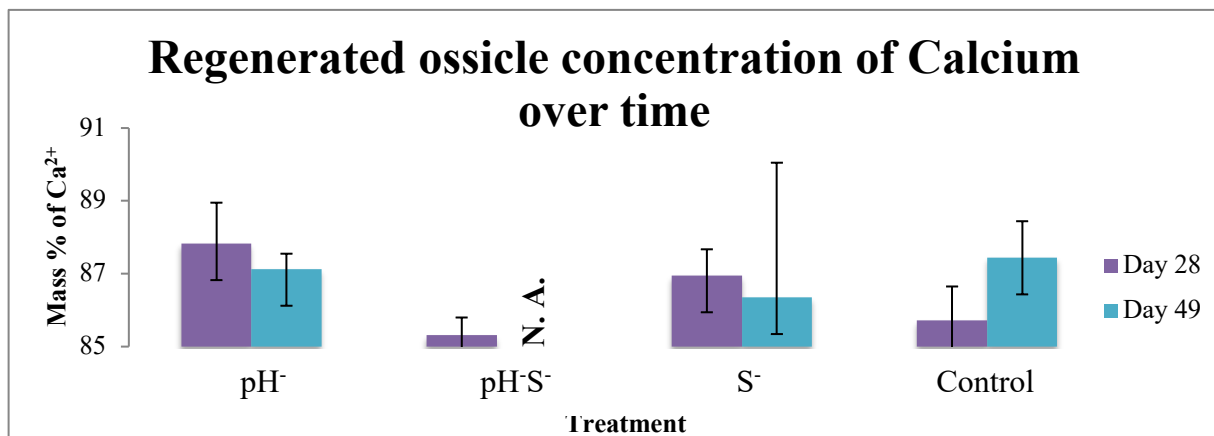


Figure 21. Average concentrations of magnesium in mass percent \pm SD present in the regenerated dorsal ossicle for each brittlestar exposed to the four treatments over time. There was no regeneration for pH^-S^- during day 49 (N.A.).

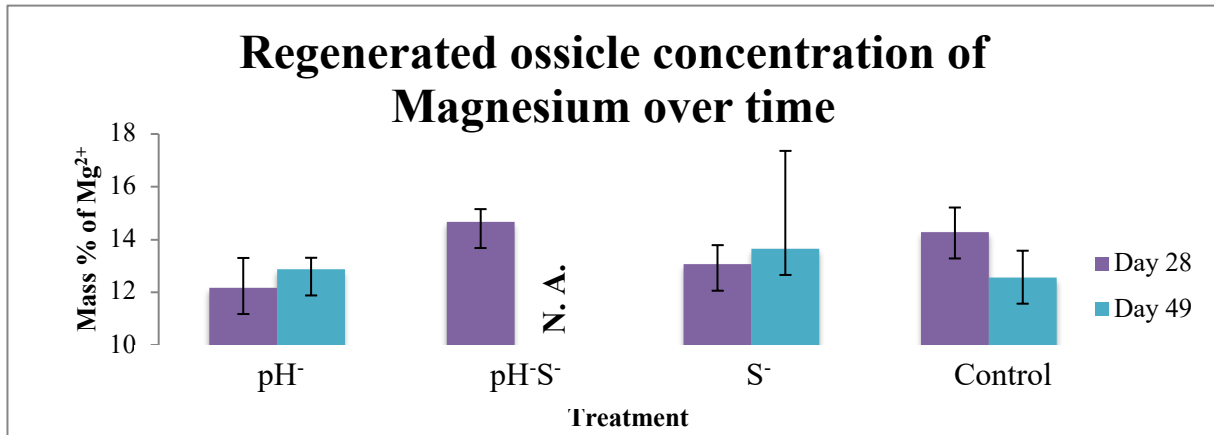


Figure 22. Average concentrations of calcium in mass percent \pm SD present in the regenerated dorsal ossicle for each brittlestar exposed to the four treatments over time. There was no regeneration for pH⁻S⁻ during day 49 (N.A.).

The Ca:Mg ratio in the regenerated brittlestar ossicles decreased over time (from day 28 to day 49) in the pH⁻, and S⁻ treatments., but increased in the control. Interestingly, the Ca:Mg ratio under control conditions in the regenerated arms reversed on Day 49 (Figure 23). The brittlestars in the control condition now expressed lower magnesium concentrations and higher calcium concentrations in the regenerated dorsal ossicles at day 49 (ANOVA: $F_{3,12} = 9.38$, $n = 4$, $p = 0.03$) as opposed to day 28. The results of the Ca:Mg ratio also resembled the results of the concentration of calcium over time (Figure 23) but at a smaller scale. The Ca:Mg ratio of the ossicles exposed to the pH⁻S⁻ treatment on day 28 looked similar to the control ratio on the same day but there was no pH⁻S⁻ data on day 49 to compare to the control to elucidate if the pattern would hold over time.

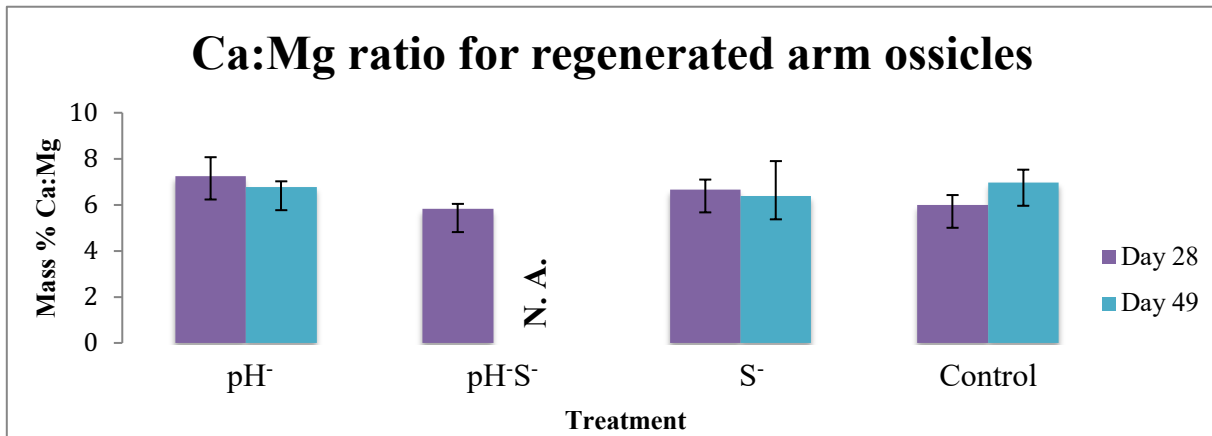


Figure 23. Ratios of calcium to magnesium in mass percent \pm SD of the regenerated dorsal ossicle for each brittlestar exposed to the four treatments over time. There was no regeneration for pH⁻S⁻ during day 49 (N.A.).

Comparison of non-regenerated and regenerated ossicles from the same arm showed an increase in calcium concentration in regenerated arms exposed to pH⁻ and S⁻ over time

The brittlestars displayed increased magnesium mass percent levels (Figure 24) and slightly lower calcium mass percent levels for day 28, in the control (ANOVA: $F_{1,6} = 2.88$, $n = 4$, $p = 0.14$) (Figure 25). This pattern held true for the brittlestars exposed to the pH⁻S⁻ treatment (ANOVA: $F_{1,6} = 6.47$, $n = 4$, $p = 0.04$). The difference in magnesium and calcium mass percent was only significant between the non-regenerated and regenerated arms between the pH⁻ treatment and the control and between the pH⁻ and the pH⁻S⁻ treatments (ANOVA: $F_{1,6} = 12.07$, $n = 4$, $p = 0.01$). The brittlestars in the pH⁻ treatment demonstrated much lower magnesium (Figure 24) and higher calcium mass percent levels (Figure 25) in the regenerated arms. The difference in magnesium and calcium mass percent levels in the non-regenerated and regenerated ossicles exposed to the S⁻ treatment were not significant (ANOVA: $F_{1,6} = 3.11$, $n = 4$, $p = 0.13$).

There was a significant difference in the control treatment between the levels of magnesium and calcium present in the non-regenerated and regenerated ossicles for day 49 (ANOVA: $F_{1,6} = 7.99$, $n = 4$, $p = 0.03$). The brittlestars in the pH⁻ treatment on day 49 also now expressed higher magnesium levels and lower calcium levels in the regenerated arm (ANOVA:

$F_{1,6} = 6.21$, $n = 4$, $p = 0.05$). The differences in the magnesium and calcium levels in the non-regenerated and regenerated ossicles on day 49 that were exposed to the S^- treatment became even more negligible (ANOVA: $F_{1,6} = 0.09$, $n = 4$, $p = 0.78$). Once again, there was no measurable ossicle regeneration in the brittlestars exposed to the pH^-S^- treatment but based off of the day 28 results, it is likely that the treatment magnesium (Figure 24) and calcium levels (Figure 25) would have been similar to the pattern of the control for the day 49 measurements.

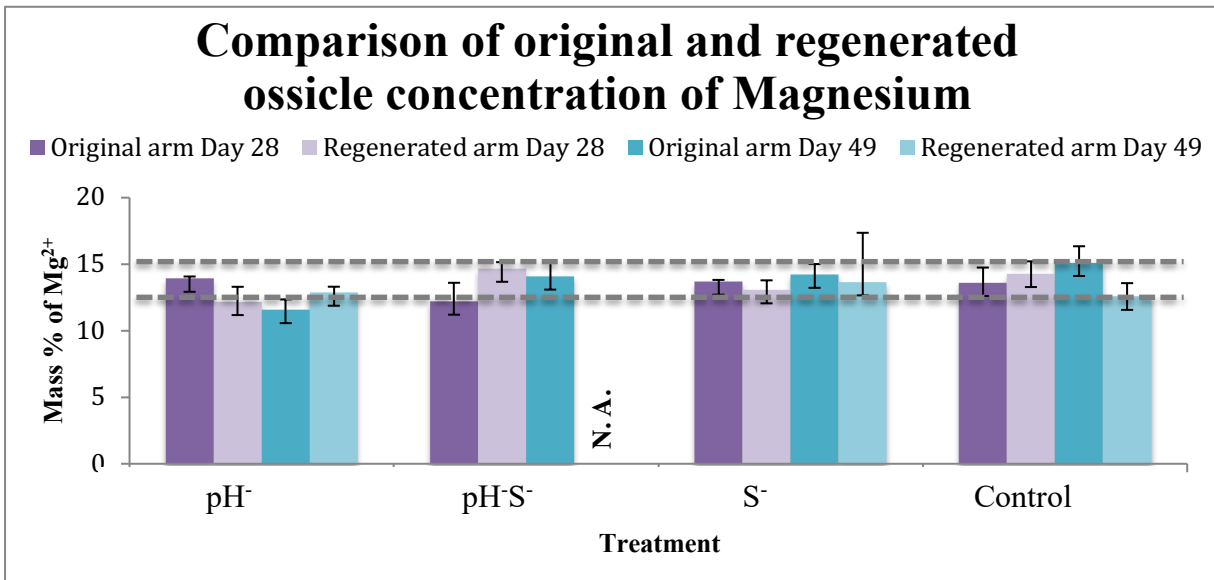


Figure 24. Comparison between average concentrations of magnesium in mass percent \pm SD present in the both the regenerated and non-regenerated dorsal ossicles for each brittlestar exposed to the four treatments over time ($n=4$ per bar). The dotted lines indicate the upper and lower limits of the control range.

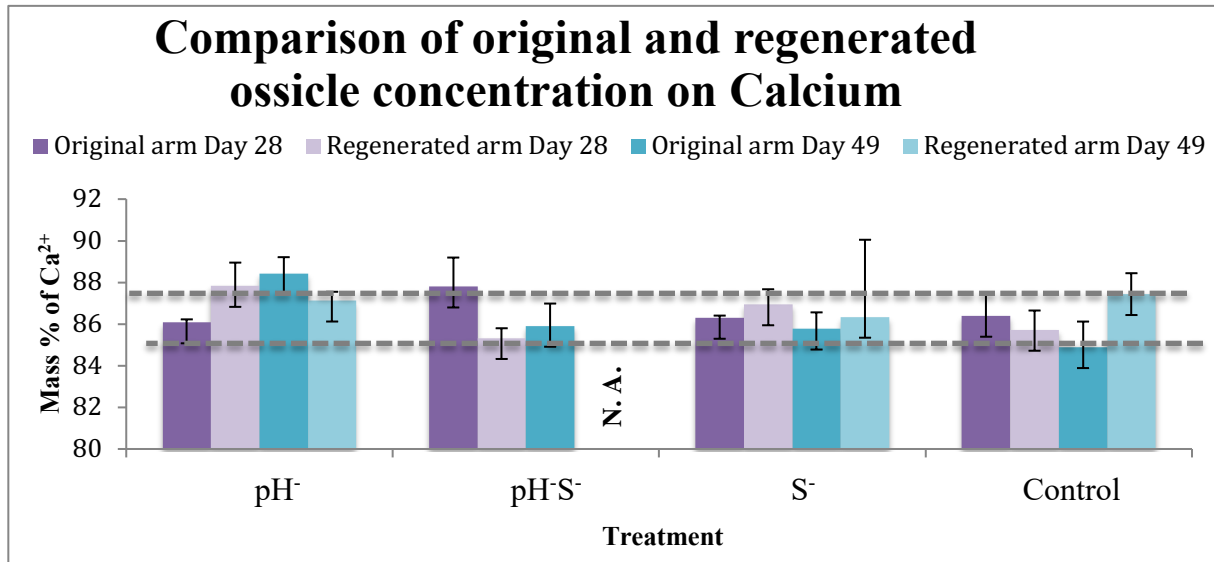


Figure 25. Comparison between average concentrations of calcium in mass percent \pm SD present in the both the regenerated and non-regenerated dorsal ossicles for each brittlestar exposed to the four treatments over time (n=4 per bar). The dotted lines indicate the upper and lower limits of the control range.

Discussion

This study analyzed the impact of future predicted climate change conditions of low pH and low salinity (both separately and combined) on the nervously controlled survival mechanisms implored by the brittlestar *Amphipholis squamata*. The brittlestars neural network controls many of their defensive mechanisms against predation such as, their flipping response, their regeneration, and their bioluminescent capabilities (Dewael and Mallefet, 2001; Kano et al., 2017). The results showed that this nervous control is challenged when the brittlestars were placed in conditions of pH⁻, S⁻ and, pH⁻S⁻. These effects indicate that the nervous system is impacted by changes in water chemistry. The results also suggest that this species of brittlestar will have a more difficult time warding off predators and surviving in conditions of altered pH and altered salinity projected in the near future if climate change conditions continue as predicted.

Brittlestars neuro-coordination ability is affected by pH and S⁻

The righting response is a natural behavioral instinct of some echinoderms including the brittlestar in this study and can be used as an indication of the health of the organism, such as if it is stressed or healthy in a variety of environmental conditions (Lawrence and Cowell, 1996). The brittlestars displayed stressed behaviors that were representative of *in situ* predator avoidance/escape behaviors (Emson and Wilkie, 1982) when they were exposed to the pH⁻, S⁻, and pH·S⁻ treatments.

One of the studies using the righting response as an indicator for organismal stress found that asteroids (sear stars), echinoids (sea urchins), and ophiuroids (brittlestars) flipped slower in conditions of low salinity (Lawrence and Cowell, 1996). In another study, the righting response of the sea stars *Stichaster striatus*, and *Luidia clathrata* were negatively impacted by conditions of low salinity (Watts and Lawrence, 1990; Lawrence and Cowell, 1996). This shows that the negative impact on the righting response is not limited to just this particular species of brittlestar under lower future projected water chemistry conditions of salinity, and could have negative ramifications for many marine organisms with either this specific flipping behavioral ability or other coordination functions under nervous control.

Unfortunately, there is not much scientific literature on the effects of low pH environmental conditions on the flipping response of echinoderms. Although, based on the results from this study, it may be appropriate to say that the flipping response is negatively impacted in situations of pH levels around 7.7. This could have severe implications on the survival of not only these brittlestars, but also on other echinoderms that use this flipping behavior (or any other neuro-coordinated movement) to escape predation. However, there are other studies that question nervous control abilities over coordination functions in other species of marine invertebrates such as the mantis shrimp, which did not express a change in the strike

effectiveness of its raptorial appendage under conditions of lower pH (deVries et al., 2016). The study's result demonstrates that not every species will react the same either under altered pH or altered salinity conditions, which is why it is important to conduct multiple experiments on various species using these future water chemistry predictions as a baseline for potential organismal survivability.

Stunted arm regeneration in pH, S, and pH·S conditions impedes brittlestar survival

In the ocean, sublethal predation on brittlestars makes it more difficult for the brittlestars to find and obtain food and the allocation of nutrients goes toward regeneration as opposed to body mass and reproduction (Lawrence and Vasquez, 1996). A study found that even a species of brittlestar *Ophiophragmus filigraneus*, that is accustomed to low salinities of 30-20 PSU, regeneration ability suffers in prolonged exposure to lower salinity (16 PSU) conditions (Talbot and Lawrence, 2002). Another species of brittlestar less tolerant to changes in salinity also demonstrated significantly less regrowth of arm ossicles at salinity levels of 23 PSU (Donachy and Watabe, 1986). This shows that although brittlestars tend to be stenohaline organisms, meaning they are only able to tolerate a narrow range of salinities, the range of tolerance can vary from species to species (Rivera-Ingraham and Lignot, 2017).

It appears from the results of this study that the lower limit of salinity the study species *A. squamata* can successfully regenerate their arms in is higher than 25 PSU. When the brittlestar was exposed to S^- and the combined stressors of $pH \cdot S^-$, the regeneration process suffered, possibly as a consequence of the brittlestar trying to maintain arguably more important functions (bioluminescence). This inability to regenerate normally could lead to a decrease in the brittlestars ability to feed, affecting its ability for growth and reproduction which are crucial necessities for their survival (Sides, 1987). Handicapping the regeneration ability in these environmental conditions could also lead to a reduction in locomotion allowing for ease of

predation (Shaeffer, 2016) that could result in a higher predation mortality rate of the brittlestars in the future.

There was also stunted arm regeneration in the brittlestars exposed to the pH⁻ treatment and the quality (width) of regenerated arms was poorer once regeneration occurred. This could be because exposure to pH⁻ causes a reduction in the metabolic rate of the brittlestars, which depletes the energy resources necessary for regeneration (Wood et al., 2010). Another study conducted on a different species of infaunal brittlestar, *Amphiura filiformis* suffered a decrease of 80% in regeneration rate and experienced delayed or depressed regeneration in decreased pH (Hu et al., 2014).

The arms that regenerated under pH⁻ conditions were much narrower than the regenerated arms in the control. This change in morphology could also negatively impact the feeding behaviors of these brittlestars as well as make locomotion more difficult which is an important function in escaping predation (Lawrence, 2010). Although the brittlestars may be able to survive based off of the length that was observed to have regenerated under pH⁻, they are allocating energy to this regeneration process that could be better used for growth and reproduction. The arms that regenerated under the stressful condition of pH⁻ also demonstrated problems in the structural mineral ratio of Ca:Mg, which could severely impact the functionality and durability of the regenerated arm and have negative consequences in terms of survival.

Ca:Mg ratio of brittlestar ossicles changes when exposed to pH⁻ and S⁻

The ratio of magnesium to calcium in both the already present and regenerated brittlestar ossicle skeleton changed during the beginning and end of the arm regeneration process. These opposing trends in the non-regenerated and regenerated ossicles suggest that the brittlestars in the pH⁻ treatment are taking up more calcium in lieu of magnesium (perhaps to fortify the

structure of the already present ossicles) while the regenerated ossicles in the pH⁻ treatment favor higher magnesium levels when exposed to stressful altered environmental conditions.

The discrepancy in calcium vs. magnesium concentration in the non-regenerated arms could be attributed to the brittlestar trying to absorb more stable elemental minerals to compensate for the stressful pH⁻ treatment conditions. This claim is supported by a study that shows the mineral deposition of Mg-calcite is less stable the higher percentage of magnesium the structure contains in relation to calcium (Loste et al., 2003). If this could also be true for *A. squamata*, it would make sense that the already formed ossicles naturally have a higher concentration of calcium compared to magnesium.

However, a high percentage of magnesium may be necessary in the regenerating ossicles to lay the structural foundation more rapidly and grow an arm that can be used for feeding as fast as possible. Even though the regenerated ossicles in the pH⁻ treatment have higher levels of magnesium, it does not mean that they are being used as effectively, this becomes apparent when looking at the length and width of the regenerated arms exposed to pH⁻ and the fact that the ossicles exposed to S⁻ and pH⁻S⁻ show high levels of concentrations of magnesium and calcium but little to no visible appearance of regeneration.

Currently the ratio of magnesium to calcium is not well documented for the species *A. squamata* so the results of this paper could help the scientific community understand the ratios of Ca:Mg in both normal seawater conditions (control) and altered conditions of low pH and low salinity. However, one study did try to quantify the elemental composition of the ossicle plates of *A. squamata* compared to another luminous and non-luminous species of brittlestar and found that there were compositional skeletal elemental differences between species although not for the element magnesium, which was the most abundant element measured at 100 mg/g concentration (the study did not measure calcium concentration) (Deheyn et al., 2015).

Dissolution/calcification of skeletal Ca^{2+} , Mg^{2+} could be increased/decreased in pH, S, pH·S

This study analyzed the elemental mineral concentrations of magnesium and calcium present in both the non-regenerated and regenerated dorsal ossicles of the brittlestars skeleton. The material needed to build the ossicles is secreted by a specialized group of cells known as sclerocytes whose main function is to produce amorphous calcium carbonate (ACC) and calcium carbonate crystals, which form the Mg-calcite endoskeleton of echinoderms (Märkel and Röser, 1985). There is also a theory that the addition of magnesium in the calcium carbonate mineral structure may give brittlestars the ability to control crystal morphologies and transform ACC into ossicles. The first phase in the ossicle formation process was always ACC and the magnesium entered the mineral structure at that phase at varying concentrations (Loste et al., 2003).

The first stage of regenerating ossicles is a secretion of ACC, which has the ability to form the Mg-calcite skeletal structure of the brittlestar. The concentration of magnesium had a direct effect on the stabilization property of the ACC and thereby the stability of the magnesium-calcite precipitate that would later form the calcium carbonate skeletal structural ossicle segments. ACC with a higher concentration of magnesium was more stable over significant periods of time (Loste et al., 2003). This could also explain why there was a higher magnesium signature in the regenerated ossicles.

The dissolution of $CaCO_3$ crystal morphologies such as Mg-calcite is favored by lower pH. (Andersson et al., 2011). Lower pH also results in a reduction in carbonate ions necessary for calcification which results in a decrease in $MgCO_3$ content that could be responsible for providing magnesium ions to the Mg-calcite structure the brittlestars ossicles are composed of (Burton and Walter, 1991). Another study found that as pCO_2 decreased observed dissolution rates decreased as well, this could mean that the dissolution rates of Mg-calcite will increase under higher pCO_2 levels which correspond to lower pH levels. It also found that salinity had

little effect on calcite precipitation rates (Finneran and Morse, 2009). However, lower salinity as a product of increased precipitation reduces all of the seawater ions concentrations (Freire et al., 2011) and thereby could inhibit or significantly slow the process of brittlestar ossicle calcification that requires ions available in seawater like Ca^{2+} and Mg^{2+} .

This integration of magnesium into the calcite mineral structure remains unique among echinoderms and may be the key to explaining the process behind the regenerative ossicle growth and structure differences between brittlestar species. Ocean acidification dissolves exposed calcium carbonate skeletons but it is still unclear how ocean acidification impacts these cellular mechanisms and disturbs the process of calcification at the molecular level. More research needs to be done on this subject to better understand how the process of ossicle formation in the brittlestar *A. squamata* will be impacted by a decrease in pH and a decrease in salinity. Once this process is better understood, we can better understand how it will be affected by future projections of low pH and low salinity and hypothesize if the effects will be representative for other marine invertebrate organisms with similar skeletal composition and morphologies.

Bioluminescence data was not systemically significant but showed a slight increase in light production in pH, S, and pH·S

Following the findings that the nervous system functionality of *A. squamata* is impaired for their flipping response and arm regeneration when the brittlestars are exposed to conditions of low pH, low salinity and their combination. To further test the integrity of the brittlestars nervous system under the predicted altered carbonate chemistry conditions by testing the brittlestars bioluminescence response, which is also nervously controlled, raw data from the brittlestars light production abilities when introduced to both a non-chemical (ASW) and chemical stimuli (ACh and KCl) was examined for each of the four treatments. The results from

the analysis of this raw data are meant to act as a suggestion for how else the brittlestars nervous system may be impacted by these changes in pH and salinity as a consequence of climate change. They are also meant to be viewed in conjunction with the results from the flipping and the arm regeneration to determine if the response will further hinder the brittlestars ability to escape predation.

Non-chemically stimulated spontaneous light production increased in pH⁻ and S⁻

The sum (integration over time; RLU/mm) of the spontaneous light production normalized to the individual arm lengths of the brittlestars and the total possible chemical light output from the KCl test (positive control) displayed significant difference between the control condition and the pH⁻, pH⁻S⁻ and S⁻ treatments. There was mostly an increase in the spontaneous light production of the brittlestar arms that had been exposed to the pH⁻ and pH⁻S⁻ treatments in the expression of peak light intensity. When the kinetics or time of the peak spontaneous light emission were analyzed, there was some difference between the pH⁻ treatment responses and the other treatments (Figure 26). The peak light intensity was reached slowly in the beginning and decreased over time for the brittlestars exposed to pH⁻, the opposite trait occurred for the brittlestars exposed to the three other treatments. This could suggest that the brittlestars exposed to low pH were becoming increasingly more stressed during the time of exposure, which is also in agreement with the flipping response findings.

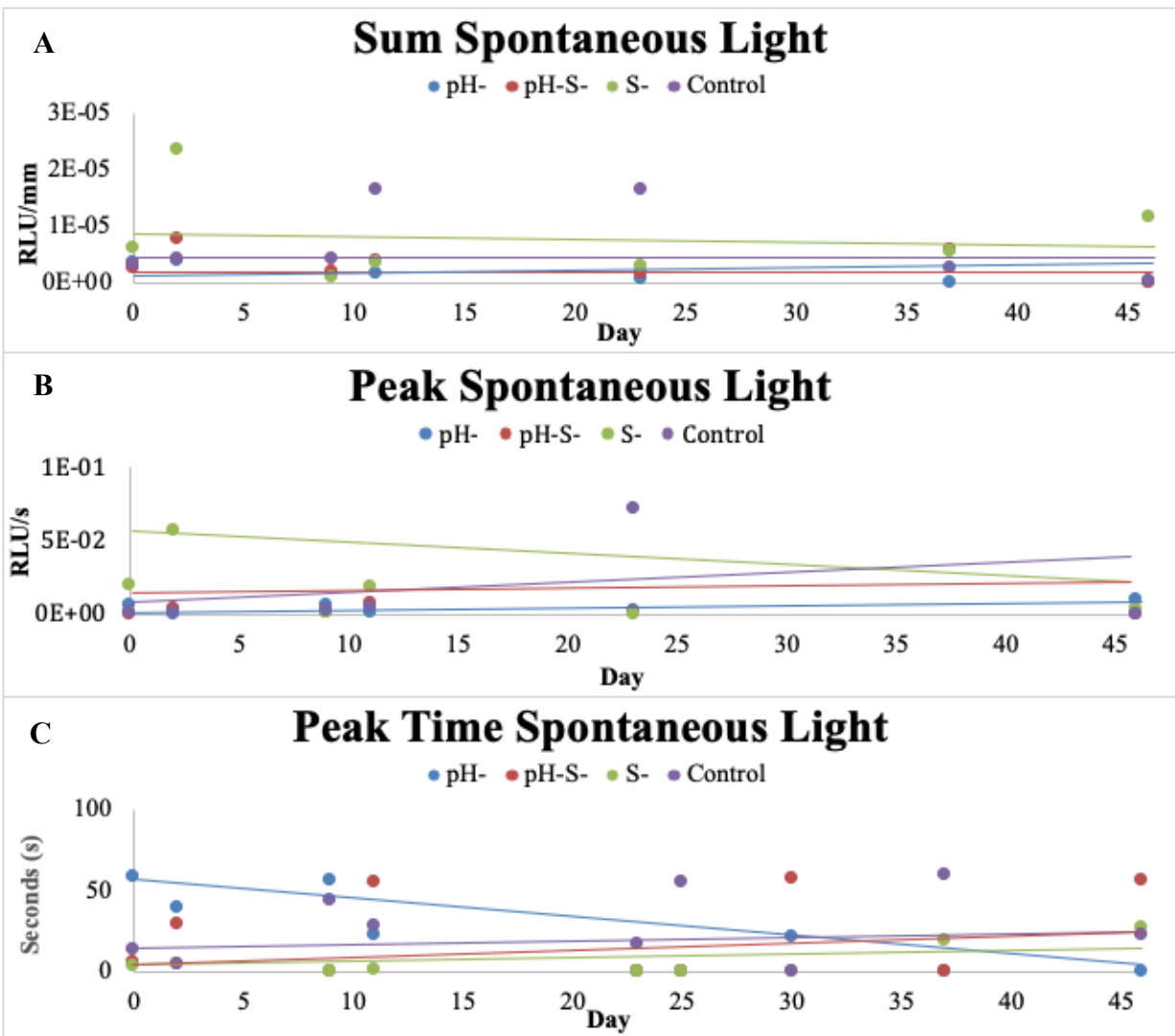


Figure 26. Raw bioluminescence data of spontaneous light showing the sum light (A), peak light intensity (B) and peak time of the light response (C) for the brittlestars exposed to each treatment. The colored lines represent the best fit lines of the raw data to show a general trend. The peak intensity plot corresponds most closely with the light profiles shown in Figure 26 (Day 0, 30, 46).

However, when the treatments were removed, the pH⁻ treatment had the lowest sum light response after the treatments were removed, while the brittlestars that were exposed to the S⁻ treatment had the largest sum light response and the pH⁻S⁻ displayed the second largest sum light response and had the highest peak intensity of light. For the spontaneous light emission, the brittlestars in the S⁻ treatment expressed the second highest peak levels of light and had the

fastest light emission after the treatments had been removed while the brittlestars in the pH⁻ and control treatments expressed the lowest peak levels and experienced slower light emission times after the treatments had been removed. Moreover, the brittlestars exposed to the pH⁻S⁻ treatment and the control condition had the slowest peak light response time when the treatments were removed (Figure 27).

The takeaway message is that the brittlestars that were exposed to low salinity conditions showed latent effects of difficulty controlling their light production response indicating there could be prolonged damage to the nervous system control of the brittlestars. This suggestion is also in agreement with the other findings regarding the flipping response behavior of the brittlestars. A loss of nervous system control would also negatively impact the brittlestars survival capabilities because *A. squamata* relies heavily on bioluminescence as a predator deterrent.

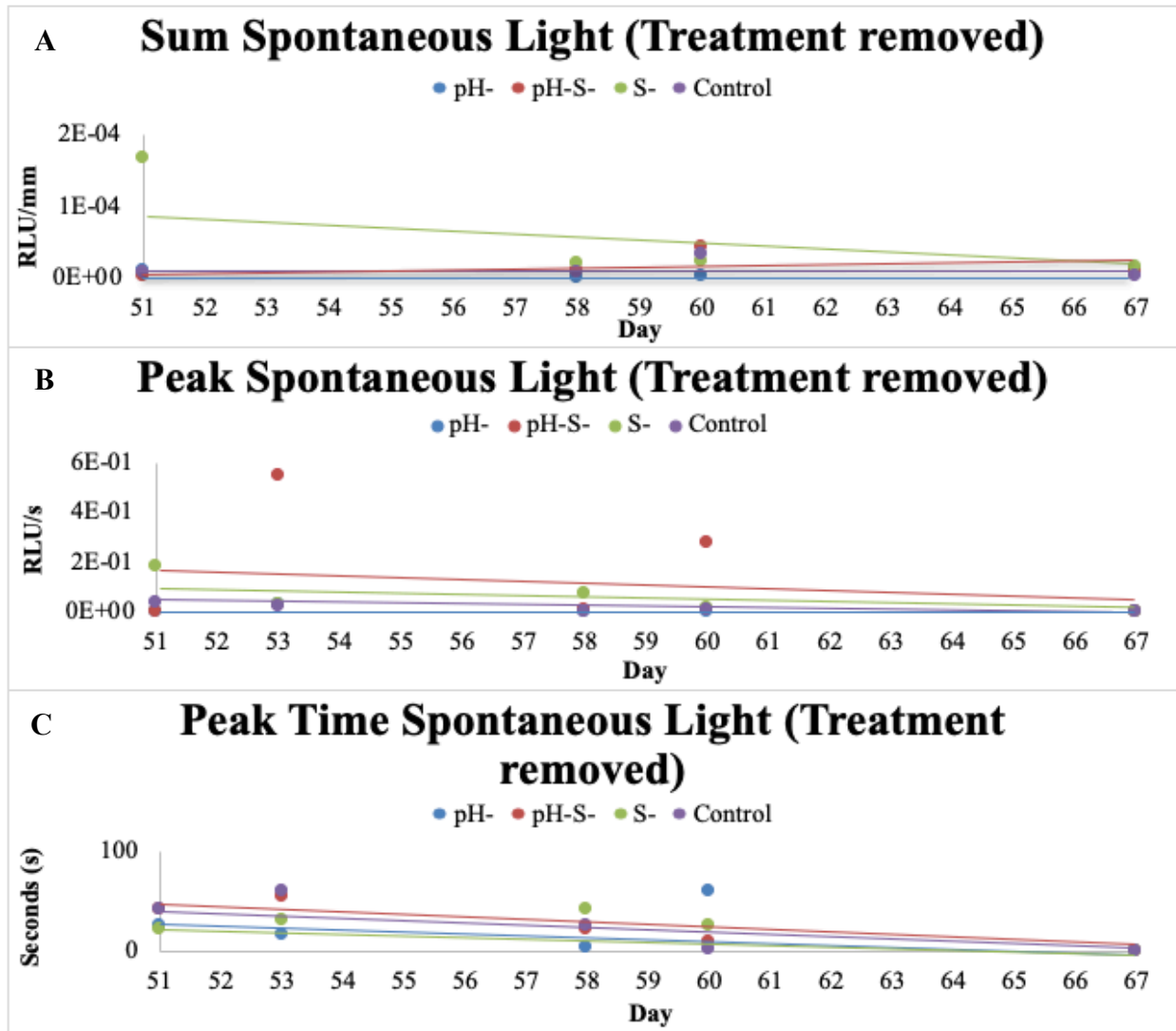


Figure 27. Raw bioluminescence data of spontaneous light showing the sum light (A), peak light intensity (B) and peak time of the light response (C) for the brittlestars after the treatments were removed. The colored lines represent the best fit lines of the raw data to show a general trend. The peak intensity plot corresponds most closely with the light profiles shown in Figure 26 (Day 67).

There is not a clear visible trend for the sum, peak and peak time of the brittlestars measured spontaneous light emission for any of the four treatments either when the treatments were present or for when the treatments were removed. However, when the entire profile for spontaneous light emission was viewed, some patterns in the data set began to emerge (Figure 28).

The brittlestars exposed to the pH^- treatment appeared to have their spontaneous light response affected more than the other treatments. This is shown by the large amount of spontaneous light on day 46 $\sim 45,000$ RLU/s at peak light emission after the brittlestars had been exposed to the condition for nearly seven weeks. However, this spike in spontaneous light production returned to normal levels ~ 500 RLU/s when the brittlestars that were exposed to pH^- conditions were placed back into control conditions. Brittlestars that were exposed to the $\text{pH}^- \text{S}^-$ (day 30) and S^- (day 46) treatments also showed a slight increase in their production of light as well, although rise in light production also decreased back to control levels when the treatments were removed (day 67; Figure 28).

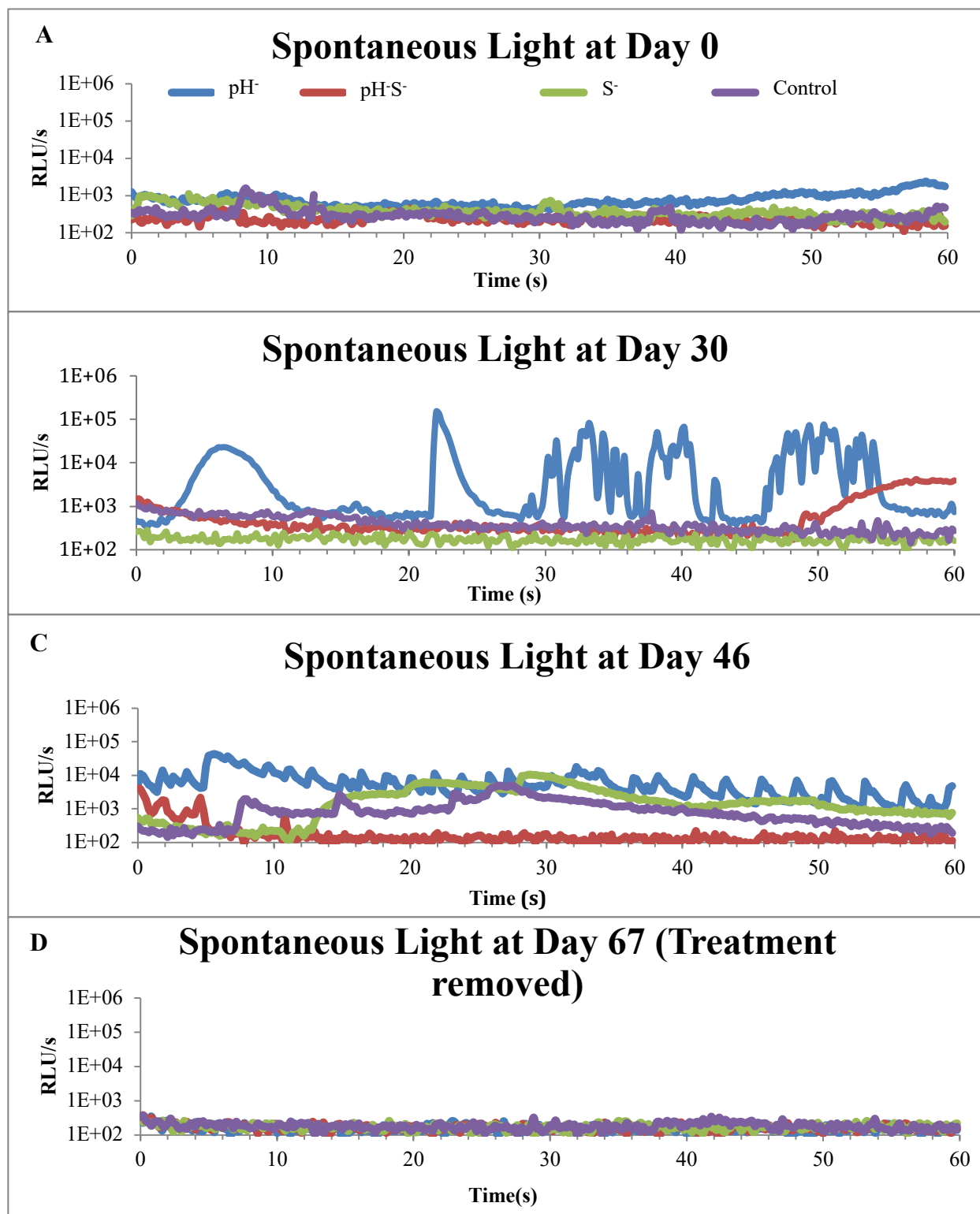


Figure 28. Typical profiles of spontaneous light production (RLU/s) for the brittlestars exposed to each treatment on Day 0 (A), Day 30 (B), Day 46 (C) and Day 67 (D). Day 67 (D) occurred while the brittlestars were placed back into the control conditions to determine if recovery was possible.

Chemically stimulated light production increased for pH⁻/ pH⁻S⁻/S⁻ (Ach) and pH⁻/ pH⁻S⁻ (KCl)

There was no significant difference in the sum value when normalized to the arm length and the KCl positive control light emission sum values between the brittlestars light production for either the Ach or KCl chemical stimulus. There was also no apparent significant difference in the brittlestars peak light emission between the treatments for any of the three stimulated light response effects tested (Figure 29 and Figure 30 respectively). Although, the brittlestars in the pH⁻, pH⁻S⁻ expressed higher Ach and KCl peak light intensity levels (Figure 29 and Figure 30 respectively). The brittlestars exposed to the pH⁻ treatment also expressed a higher level of sum Ach stimulated light (Figure 29). The takeaway message from the trends in these raw data measurements is that the brittlestars that experienced low pH conditions had a more difficult time controlling their nervous system dependent light production when they were chemically stimulated.

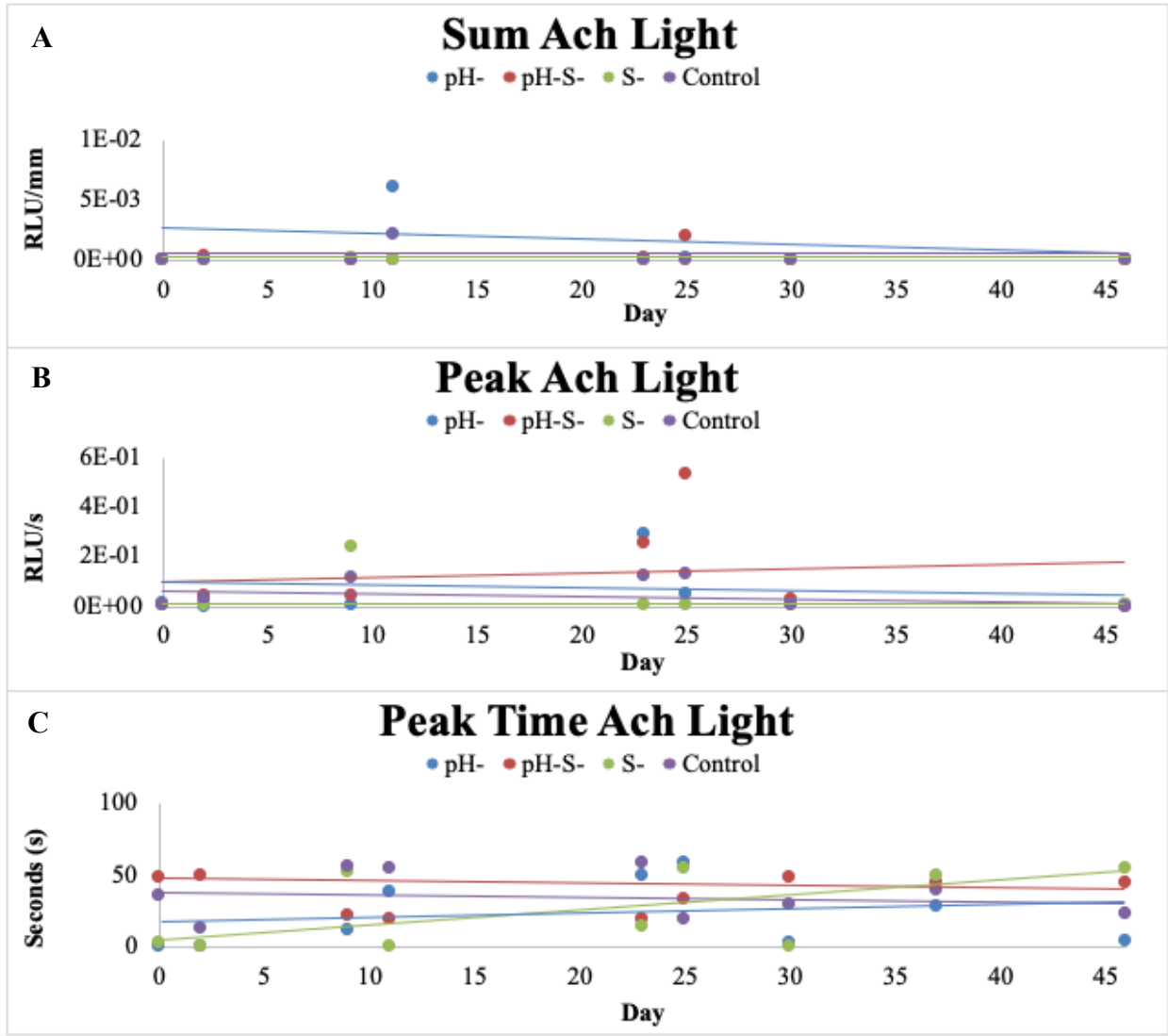


Figure 29. Raw bioluminescence data of Ach light showing the sum light (A), peak light intensity (B) and peak time of the light response (C) for the brittlestars exposed to each treatment. The colored lines represent the best fit lines of the raw data to show a general trend. The peak intensity plot corresponds most closely with the light profiles shown in Figure 31 (Day 0, 30, 46).

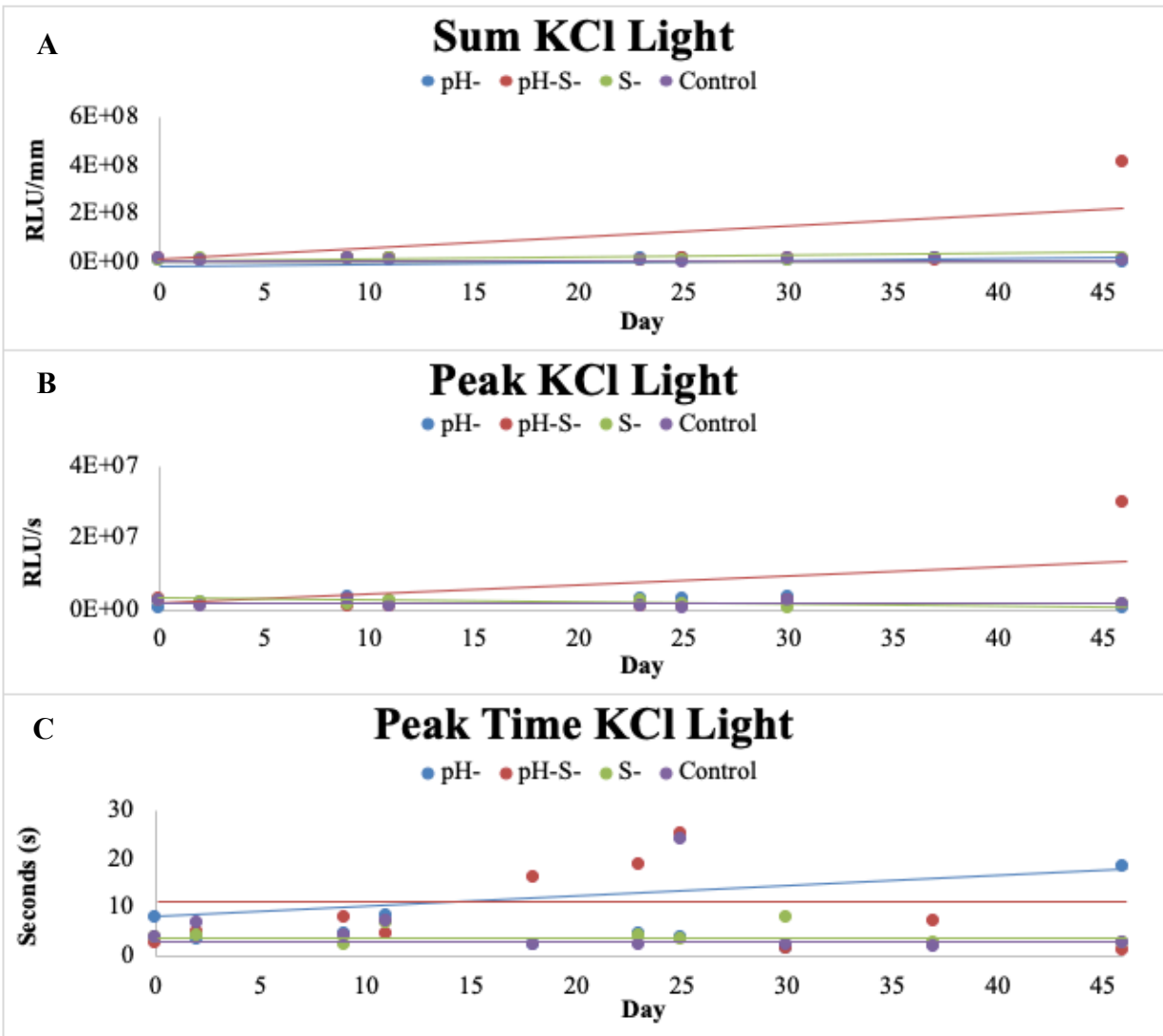


Figure 30. Raw bioluminescence data of KCl light showing the sum light (A), peak light intensity (B) and peak time of the light response (C) for the brittlestars exposed to each treatment. The colored lines represent the best fit lines of the raw data to show a general trend. The peak intensity plot corresponds most closely with the light profiles shown in Figure 32 (Day 0, 30, 46).

The brittlestars in the pH⁻ and pH⁻S⁻ treatments displayed the highest sum light emission responses for the Ach stimulated tests after the treatments were removed (Figure 31 and Figure 32 respectively). The KCl stimulated light production also had the lowest values for the S⁻ exposed brittlestars after the treatments were removed indicating that there was an issue with the brittlestars arms ability to produce a maximum light response initiated by the KCl. This could

suggest that there was sustained nervous system damage of the brittlestars that were exposed to the low salinity treatment. A similar trend in the luminescence sum of the S- treatment emitting a total higher sum light production, after the treatments were removed and the brittlestars were re-exposed to ambient seawater conditions, was also represented for the peak Ach light response (Figure 31) further supporting this claim. There was not much change in peak RLU/s light emission time from the time the treatments were present to when the treatments were absent for any of the four experimental treatments.

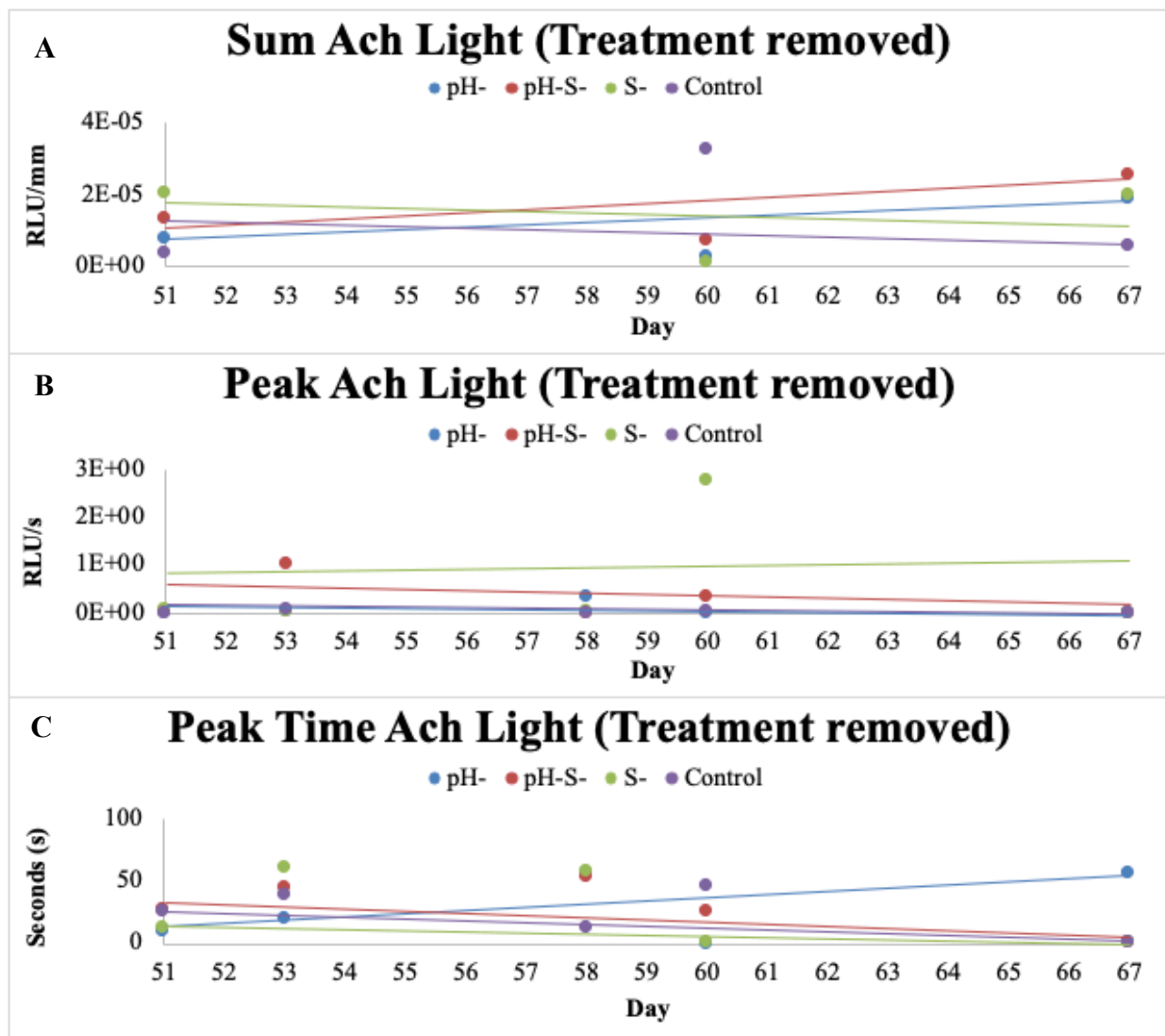


Figure 31. Raw bioluminescence data of Ach light showing the sum light (A), peak light intensity (B) and peak time of the light response (C) for the brittlestars after the treatments were removed. The colored lines represent the best fit lines of the raw data to show a general trend. The peak intensity plot corresponds most closely with the light profiles shown in Figure 31 (Day 67).

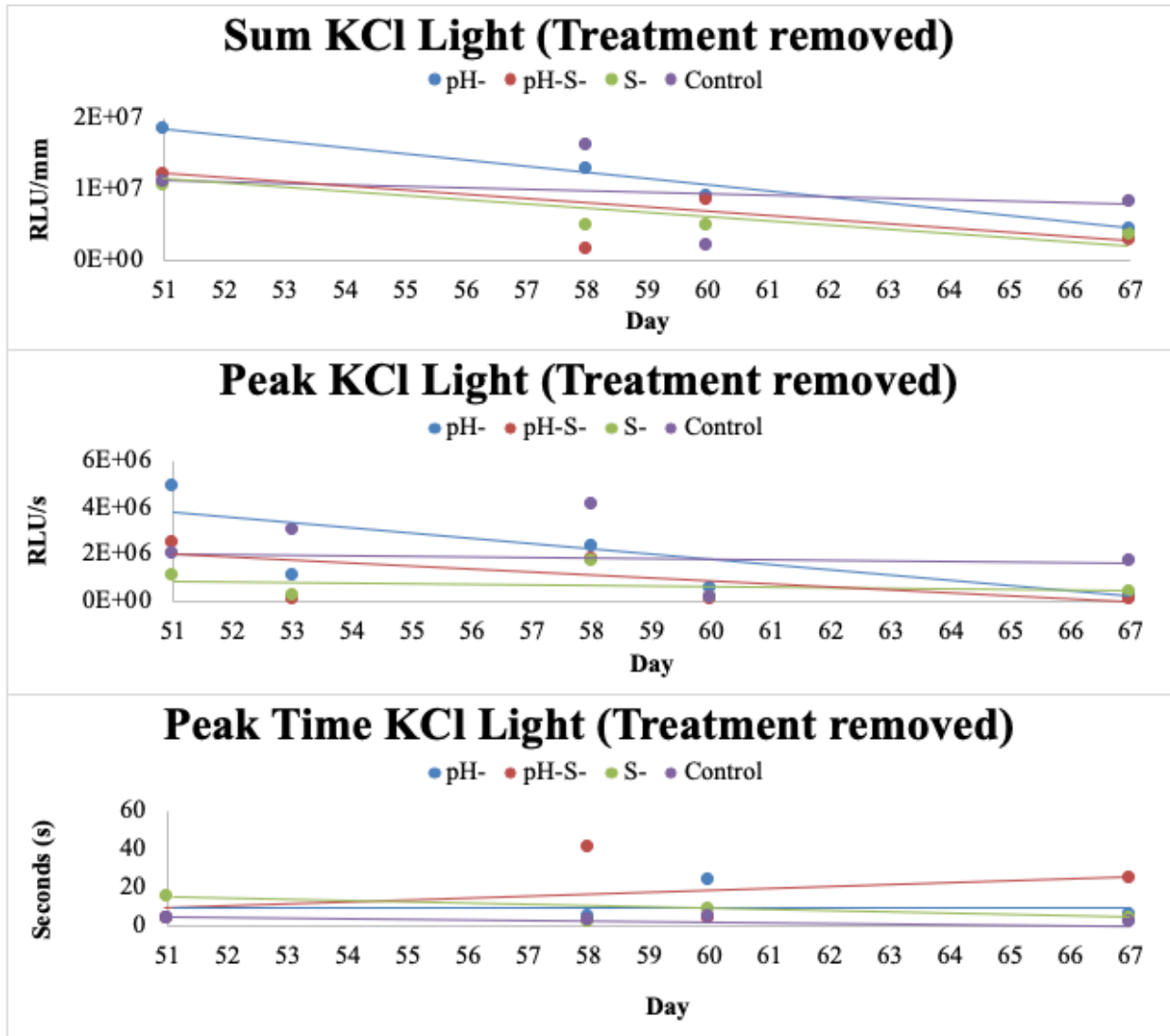


Figure 32. Raw bioluminescence data of KCl light showing the sum light (A), peak light intensity (B) and peak time of the light response (C) for the brittlestars after the treatments were removed. The colored lines represent the best fit lines of the raw data to show a general trend. The peak intensity plot corresponds most closely with the light profiles shown in Figure 32 (Day 67).

Although there was no visible pattern of effect on the brittlestars sum, peak, and peak kinetics luminescence abilities when exposed to pH^- and S^- conditions, both individually and together, a trend became apparent when the light profile was considered for the tests where the brittlestars light response was chemically stimulated by either Ach or KCl (Figure 33 and Figure 34 respectively). Under neurostimulation from the added chemical Ach, the brittlestars in all of

the treatments produced ~500 RLU/s on day 0 before they were exposed to the altered water chemistry treatments. However, after the brittlestars were exposed to the pH^- treatment on day 30 and 46 (Figure 33), they released large amounts of light (~800,000 RLU/s and ~80,000 RLU/s respectively) in flashes. The method of light released was in flashes after neuro-stimulation by the addition of Ach. The light profiles oscillating up and down quickly signified the light response of the brittlestar as flashing on and off repeatedly, similar to a nervous system pacemaker. This behavior ceased when the brittlestars that were first exposed to pH^- conditions were placed back into ambient conditions for a period of three weeks (Day 67, Figure 33).

When the brittlestars were chemically stimulated by KCl, the light cells were depolarized and released any remaining light-producing reagents from within the brittlestar arm. After exposure to the pH^- and S^- treatments for seven weeks (Day 46, Figure 34) the brittlestars were unable to release as much light <1,000,000 RLU/s as they were in the control conditions. Unlike the spontaneous and Ach stimulated light productions, the brittlestars still expressed poor light control after being placed into ambient seawater conditions for three weeks (Day 67, Figure 34) indicated by the low light response <500,000 RLU/s in the brittlestars that were exposed to the pH^- , S^- , and pH^-S^- treatments.

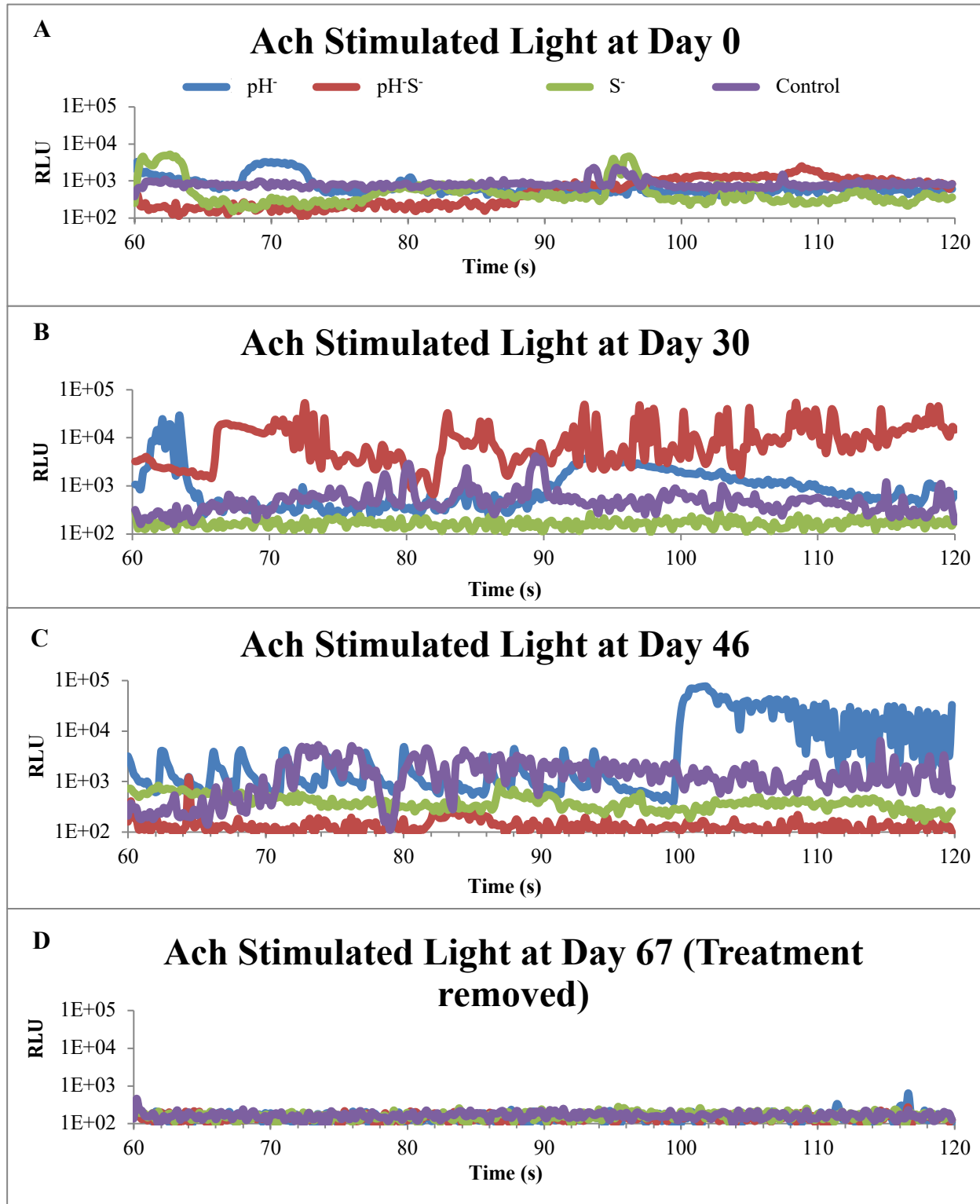


Figure 33. Typical profiles of Ach light production (RLU/s) for the brittlestars exposed to each treatment on Day 0 (A), Day 30 (B), Day 46 (C) and Day 67 (D). Day 67 (D) occurred while the brittlestars were placed back into the control conditions to determine if recovery was possible.

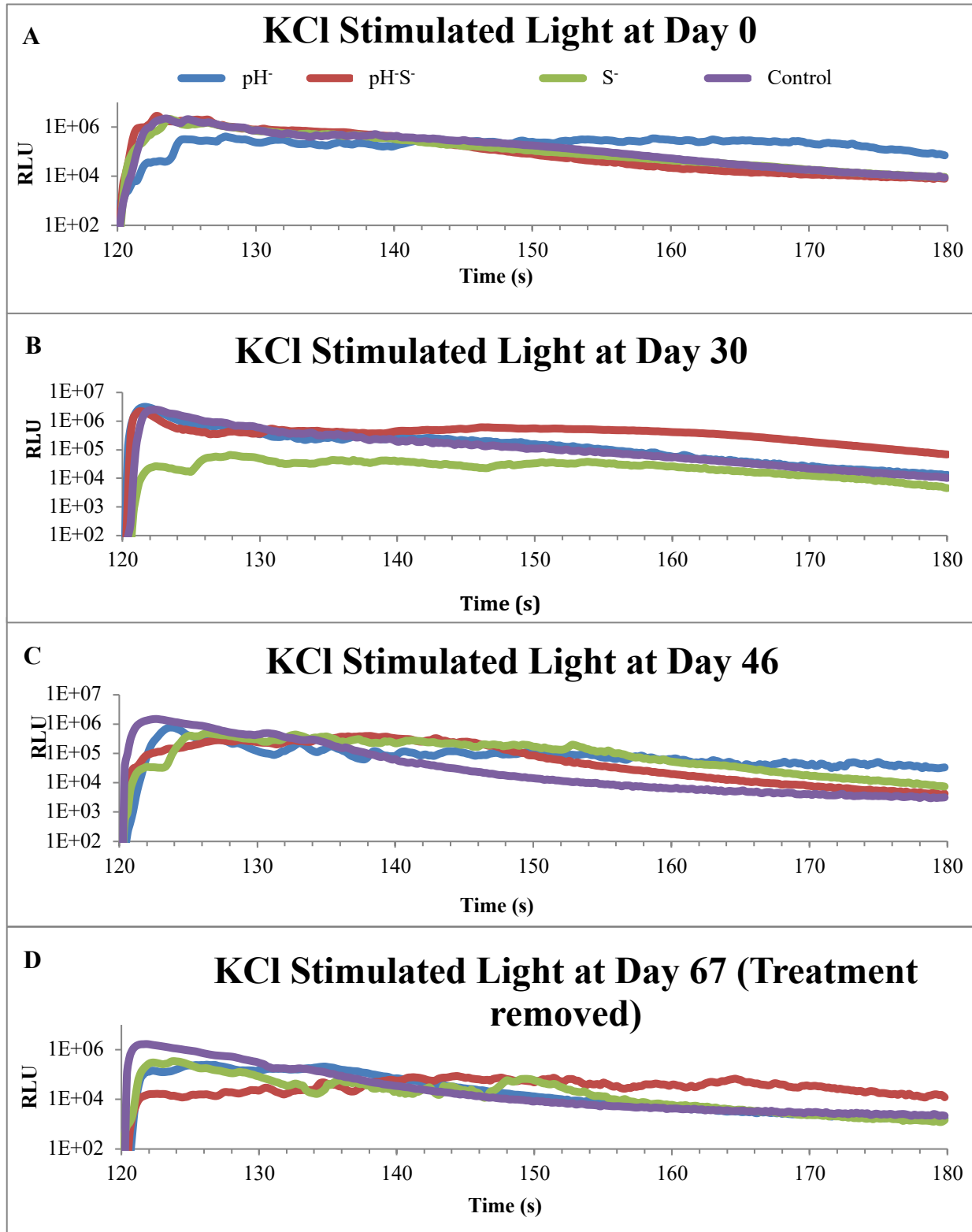


Figure 34. Typical profiles of KCl light production (RLU/s) for the brittlestars exposed to each treatment on Day 0 (A), Day 30 (B), Day 46 (C) and Day 67 (D) and measured without the use of the filter. Day 67 (D) occurred while the brittlestars were placed back into the control conditions to determine if recovery was possible.

Nervous control of bioluminescence is affected by changes in pH and salinity

The biochemical production of light from organisms is influenced by pH and salinity and both the light intensity and duration (kinetics) depend heavily on the neuro physiological status of the organism (Deheyn et al., 1999). The photogenic cells lie close to the nerve cord in each of the brittlestars arms further indicating that the light production is under nervous control.

Furthermore, spontaneous light production is rare without mechanical stimulation involved (Deheyn et al., 1996), so the increase in this type of light production could be a result of stress (biochemical and tissue damage) from the altered water chemistry treatment effects.

The S⁻ treatment did not seem to have a noticeable impact on the bioluminescence ability of the brittlestars while the treatments were present. Another study also found that changes in salinity did not affect the production of bioluminescence of the brittlestar species *A. squamata*. Although, they found that changes in temperature (not considered in this study) did have an impact on the bioluminescence production (Deheyn et al., 2000c). Projected rising sea surface temperatures and lower pH levels often seem to be linked in the scientific literature, whereby one strengthens the environmental presence of the other. Although, the combined pH-S⁻ treatment did not appear to have the same additive effects in this study and also did not show significant change in the brittlestar bioluminescent response while the treatments were present. However, the low salinity treatments were shown to possibly have lasting effects on the bioluminescent capabilities of the brittlestars either having to do with leaking the physical leaking of the light cells or failure in nervous system control of the light production, which caused an increase in the stimulated light response of the brittlestars.

Despite this, the pH⁻ treatment seemed to influence the brittlestars control over their spontaneous light production and their response of chemically stimulated light production. Although the bioluminescence reaction of the brittlestars showed some change in their light

production under conditions of pH, the results did not show enough of a pattern for the findings to be significant. There is also a deficit of experimental evidence concerning bioluminescence and low pH so it is still unclear how this future environmental condition will impact the brittlestars natural light defense ability. The brittlestars exposed to low pH also seemed to recover normal nervous bioluminescent control after the treatments were removed.

There are two main defense methods where the brittlestars use their flashing light ability. The first one is the “startle effect” to warn and scare predators away, and the second is the “burglar alarm effect”, which illuminates their predator so they can be eaten by another predator (Jones and Mallefet, 2013). The brittlestar can also autotomize (detach) its own arm while the arm is still flashing as a final attempt to distract the predator. The predator is then attracted to the flashing arm stump while the rest of the brittlestar body stops producing light and escapes into the darkness (Wilkie, 1978; Deheyn et al., 2000c). There is also the possibility of the brittlestars bioluminescence being used as an aposematic signal to warn potential predators of their unpalatability (Herring, 1995). If this is true, this light ability could be used for aposematic purposes and highlight the impalpability of these brittlestars to predators as another method of a predator deterrent (Grober, 1988).

A study using crab predators showed that there was higher avoidance, rejection, and less damage to luminescent brittlestars than non-luminescent brittlestars. The study also found that the crabs caused more damage to the luminescent brittlestars when they were manually blinded so they could not perceive the luminescence (Grober, 1988). If the production of light from the brittlestar is in fact altered by the changes in pH and salinity, this could have an impact on the predation rates because the predators are accustomed to a specific light color, in nm wavelength, and might not be deterred by variations in light production as a consequence of climate change.

However, the lack of systematically significant effects of pH, S⁻ and pH·S⁻ treatments on the bioluminescence ability of the brittlestars could alternatively mean that this particular defense mechanism is far too important to compromise even under conditions of stress. If this is proven to be the case, then perhaps the other parameters in this study that did show an effect from the altered water chemistry treatments, such as the brittlestars flipping response and regeneration abilities functionality were sacrificed in a sort of trade-off relationship to maintain control of the normal function of bioluminescence and conserve this particular defense mechanism to avoid predation. Regardless, the process of how the bioluminescence reaction works in these brittlestars needs to be more closely studied so that we can understand how this crucial predation defense/deterrent mechanism may be altered under the projected future environmental conditions concerning salinity, pH and temperature.

Role of calcium in nervous control for both the brittlestar flipping and bioluminescent responses

Calcium could play a very important role as a cofactor in the biochemical bioluminescence reaction of these brittlestars. Although, it is still unclear how exactly this intercellular calcium triggers this reaction (Dewael, and Mallefet, 2001; Haddock et al., 2010). Calcium is also a very important element for intercellular signaling and sending messages of response due to external stimuli, such as during the flipping response, arm regeneration, and the bioluminescence response (which are all nervously controlled). The brittlestars nervous system could be using calcium to relay and maintain the message of locomotion to the muscles in the arms and flip the brittlestar upright, start the regeneration process, and to trigger the luminescent reaction of the brittlestars.

Studies have found that light production of three different species of brittlestars decreased and the light responses became slower or halted entirely in conditions of lowered concentrations of calcium. Removal of calcium from an external medium also results in the inhibition of the

KCl stimulated light response in brittlestars (Dewael and Mallefet, 2001). Based on these results, calcium appears to be a crucial element of luminescent control.

Decreasing the salinity also decreases the amount of calcium in the environment and that could have disastrous implications of the brittlestars neural network, which relies on calcium to send important messages to enzymes for crucial chemical reactions such as the production of light necessary to the brittlestars main predator defense mechanism (Dewael and Mallefet, 2001). Decreasing the pH could potentially have negative consequences on the Ca^{2+} voltage-gated channels and active transport mechanisms by reducing the amount of ATP (energy) available, which could make it more difficult for the calcium to enter the organism and trigger the biochemical reaction of bioluminescence (Fieber, 2017).

Comparison between continuous (pH) and pulsed (pH·S⁻, and S⁻) exposure treatments, recovery

In experiments involving chemicals, exposure duration and concentration can have large impacts on organismal stress and recovery. If we assume the treatments of low pH and low salinity both independently and combined are like toxicants, the brittlestars experienced chronic continuous low pH exposure and chronic pulsed low salinity exposure in this study. The difference in exposure period between the pH⁻ treatment and the pH·S⁻ and S⁻ treatments could help to explain the variations in the results between each treatment.

For example, the pH·S⁻ and S⁻ treatments were administered to the brittlestars in pulses of 7 out of 24 hours each day when the water flow to all tanks was stopped, to simulate the effects of increased precipitation rates predicted in the future as a consequence of climate change. The temperature was also allowed to fluctuate to keep experimental conditions as representative of natural conditions as possible. Rainstorms can be frequent and temporally short but they can have a large impact on the salinity levels in coastal areas (Richmond and Woodin, 1996). These

stochastic events can have significant impact on the physiological development of marine invertebrates exposed to these changes.

However, when comparing consistent to pulsed exposure of toxicants, many studies have found that organisms accumulated less toxicants from intermittent exposure although the toxicity was dependent on exposure duration and frequency (Handy, 1994; Amachree et al., 2014). This minimized response also seemed relevant for a salinity pulsed exposure study (Cañedo-Argüelles et al., 2014). The repeated lower exposure times (3-6 hours) additionally seemed to affect marine organisms less when pH pulsing was tried compared to prolonged exposure of lower pH (Kim et al., 2013).

This result could be in part due to the slight increase in pH that naturally occurred when the salinity and pH water parameters were combined in both the pH-S⁻ treatment and the S⁻ treatment (refer to Table 1). Understanding the interactions between the various carbonate parameters of water chemistry such as the interaction between pH and salinity could help explain why the brittlestars in the pH-S⁻ treatment behavioral and physiological responses more closely resembled the control and the brittlestars in the S⁻ treatment less strongly (flipping response, and bioluminescence) in comparison to the brittlestars exposed to the pH⁻ treatment.

There was a noticeable change in the impact of the pH-S⁻ and S⁻ treatments when the experimental treatment conditions were removed and the brittlestars were all exposed to ambient (control) seawater conditions (otherwise known as a depuration period) to determine if recovery from some of the treatment effects was possible. There appeared to be more cumulative damage to the brittlestars that were exposed to low salinity intermittently than the brittlestars continuously exposed to low pH. This latent damage can occur in toxicology if the toxicant is too difficult to get rid of during the organism's depuration period or if the recovery time between exposures is too short (Zhao and Newman, 2006; Diamond et al., 2006). It is possible that the

brittlestars could have also experienced osmotic shocks from the intermittent exposure to low salinity for such a long duration (7 weeks) making it more difficult to behaviorally and physiologically recover in ambient seawater conditions. Although, these shocks seemed to have been slightly buffered by the presence of low pH in the pH⁻S⁻ treatment. The brittlestars that were in the pH⁻ treatment demonstrated no issues in their recovery ability, indicating that low pH administered continuously has no latent behavioral or physiological effects for the parameters tested during recovery (flipping response and bioluminescence) after the treatment is removed.

Energetic costs of pH⁻ and S⁻ conditions on brittlestars

Research showed that the sea star *Luidia cathrata* has more difficulty maintaining normal energy levels for maintenance and growth functions in low salinity conditions (Forcucci and Lawrence, 1986). The slowed flipping and regeneration results of the brittlestars exposed to low salinity conditions for extended periods of time suggest that low salinity could also have a large impact on their energy efficiency to maintain normal functions while stressed. Studies showed that absorption efficiency of energy sources from feeding was also shown to decrease in various sea star species exposed to low salinity conditions (Forcucci and Lawrence, 1986).

A change in salinity can have large implications on basic components of physiology, such as regeneration. There was an observed decrease in regeneration ability in organisms exposed to low salinity conditions (Kaack and Pomory, 2011). A large portion of a reduction in energetic functions could be due to a trend of decreasing metabolic rate when organisms are exposed to environmental conditions of low pH, high temperature and altered salinity (Talbot and Lawrence, 2002; Hu et al., 2014). Stress of an organism is often accompanied by a reduction in metabolic rate. This occurred when the brittlestar was exposed to the pH⁻, S⁻ and pH⁻S⁻ experimental treatments and could be due to an excess production of ROS in response to the environmental stressors of altered pH and altered salinity (Rivera-Ingraham and Lignot, 2017).

Importance of Amphipholis squamata as an indicator species

Many other marine species, mainly invertebrates, utilize similar survival mechanisms as *A. squamata* so they could also potentially be adversely affected by projected future changes of low pH and low salinity. There are studies in the literature that found that sea urchins have a more difficult time calcifying in conditions of low pH (Courtney et al., 2013). Sea stars flipping ability has also suffered similarly to the brittlestar in conditions of low salinity (Watts and Lawrence, 1990; Lawrence and Cowell, 1996). Using these brittlestars as model organisms and their behavioral and physiological responses to low pH and low salinity conditions (both individually and combined) as proxies for organismal stress could be very beneficial to understanding how other marine organisms could be affected in a changing climate. It is important to remember that the brittlestars used in this study were self-fertilized clones collected from approximately five individuals so the change of genetic variation among test specimens is slim. Therefore, it can be appropriate to say the variation in flipping, regeneration and bioluminescence responses are physiologically driven and may vary from individual to individual across species.

Conclusions

The findings of this experiment were four-fold. The brittlestars exposed to pH⁻ flipped slower but this change returned back to normal when the treatment was removed. The brittlestars expressed stunted regenerative growth in both length and width when exposed to the pH⁻, S⁻, and pH⁻S⁻ treatments. The brittlestars displayed more difficulty controlling their natural bioluminescence response in all of the altered water chemistry treatments S⁻ and pH⁻S⁻ and pH⁻ despite the overall light production process being unaffected. And when the experimental treatments were removed, the brittlestars seemed to have the most difficulty recovering from the

previous S- treatment to some degree in all the behavioral and physiological parameters tested. Based on these findings, the brittlestars might be preferentially conserving the functionality of their bioluminescence response at the expense of their ability to flip and regenerate normally because of their strong dependence on bioluminescence as a crucial predator deterrent. It also seems that the nervous system of these brittlestars is negatively impacted (flipping response and bioluminescence) and that the brittlestars ability of calcification suffers (arm regeneration) under conditions of low pH and low salinity. This study intended to use the behavioral and physiological survival mechanism properties of *A. squamata* as a representative for how other marine organisms with similar functions may react under the same conditions but further research on other marine organisms is required to determine the validity of this objective.

Future Directions

To obtain a clearer understanding of the results of this study, the compensation mechanisms that allow *Amphipholis squamata* to know which function preferentially it should allocate resources and energy to should be studied further. How did the brittlestar sense to conserve the bioluminescence function over the flipping response and arm regeneration capabilities? It is also unclear what chemical pathways the nervous system of the brittlestar relies on to send messages to the rest of the body to initiate such rapid escape and defense responses required for flipping and bioluminescence. These mechanisms should be studied further in not only this specific species of brittlestar but also in other species of invertebrates to achieve a more well-rounded understanding of the physicochemical processes required for survival and how these processes may change in the wake of IPCC future climate change predictions of low pH and low salinity.

References

- Amachree, D., Moody, A. J., and Handy, R. D. (2014). "Comparison of intermittent and continuous exposures to inorganic mercury in the mussel, *Mytilus edulis*: Accumulation and sub-lethal physiological effects." *Ecotoxicology and Environmental Safety* 109, 133-142.
- Andersson, A. J., Bates, N. R., Jeffries, M. J., Freeman, K., Davidson, C., Stringer, S., Betzler, E., and Mackenzie, F. T. (2013) "Clues from current high CO₂ environments on the effects of ocean acidification on CaCO₃ preservation." *Aquatic Geochemistry* 19.5-6, 353-369.
- Andersson, A. J., Mackenzie, F. T. and Gattuso, Jean-Pierre. (2011). "Ch. 8 Effects of ocean acidification on benthic processes, organisms, and ecosystems." *Ocean Acidification* edited by Jean-Pierre Gattuso and Lina Hansson, Oxford University Press, 122-153.
- Barry, J. P., Widdicombe, S., and Hall-Spencer, J.M. (2011). "Ch. 10 Effects of ocean acidification on marine biodiversity and ecosystem function." *Ocean Acidification* edited by Jean-Pierre Gattuso and Lina Hansson, Oxford University Press, 192-209.
- Brehm, P. (1977). "Electrophysiology and luminescence of an ophiuroid radial nerve." *Journal of Experimental Biology*, 71.1, 213-227.
- Brehm, P., and Morin, J. G. (1997). "Localization and characterization of luminescent cells in *Ophiopsila californica* and *Amphipholis squamata* (Echinodermata: Ophiuroidea)." *The Biological Bulletin* 152.1, 12-25.
- Burton, E. A., and Walter, L. M. (1991). "The effects of PCO₂ and temperature on magnesium incorporation in calcite in seawater and MgCl₂-CaCl₂ solutions." *Geochimica et Cosmochimica Acta* 55.3, 777-785.
- Cañedo-Argüelles, M., Bundschuh, M., Gutiérrez-Cánovas, C., Kefford, B. J., Prat, N., Trobajo, R., and Schäfer, R. B. (2014). "Effects of repeated salt pulses on ecosystem structure and functions in a stream mesocosm." *Science of the Total Environment* 476-477.1, 634-642.
- Carter, B. R., Radich, J. A., Doyle, H. L., and Dickson, A. G. (2013). "An automated system for spectrophotometric seawater pH measurements." *Limnology and Oceanography: Methods* 11.1, 16-27.
- Courtney, T., I. Westfield, and J. B. Ries. (2013). "CO₂-induced ocean acidification impairs calcification in the tropical urchin *Echinometra viridis*." *Journal of Experimental Marine Biology and Ecology* 440, 169-175.
- De Bremaeker, N. D., Baguet, F., Thorndyke, M. C., & Mallefet, J. (1999). "Modulatory effects of some amino acids and neuropeptides on luminescence in the brittlestar *Amphipholis squamata*." *Journal of experimental biology*, 202.13, 1785-1791.

- Deheyn, D. D., Allen, M. C., and De Meulenaere, E. (2015). "On the biophotonic properties of brittlestar ossicles." *Organic Photonic Materials and Devices XVII*. International Society for Optics and Photonics 9360, 1-9.
- Deheyn, D. D., Alva, V., and Jangoux, M. (1996). "Fine structure of the photogenous areas in the bioluminescent ophiuroid *Amphipholis squamata* (Echinodermata, Ophiuridea)." *Zoomorphology* 116.4, 195-204.
- Deheyn, D. D. (2001). "Bioluminescence in the brittle star *Amphipholis squamata* (Echinodermata): an overview of 10 years of research." *Proceedings of the 11th International Symposium on Bioluminescence And Chemiluminescence* edited by, Case, J. F., Herring, P. J., Robison, B. H., Haddock, S. H. D., Kricka, L. J., and Stanley, P. E. World Scientific, 35-38.
- Deheyn, D. D., Mallefet, J., and Jangoux, M. (1999). "Variation in bioluminescence with ambient illumination and diel cycle in a cosmopolitan ophiuroid (Echinodermata)." *Cahiers de Biologie Marine* 40, 57-63.
- Deheyn, D. D., Mallefet, J., and Jangoux, M. (2000a). "Cytological changes during bioluminescence production in dissociated photocytes from the ophiuroid *Amphipholis squamata* (Echinodermata)." *Cell and Tissue Research* 299.1, 115-128.
- Deheyn, D. D., Mallefet, J., and Jangoux, M. (2000b). "Evidence from polychromatism and bioluminescence that the cosmopolitan ophiuroid *Amphipholis squamata* might not represent a unique taxon." *Comptes Rendus de l'Académie des Sciences-Series III-Sciences de la Vie* 323.5, 499-509.
- Deheyn, D. D., Mallefet, J., and Jangoux, M. (2000c). "Evidence of seasonal variation in bioluminescence of *Amphipholis squamata* (Ophiuroidea, Echinodermata): effects of environmental factors." *Journal of Experimental Marine Biology and Ecology* 245.2, 245-264.
- deVries, M. S., Webb, S. J., Tu, J., Cory, E., Morgan, V., Sah, R. L., Deheyn, D. D., and Taylor, J. R. A. (2016). "Stress physiology and weapon integrity of intertidal mantis shrimp under future ocean conditions." *Scientific Reports* 6: 38637, 1-15.
- Dewael, Y., and Mallefet, J. (2001). "Involvement of calcium in the luminescence control of three Ophiuroid species (Echinodermata): a comparative study." *Proceedings of the 11th International Symposium on Bioluminescence And Chemiluminescence* edited by, Case, J. F., Herring, P. J., Robison, B. H., Haddock, S. H. D., Kricka, L. J., and Stanley, P. E. World Scientific Publishing, 39-42.
- Diamond, J. M., Klaine, S. J., and Butcher, J. B. (2006). "Implications of pulsed chemical exposures for aquatic life criteria and wastewater permit limits." *Environmental Science & Technology* 40.16, 5132-5138.

- Donachy, J. E., and Watabe, N. (1986). "Effects of salinity and calcium concentration on arm regeneration by *Ophiothrix angulata* (Echinodermata: Ophiuroidea)." *Marine Biology* 91.2, 253-257.
- Dupont, S., Ortega-Martinez, O., and Thorndyke, M. (2010). "Impact of near-future ocean acidification on echinoderms." *Ecotoxicology* 19.3, 449-462.
- Dupont, S., Vandemeulebroecke, G., Mallefet, J., Costanzo, M. T., and Salpietro, L. (2001). "Effect of habitat on intraspecific diversity of bioluminescence of the Ophiuroid *Amphipholis squamata*." *Proceedings of the 11th International Symposium on Bioluminescence and Chemiluminescence* edited by, Case, J. F., Herring, P. J., Robison, B. H., Haddock, S. H. D., Kricka, L. J., and Stanley, P. E. World Scientific Publishing, 51-54.
- Emson, R. H., and Wilkie, I. C. (1982). "The arm coiling response of *Amphipholis squamata* (Delle Chiaje)." *Proceedings of the International Echinoderm Symposium Tampa Florida. Balkema, Rotterdam* edited by Lawrence, J. M. A. A. Balkema, 11-18.
- Feely, R. A., Sabine, C. L., Lee, K., Berelson, W., Kleypas, J., Fabry, V. J., and Millero, F. J. (2004). "Impact of anthropogenic CO₂ on the CaCO₃ system in the oceans." *Science* 305.5682, 362-366.
- Fieber, L. A. (2017). "Neurotransmitters and Neuropeptides of Invertebrates." *The Oxford Handbook of Invertebrate Neurobiology* edited by Fieber, L. A. Oxford University Press, 1-27.
- Finneran, D. W., and Morse, J. W. (2009). "Calcite dissolution kinetics in saline waters." *Chemical Geology* 268.1-2, 137-146.
- Forcucci, D., and Lawrence, J. M. (1986). "Effect of low salinity on the activity, feeding, growth and absorption efficiency of *Luidia clathrata* (Echinodermata: Asteroidea)." *Marine Biology* 92.3, 315-321.
- Freire, C. A., Santos, I.A., and Vidolin, D. (2011). "Osmolality and ions of the perivisceral coelomic fluid of the intertidal sea urchin *Echinometra lucunter* (Echinodermata: Echinoidea) upon salinity and ionic challenges." *Zoologia (Curitiba)* 28.4, 479-487.
- Gattuso, Jean-Pierre, and Hansson, L. (2011). "Ch.1 Ocean acidification: background and history." *Ocean Acidification* edited by Jean-Pierre Gattuso and Lina Hansson, Oxford University Press, 1-20.
- Grober, M. S. (1988). "Brittle-star bioluminescence functions as an aposematic signal to deter crustacean predators." *Animal Behaviour* 36.2, 493-501.
- Haddock, S., Moline, M.A., and Case, J. F. (2010). "Bioluminescence in the sea." *Annual Review of Marine Science* 2, 443-493.

- Handy, R. D. (1994). "Intermittent exposure to aquatic pollutants: assessment, toxicity and sublethal responses in fish and invertebrates." *Comparative Biochemistry and Physiology Part C: Pharmacology, Toxicology and Endocrinology* 107.2, 171-184.
- Herring, P. J. (1995). "Bioluminescent echinoderms: unity of function in diversity of expression." *Echinoderm Research* edited by Herring, P. J., Emson, R., Smith, A., and Campbell, A. Balkema, 9-17.
- Huet, M. (1975) "Role of the nervous system during the regeneration of an arm in a starfish: *Asterina gibbosa* Penn. (Echinodermata, Asteroidea)." *J. Embryology and Experimental Morphology* 33, 535-552.
- Hu, M. Y., Casties, I., Stumpp, M., Ortega-Martinez, O., and Dupont, S. T. (2014). "Energy metabolism and regeneration impaired by seawater acidification in the infaunal brittlestar, *Amphipura filiformis*." *Journal of Experimental Biology* 217, 2411-2421
- IPCC, (2014): Climate Change 2014: Synthesis Report. Contribution of Working Groups I, II and III to the Fifth Assessment Report of the Intergovernmental Panel on Climate Change [Core Writing Team, R.K. Pachauri and L.A. Meyer (eds.)]. IPCC, Geneva, Switzerland, 151 pp.
- Jones, A., and Mallefet, J. (2013). "Why do brittle stars emit light? Behavioural and evolutionary approaches of bioluminescence." *Cahiers de Biologie Marine* 54, 729-734.
- Kaack, K. E., and Pomory, C. M. (2011). "Salinity effects on arm regeneration in *Luidia clathrata* (Echinodermata: Asteroidea)." *Marine and Freshwater Behaviour and Physiology* 44.6, 359-374.
- Kano, T., Sato, E., Ono, T., Aonuma, H., Matsuzaka, Y., and Ishiguro, A. (2017). "A brittle star-like robot capable of immediately adapting to unexpected physical damage." *Royal Society Open Science* 4.12, 171200.
- Kim, T. W., Barry, J. P., & Micheli, F. (2013). "The effects of intermittent exposure to low-pH and low-oxygen conditions on survival and growth of juvenile red abalone." *Biogeosciences* 10.11, 7255-7262.
- Kumar, A., and Brockes, J. P. (2012). "Nerve dependence in tissue, organ, and appendage regeneration." *Trends in neurosciences* 35.11, 691-699.
- Lawrence, J. M., and Cowell, B.C. (1996). "The righting response as an indication of stress in *Stichaster striatus* (Echinodermata, Asteroidea)." *Marine & Freshwater Behaviour and Physiology* 27.4, 239-248.
- Lawrence, J. M. (2010). "Energetic costs of loss and regeneration of arms in stellate echinoderms." *Integrative and Comparative Biology* 50.4, 506-514.
- Lawrence, J. M., and Vasquez, J. (1996). "The effect of sublethal predation on the biology of echinoderms." *Oceanologica Acta* 19.3-4, 431-440.

- Le François, N. R., Picq, S., Savoie, A., Boussin, J.C., Plante, S., Wong, E., Misserey, L., Rojas, S., and Genet, J.P. (2015). "Coupling salinity reduction to aquatic animal well-being and ecosystem representativeness at the Biodôme de Montréal." *Journal of Zoo and Aquarium Research* 3.2, 70-76.
- Lesser, M. P. (2006). "Oxidative stress in marine environments: biochemistry and physiological ecology." *Annual Review of Physiology* 68, 253-278.
- Loste, E., Wilson, R. M., Seshadri, R., and Meldrum, F. (2003). "The role of magnesium in stabilizing amorphous calcium carbonate and controlling calcite morphologies." *Journal of Crystal Growth* 254.1-2, 206-218.
- Märkel, K., and Röser, U. (1985). "Comparative morphology of echinoderm calcified tissues: Histology and ultrastructure of ophiuroid scales (Echinodermata, Ophiuroidea)." *Zoomorphology* 105.3, 197-207.
- Murtey, M. D., and Ramasamy, P. (2016). "Ch.8 Sample Preparations for Scanning Electron Microscopy–Life Sciences." *Modern Electron Microscopy in Physical and Life Sciences* edited by Janecek M. InTech, 161-185.
- National Research Council. (2010). *Ocean Acidification: a National Strategy to Meet the Challenges of a Changing Ocean*. Washington, DC: The National Academies Press. 1-187.
- Orr, J. C. (2001). "Ch.3 Recent and future changes in ocean carbonate chemistry." *Ocean Acidification* edited by Jean-Pierre Gattuso and Lina Hansson, Oxford University Press, 41-66.
- Richmond, C. E., and Woodin, S. A. (1996). "Short-term fluctuations in salinity: effects on planktonic invertebrate larvae." *Marine Ecology Progress Series* 133, 167-177.
- Rivera-Ingraham, G. A., and Lignot, Jehan-Hervé. (2017). "Osmoregulation, bioenergetics and oxidative stress in coastal marine invertebrates: raising the questions for future research." *Journal of Experimental Biology* 220.10, 1749-1760.
- Shaeffer, C. M. (2016). "The effects of autotomy and regeneration on the locomotion and behavior of brittle stars (Echinodermata: Ophiuroidea) of Moorea, French Polynesia." *PeerJ Preprints* 4:e2471v1.
- Shimomura, O., and Shimomura, A. (1985). "Halostaurin, phialidin and modified forms of aequorin as Ca²⁺ indicator in biological systems." *Biochemical Journal* 228.3, 745-749.
- Shimomura, O. (1986). "Bioluminescence of the brittle star *Ophiopsila californica*." *Photochemistry and Photobiology*, 44.5, 671-674.
- Shimomura, O. (2006) *Bioluminescence: Chemical Principles and Methods*. World Scientific. 1-470

- Sides, E. M. (1987). "An experimental study of the use of arm regeneration in estimating rates of sublethal injury on brittle-stars." *Journal of Experimental Marine Biology and Ecology* 106.1, 1-16.
- Talbot, T. D., and Lawrence, J. M. (2002). "The effect of salinity on respiration, excretion, regeneration and production in *Ophiophragmus filigraneus* (Echinodermata: Ophiuroidea)." *Journal of Experimental Marine Biology and Ecology* 275.1, 1-14.
- Turner, R. L., and Meyer, C. E. (1980). "Salinity tolerance of the brackish-water echinoderm *Ophiophragmus filigraneus* (Ophiuroidea)." *Marine Ecology Progress Series* 2, 249-256.
- Watts, S. A., and Lawrence, J. M. (1990). "The effect of temperature and salinity interactions on righting, feeding and growth in the sea star *Luidia clathrata* (Say)." *Marine and Freshwater Behaviour and Physiology* 17.3, 159-165.
- Wilkie, I. C. (1978). "Arm autotomy in brittlestars (Echinodermata: Ophiuroidea)." *Journal of Zoology* 186.3, 311-330.
- Wilt, F. H., Killian, C. E., and Livingston, B. T. (2003). "Development of calcareous skeletal elements in invertebrates." *Differentiation* 71.4-5, 237-250.
- Wood, H. L., Spicer, J. I., Lowe, D. M., and Widdicombe, S. (2010). "Interaction of ocean acidification and temperature; the high cost of survival in the brittlestar *Ophiura ophiura*." *Marine Biology* 157.9, 2001-2013.
- Wood, Hannah L., Spicer, J. I., and Widdicombe, S. (2008). "Ocean acidification may increase calcification rates, but at a cost." *Proceedings of the Royal Society of London B: Biological Sciences* 275.1644, 1767-1773.
- Zeebe, R. E., and Ridgwell, A. (2011). "Ch.2 Past changes of ocean carbonate chemistry." *Ocean Acidification* edited by Jean-Pierre Gattuso and Lina Hansson, Oxford University Press, 1-28.
- Zhao, Y., and Newman, M. C. (2006). "Effects of exposure duration and recovery time during pulsed exposures." *Environmental Toxicology and Chemistry* 25.5, 1298-1304.